

RESEARCH TRIANGLE INSTITUTE

TRR-33

RTI Report No. TRR-33

Final Report, RTI Program RU-277

SURVEYOR LANDING RADAR TEST PROGRAM REVIEW

CONTRACT NO. 951603

(THRU)
(CODE)
(CATEGORY)

N67-37922
(ACCESSION NUMBER)
194
(PAGES)
CR-88883
(NASA CR OR TMX OR AD NUMBER)

Prepared for

Jet Propulsion Laboratory
California Institute of Technology
Pasadena, California

January 24, 1967

FACILITY FORM 802



RTI Report No. TRR-33

SURVEYOR LANDING RADAR TEST PROGRAM REVIEW

CONTRACT NO. 951603
RTI PROJECT NO. RU-277

Submitted to:

Jet Propulsion Laboratory
California Institute of Technology
Pasadena, California

D. F. Palmer
D. F. Palmer

P. Gene Smith
P. Gene Smith

G. V. Borgiotti
G. V. Borgiotti

Approved by:

P. Gene Smith
P. Gene Smith, Director
Radiation Systems Laboratory

FOREWARD

This report was prepared by the Radiation Systems Laboratory of the Research Triangle Institute, Research Triangle Park, North Carolina, under California Institute of Technology (JPL) Contract 951603, a subcontract of NAS7-100. The work was administered by Section 273 of the Jet Propulsion Laboratory, Pasadena, California. Mr. S. A. Cohen was the JPL coordinator for the contract.

The program studies began on June 1, 1966 and were completed January 31, 1967. Participating RTI Staff Members were:

- P. G. Smith, Director of Radiation Systems Laboratory
- D. F. Palmer, Project Leader
- G. V. Borgiotti, Member of Technical Staff

TABLE OF CONTENTS

	<u>Page</u>
I. CONCLUSIONS AND RECOMMENDATIONS	1-1
A. GENERAL RESULTS	1-1
B. SPECIFIC RECOMMENDATIONS	1-1
II. INTRODUCTION	2-1
III. BACKGROUND INFORMATION	3-1
A. INTRODUCTION	3-1
B. ENVIRONMENTAL AND SYSTEM-PERFORMANCE DEFINITION	3-1
C. SUMMARY OF RADVS CHARACTERISTICS	3-5
D. OUTLINE OF ANTICIPATED RADVS OPERATIONAL PROBLEMS	3-12
E. OUTLINE OF RADVS FUNCTIONAL DETAILS	3-15
IV. "DESIRABLE" TEST PROGRAM DESCRIPTION	4-1
A. PHILOSOPHY OF A "DESIRABLE" TEST PROGRAM	4-1
B. "DESIRABLE" FLIGHT-READINESS TEST PROGRAM	4-5
C. "DESIRABLE" SPECIAL TEST PROGRAM	4-16
V. PRESENT TEST PROGRAM DESCRIPTION	5-1
A. OVERALL PROGRAM OUTLINE	5-1
B. TEST EQUIPMENT	5-1
C. DEVELOPMENTAL AND TYPE ACCEPTANCE TESTS	5-2
D. VERIFICATION AND ACCEPTANCE TESTS	5-10
VI. EVALUATION OF PRESENT TEST PROGRAM	6-1
A. INTRODUCTION	6-1
B. COMPARISON OF TEST SPECIFICATIONS WITH MISSION REQUIREMENTS	6-1
C. COMPARISON OF PRESENT AND "DESIRABLE" PROGRAMS	6-10
D. DOCUMENTATION ADEQUACY	6-18
E. TESTING CONSISTENCY	6-18
VII. SUGGESTED TEST MODIFICATIONS	7-1
A. FLIGHT-READINESS PROGRAM	7-1
B. SPECIAL-TEST PROGRAM	7-11
 APPENDICES	
A. BIBLIOGRAPHY OF DOCUMENTATION AND LIST OF REFERENCES	A-1
B. RADVS TRANSMITTER RECEIVER LEAKAGE	B-1
C. SIDELobe EFFECTS AS RELATED TO RADVS TEST PROGRAM REVIEW	C-1

Table of Contents (continued)

	<u>Page</u>
D. AVAILABLE DETAILS OF VENDOR UNIT TESTS	D-1
E. DETAILS OF THE VENDOR SYSTEM ACCEPTANCE TEST	E-1
F. BUYER FAT REQUIREMENTS LISTING	F-1
G. DISCUSSION OF THE STEA SIGNAL SIMULATION TECHNIQUE	G-1

LIST OF ILLUSTRATIONS

<u>Figure No.</u>		<u>Page</u>
3-1	Antenna and beam configuration, RADVS. (Z-axis points downward into plane of paper.)	3-6
3-2	RADVS block diagram.	3-7
3-3	RF and preamp sections of the DVS. (Section for RA is similar.)	3-8
3-4	Frequency tracker, simplified block diagram	3-11
5-1	Diagram of the RADVS signal simulation portion of STEA. The channel shown is typical of all DVS and RA channels except as shown.	5-3
6-1	Spectral width and velocity misalignment angle vs velocity magnitude. (See Fig. 6-2 for relationships assumed.)	6-5
6-2	Relationships assumed to computed curves of Fig. 6-1.	6-6
7-1	Stability and deviation-linearity measurement circuit.	7-6
7-2	Simplified version of discriminator circuit using audio detection and amplification.	7-8
7-3	Addition to STEA for implementing spread-spectrum testing. Blocks shown in double lines are existing system; dotted lines from phase splitter to switches show existing mode; switches are in spread-spectrum position.	7-10
7-4	Block diagram for an on-board spectrum analyzer.	7-13
B-1	Illustration of transmitter-receiver leakage	B-2
B-2	Illustration of experimental configuration. Antenna shown is a part of the system illustrated in Fig. B-1.	B-7
C-1	Acquisition circuit, block diagram	C-7
C-2	Response curves of lowpass and bandpass filters in Fig. C-1.	C-8
C-3	Detector outputs (Fig. C-1) versus cross-coupled side-lobe power, with P_M/P_{CCSL} as a parameter.	C-8

List of Illustration (continued)

<u>Figure No.</u>		<u>Page</u>
C-4	Sidelobe suppression capability of circuit in Fig. C-1 for $B_b = 8$ kHz, $B_t = 300$ Hz (N.B.), 1500 Hz (W.B.), $B_d = 4$ Hz, and $\alpha = 1/2$. Acquisition thresholds apply when P_{CCSL} and P_M are interchanged and $P_{CCSL} = 0$.	C-12
C-5	Attenuator characteristic.	C-11
C-6	Illustration of limiting action on the resultant of a large signal plus a small signal. For well separated signals (i.e., non-overlapping), the effect is to change a non-symmetrical spectrum of the resultant (before limiting) to a symmetrical spectrum, centered at the center of the large-signal spectrum. For fluctuating signals, the effect is slightly different; small shifts of the resultant-spectrum center from that of the larger signal do occur after limiting.	C-15
G-1	Sideband levels relative to the signal acquisition threshold vs roll axis slant range for the upper DVS beam of a spacecraft at 5° angle to the lunar vertical.	G-4
G-2	Signal component levels vs. range for sinusoidal frequency modulation of 1 kHz deviation at modulating frequencies up to about 1.5 kHz.	G-5

circuit has been suggested (see Appendix C). Finally, the possibility of antenna modification could be more extensively investigated. These solutions should be analyzed and tested thoroughly in order to determine their adequacy and to detect any adverse conditions imposed by their use. In addition, tests of the simultaneous presence of two signals in one receiver channel should be made to determine whether any natural suppression of the weaker signal exists.

Without the modifications and associated testing, the CCSL problem is considered to be sufficiently serious to decrease appreciably the the probability of mission success; although restriction of roll angle appears capable of reducing the danger of CCSL effects to acceptable levels for certain lunar approach angles [52], it is not an adequate solution to the problem for all anticipated missions.

The testing recommended above is estimated to require about six man months engineering time over a four month period.

- (2) More carefully evaluate the transmitter-receiver leakage problem situation.

Further tests are recommended to obtain additional information about the characteristics of the transmitter-receiver leakage signal under actual lunar descent conditions. The following two tasks are desirable: a) review previous vibration test and compare levels with those measured on the Surveyor 1 spacecraft to determine adequacy and possible need for retest; and b) perform on-board measurement of the transmitter-receiver leakage spectrum. (These tests are described in Section VII.)

Such investigations are important because the actual nature of the transmitter-receiver leakage signal during lunar descent is still unknown. It is very desirable to learn these characteristics to determine their effect on the remainder of the Surveyor program and future programs involving similar radar-controlled landing systems.

Performance of the item (a) recommended above is primarily a matter of data gathering and analysis. It is quite possible that no further vibration tests will be necessary if results obtained previously can be interpolated or extrapolated to Surveyor 1 conditions. This analytical work is estimated to require about four man-months of engineering effort. The implementation of item (b) is estimated to require approximately three man-months engineering for design, construction, and testing of a breadboard unit. An additional period of about

I. CONCLUSIONS AND RECOMMENDATIONS

A. GENERAL RESULTS

The major weakness of the present RADVS test program appears to be in the area of design verification (as opposed to flight acceptance testing). In particular, deficiencies are believed to exist in investigations of sidelobe signal pickup, transmitter-receiver leakage effects, and retro tankage echo discrimination. Of lesser importance is the apparent lack of design margin determination in environmental tests. Finally, the adequacy of the ionization layer environmental test remains in question because of unavailability of documentation.

The present flight acceptance test program seems to be basically complete except for absence of full simulation of retro engine induced stresses. The adequacy of certain portions, however, is of concern because of lack of realism in the signal simulation. Tests of acquisition sensitivity, tracker and converter operation, range mark accuracy, and cross-coupled sidelobe circuitry performance are involved.

Documentation of the present program appears to be adequate except for procedures listings. This particularly affects unit level testing, where test equipment tends to be less permanently assembled. Test requirements are generally consistent, with the exception of acquisition levels, which seem to be variable. Environmental levels for unit and system tests are not completely consistent.

B. SPECIFIC RECOMMENDATIONS

The purpose of this section is to summarize specific recommendations resulting from the present study. Most of these recommendations are discussed in greater detail in Section VII, "Suggested Test Modifications." A rough estimate of time and manpower required to fulfill each modification is given here, based on past experiences.

The recommendations are listed below in order of decreasing importance in assuring mission success:

- (1) Perform thorough analyses and experimentation of cross-coupled sidelobe problems.

As a result of previous studies [52],* the cross-coupled-sidelobe (CCSL) logic is currently being modified [66] to eliminate potential problem situations. Also, an alternate solution of adding a small-signal suppression

* Bracketted numbers refer to references listed in Appendix A.

three months would be required for complete incorporation of the circuit into a flight spacecraft.

- (3) Provide additional test equipment and procedures to incorporate measurement of klystron frequency coherence and sweep linearity into the flight acceptance program.

Problems involving frequency incoherence and sweep nonlinearity cannot be detected with use of the present test equipment. Yet, they can cause loss of sensitivity and false locks, as discussed in Appendix G. Loss of range accuracy is also a common effect of sweep nonlinearity.

The equipment needed, which is described in Section VII, is estimated to require about six engineering man-months and eight technician man-months for completion of six units. An additional two man-months would be required for installation at test facilities and modifications of test requirements.

- (4) Provide additional test equipment and procedures to allow testing with realistic signal spectra in the flight acceptance program.

The tracker, analog converter, range mark, and cross-coupled sidelobe circuitry are not completely checked using the present line spectrum inputs, as noted in Appendix G. In addition, closed-loop descent testing lacks the realism necessary to fully check subsystem interaction.

The required circuitry, which is described in Section VII, would necessitate about two man-months of engineering and two man-months of technician time to complete a prototype. Construction and installation of all units would probably consume an additional six man-months of technician time. The possibility exists, however, that Ryan already has some of the circuitry designed.

- (5) Thoroughly examine the sufficiency of system design and test requirements in view of retro-tankage effects.

Further analytical and experimental work should be performed to determine the range of effects the retro-tankage can cause. The analysis would consist of determining the possible profiles of retro-tankage separation from the spacecraft, and the use of these profiles for estimating the retro-tankage signal level and velocity combinations. Signals having these characteristics should then be applied to the RADVS from a signal simulator such as STEA to evaluate the rejection capability and response of the SDC.

The analytical work described above is estimated to require about three engineering man-months. The requirements for performing the experimental work depends upon the range of signal levels and velocities obtained from the analytical study. If the present STEA can supply these required signals, the test will be relatively simple; otherwise, special tests will have to be planned.

(6) Modify present flight-acceptance test program to fill gaps.

Table 7-1 of Section VII indicates portions of the existing flight-acceptance program which are not considered to be adequate. With the exception of the unit acceleration tests, which are discussed separately below (8), these changes are mainly small items to increase system confidence.

About two man-months of engineering time is expected to be required to institute the changes in Table 7-1 which do not appear elsewhere in this enumeration. Full conformity to Table 7-1 also requires performance of items 3, 4, and 8 of the present summary of recommendations.

(7) Renew type-acceptance testing to determine margins of operation within the expected environmental conditions and to analyze fatigue effects of flight-acceptance testing.

Previous type-acceptance testing appeared to lack the thoroughness needed to make it valuable for RADVS, as described in Sections IV.C.4 and VII.B.3. Completion of the program would probably require about 18 man-months of combined engineering-technician time.

(8) Add a constant acceleration test in the flight acceptance program to simulate retro engine deceleration.

The argument for the need of this test is given in Section VII.A.1. Basically, the reason is that such an environment could easily impose the most severe mechanical stress on the system, and, therefore, each unit should be tested for ability to withstand it.

It is estimated that about 12 man-months would be needed to place this test in the program.

- (9) Add a sinusoidal vibration test with the RADVS operating to match the retro-descent specification (if the specification is realistic).
- (10) Provide unit level test procedure documentation to insure thoroughness and uniformity.
- (11) Set rigid acquisition sensitivity levels to assure rejection of sub-standard systems.
- (12) Circulate to JPL all Ryan engineering change proposals (ECP) to help make known system peculiarities which might otherwise be evident only to those engaged in design and construction.

II. INTRODUCTION

The purpose of the study program reported herein was to review the present Surveyor landing radar test program and to recommend desirable and realistic modifications. This effort was defined as Phase 1 of an overall program for achieving a higher confidence level in the ability of the Surveyor Radar Altimeter and Doppler Velocity Sensor (RADVS) system to perform its function of enabling soft lunar landings.

The first task of the study was to become familiar with the radar system and certain parts of the test program. During this early period, the basic tenets of a test-program philosophy were also developed. Subsequently, detailed studies of a "desirable" test program and of the current test program were conducted; to reduce biases of the former program by knowledge of the latter, these tasks were undertaken as independently as possible. This approach is clearly indicated by the report outline: Sections III, IV, and V contain background information, a "desirable" test program description, and the present program description, respectively. Following sections contain an evaluation of the present test program (mainly by comparison with the "desirable" program) and a set of suggested test modifications. Section I contains a summary of conclusions and recommendations.

Several important conditions influenced the conduct and conclusions of the program. First, the time schedule of the Surveyor Program is determined by important factors outside the purview of the test-program review and is not likely to be caused to change materially unless serious problems are encountered. Second, from a time-duration viewpoint the Surveyor Program is entering its latter stages. Consequently, the current practicality of implementing suggested modifications to the program is an uppermost consideration. These two factors dictate that the test program be reviewed from an adequacy standpoint rather than from a standpoint of improvement. A third condition which enters very strongly into the program is that completely realistic earth testing is out-of-the-question. Compromises between realistic testing under lunar conditions and reasonable testing costs and delays are clearly in order.

Although careful consideration has been given to the desirability and usefulness of suggested test program modifications, no attempt has been made to place numerical values on the confidence levels (for successful RADVS performance) to be achieved by the various recommendations. The RTI team believes that such numerical assignments would have little basis and therefore little value. Indications are given in the Recommendations Section of the relative importance attached to the recommendations.

ALONG THRUST AXIS

<u>Frequency (Hz)</u>	<u>Level</u>	<u>Duration</u>
5-40	2.5 g peak sinusoidal	Throughout powered flight
40-1500	2.0 g peak sinusoidal	Throughout powered flight
100-1500	2.0 g rms, white gaussian random	Throughout powered flight except lift-off and/or Mach 1
100-1500	4.5 g rms white gaussian random	Liftoff or Mach 1

ALONG LATERAL AXIS

<u>Frequency (Hz)</u>	<u>Level</u>	<u>Duration</u>
1-2.5	4.0 inches double amplitude	Power flight
2.5-40	1.25 g peak sinusoidal	Power flight
40-1500	2.0 g peak sinusoidal	Power flight
100-1500	2.0 g rms, white gaussian random	Power flight except lift-off or Mach 1
100-1500	4.5 g rms, white gaussian random	Lift-off or Mach 1

(c) Acoustic Environment

During the Centaur firing, the overall sound pressure level inside the Centaur fairing is estimated to be no greater than 145 db over $2 \cdot 10^{-4}$ dynes/cm² (with a flat spectrum from 20 Hz to 10 kHz).

(d) Pressure

The pressure changes from atmospheric to 10^{-4} torr within three minutes.

(e) Pitch rate

The maximum pitch rate will not exceed 5 deg/sec during thrust, coast, or turn periods.

2. Transit Phase

(a) Shock and Vibration

Not appreciable.

(b) Pressure

The pressure is anticipated to be less than 10^{-12} torr.

(c) Temperature

The incident radiant flux is 4.40 BTU/Hr - Ft²; reradiation is into a background at -460°F.

III. BACKGROUND INFORMATION

A. INTRODUCTION

Thorough investigation of RADVS testing demands detailed knowledge of the three fundamental elements of the problem:

- (1) the environmental conditions to be imposed upon the system,
- (2) the system performance required within the environments, and
- (3) the characteristics of the system.

(Few of the parameters can be known with complete certainty, of course.)

Presentation in this report of all information gathered would be of little value to those familiar with the Surveyor program. Certain details must be listed to support the analyses and conclusions, however. The purpose of the section being introduced, therefore, is to provide many of the necessary details in a concise manner.

A by-product of gathering the background information was the uncovering of areas in which RADVS operational problems might be anticipated. An outline of these ideas is presented as a logical extension of the details listed; more complete analyses are contained in Appendices B and C.

B. ENVIRONMENTAL AND SYSTEM-PERFORMANCE DEFINITION

Environmental conditions are ascribable to the four main mission phases: boost, transit, midcourse, and descent. RADVS must operate only in the last phase noted (but must survive the others, of course). Details are outlined below and consolidated in Table 3-1: (The main source of environmental information is HAC document 224800, Detail Specification, Environmental Conditions, Surveyor Spacecraft [5]. Also see [1,2].)

1. Boost Phase (11 minutes)

(a) Static Acceleration

During the Boost Phase, a static acceleration of 2.8 g will be experienced. The acceleration will have increased to a maximum of 5.9 g's at the instant of booster engine cutoff. At Centaur cutoff, the acceleration will be approximately 5 g's. In the transverse direction, the maximum acceleration will be 0.1 g.

(b) Vibration

The following vibration levels are experienced at the S/C--Centaur separation plane:

3. Midcourse

The expected environments are less severe than in other conditons.

4. Descent Phase

(a) Shock

Shock from retro-rocket ignition: Terminal peak sawtooth acceleration pulse with a magnitude of 5 g and a duration of 250-350 msec.

(b) Static Acceleration

Due to retro-rocket burning, the static acceleration reaches 10.8 g along the thrust axis at the end of engine burn-out. (No significant static acceleration appears along the lateral axis.)

(c) Vibration (retroburning)

Vibration due to retroburning is a combination of 2g (peak) sinusoidal at 100-1500 Hz and 0.2 g rms white gaussian excitation independently applied along any axis for a maximum time of 50 seconds.

Table 3-1. Summary of the main mission environments expected

PHASE	STATIC ACCELERATION	VIBRATION	TEMPERATURE	OTHER
Boost	Max. 5.9 g (thrust axis)	Max 4.5 g rms white Gaussian (both on thrust and lateral axis at the S/C - Centaur Separation plane	50° to 100°F (Data from Surveyor I Flight)	Pressure: In three minutes from atmospheric to 10 ⁻⁴ torr Acoustic: White Spectrum from 20 Hz to 10 kHz, 145 db over 2.10 ⁻⁴ torr
Transit	--	Not Appreciable	KPSM: 0° to 50°F SDC: 25° to 75°F Preamps: 0° to 75°F (Data from S/C 1 flight)	Pressure: 10 ⁻¹² torr Radiation: At the center of the outer Van Allen belt Max. 1 x 10 ⁶ pro- tons/cm ² sec. (> 40 MeV) and 1 x 10 ⁸ elec- trons/cm ² sec.
Descent	Max 10.8 g along the thrust axis (retro- rocket)	Along any axes; Combined 100-1500 Hz, 2 g peak sin- usoidal and 0.2 g rms white Gaussian for a maximum time of 50 sec.	Same as in Transit Phase	Shock: Sawtooth Accelera- tion pulse of 5 g magnitude and a duration of ~ 300 milliseconds

(d) Description of Descent Profile

Details of the terminal descent profile are outlined below and consolidated in Table 3-2:

The relative speed of approach to the moon at the slant range of about 60 miles is about 9000 fps. At the 60 miles slant range, the altitude marking radar (AMR) generates a trigger signal. The following sequence of events then occurs: (1) After a delay commanded into Flight Control Programmer storage, the vernier engines are ignited; (2) one second (nominally) later the main retro rocket engine is ignited; (3) about one half second later, power is supplied to RADVS.

During the retrophase, the S/C attitude remains fixed and the S/C is in the inertial mode. The RADVS altitude, velocity, and reflectivity data are telemetered back to earth. Control of attitude is fulfilled using the vernier engines. Roll control is obtained by swivelling one of the vernier engines about a radial line perpendicular to the roll axis. The retro-rocket thrust slowly increases until a certain point after which it rapidly decreases. When the acceleration reaches a nominal value of 3.5 g, an inertia switch provides a signal to the Flight Control Programmer (FCP) to initiate the retro-rocket separation sequence. The thrust level of the verniers is increased to the maximum programmed level. After a fixed time delay (to allow the retrorocket thrust to be reduced to a negligible value), the retro-separation units are blown apart. After another delay to permit the retro-rocket engine to clear the S/C, the FCP provides an arming signal which enables transfer of yaw and pitch control to the doppler reference if the RODVS signal is present. Otherwise, the S/C will remain in the inertial mode until the signal appears. In the time before RODVS is present and in any case before reaching the optimum (fuel-wise) descent curve, the vernier engine thrust is servoed to maintain a constant thrust-to-mass ratio equivalent to 0.9 lunar g. The burnout condition must be within the operational ranges of the doppler sensors. The doppler radars are required to operate within the desired accuracy only for velocity smaller than 850 fps.

When the optimum descent trajectory is reached, the thrust is controlled to bring the vehicle down the desired range-velocity curve. At 1000 feet, a signal from the radar altimeter will change the Doppler System scale factor.

At a speed of 10 fps the thrust control is switched to the doppler velocity reference. A constant velocity of nominally 5 fps is commanded, and the pitch and yaw control is switched to the inertial hold mode.

A signal from the radar altimeter shuts off the vernier engines at an altitude of 14 feet. The RADVS is turned off after landing.

Table 3-2. Chronological sequence of events during the descent phase

EVENTS AND CONDITIONS	RADVS REQ'T
<ol style="list-style-type: none"> 1. AMR on 2. Vernier Engine Ignition 3. Main Retro Ignition (Vehicle attitude relative to the lunar verticle not to exceed 45°. Attitude at acquisition not to exceed 25° for engineering missions, 45° for scientific missions. Max. slant range for acquisition, 50 kft. Static acceleration not to exceed 380 ft/sec^2. Velocity magnitude is +3000 to 100 fps.) 4. Main Retro Motor Burnout (BO) 5. Main Retro Casing Separation (12 sec after BO) (Vehicle Static Accelerations along the vehicle roll axis not to exceed 12 ft/sec^2. Max velocity is 850 ft/sec.) 6. Inertial Mode at 10 fps velocity mark. 7. Verniers off at 14 ft mark. 8. Landing 	<p>Inactive</p> <p style="text-align: center;">↓</p> <p>turn-on 0.55 sec after retro ignition (acquire when possible)</p> <p style="text-align: center;">↓</p> <p>RADVS control enable after 3 sec.</p> <p>RADVS Descent Control</p> <p style="text-align: center;">↓</p> <p>Generate 14 ft mark</p> <p>RADVS off</p>

C. SUMMARY OF RADVS CHARACTERISTICS

The antenna and beam configuration of the RADVS is shown in Fig. 3-1, looking downward from above the spacecraft. Fig. 3-2 shows an overall, simplified block diagram of this sub-system. Because of the similarity of the four frequency trackers, only one of the DVS channels will be described here.

Referring to Fig. 3-3, each DVS receive channel is split into two quadrature channels, $P_1 / 0^{\circ}$ and $P_1 / 90^{\circ}$ for Beam 1, in order to retain doppler sense of received signals. The two doppler signals are then passed through separate but balanced preamplifiers, one of which is shown in Fig. 3-3. The signal contained in the entire doppler band (100 Hz - 100 kHz) is used to control the gain-state of the preamplifier (i.e., whether the P_1 signals are taken from the 40 db, 65 db, or 90 db gate). These gain-state switches keep the output signals within a limited dynamic range (maximum signal approximately 33 db above the acquisition threshold). Major characteristics of this portion of RADVS are summarized in Table 3-3.

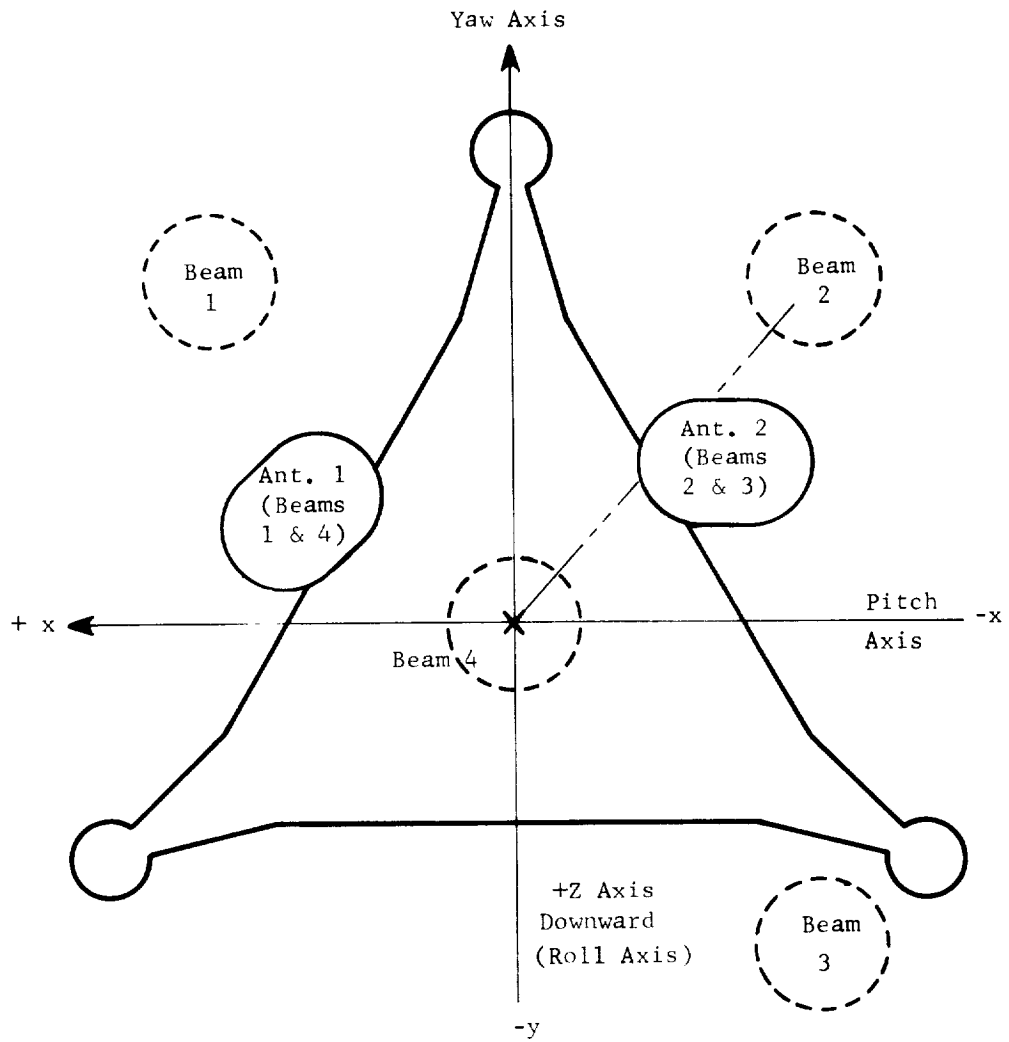
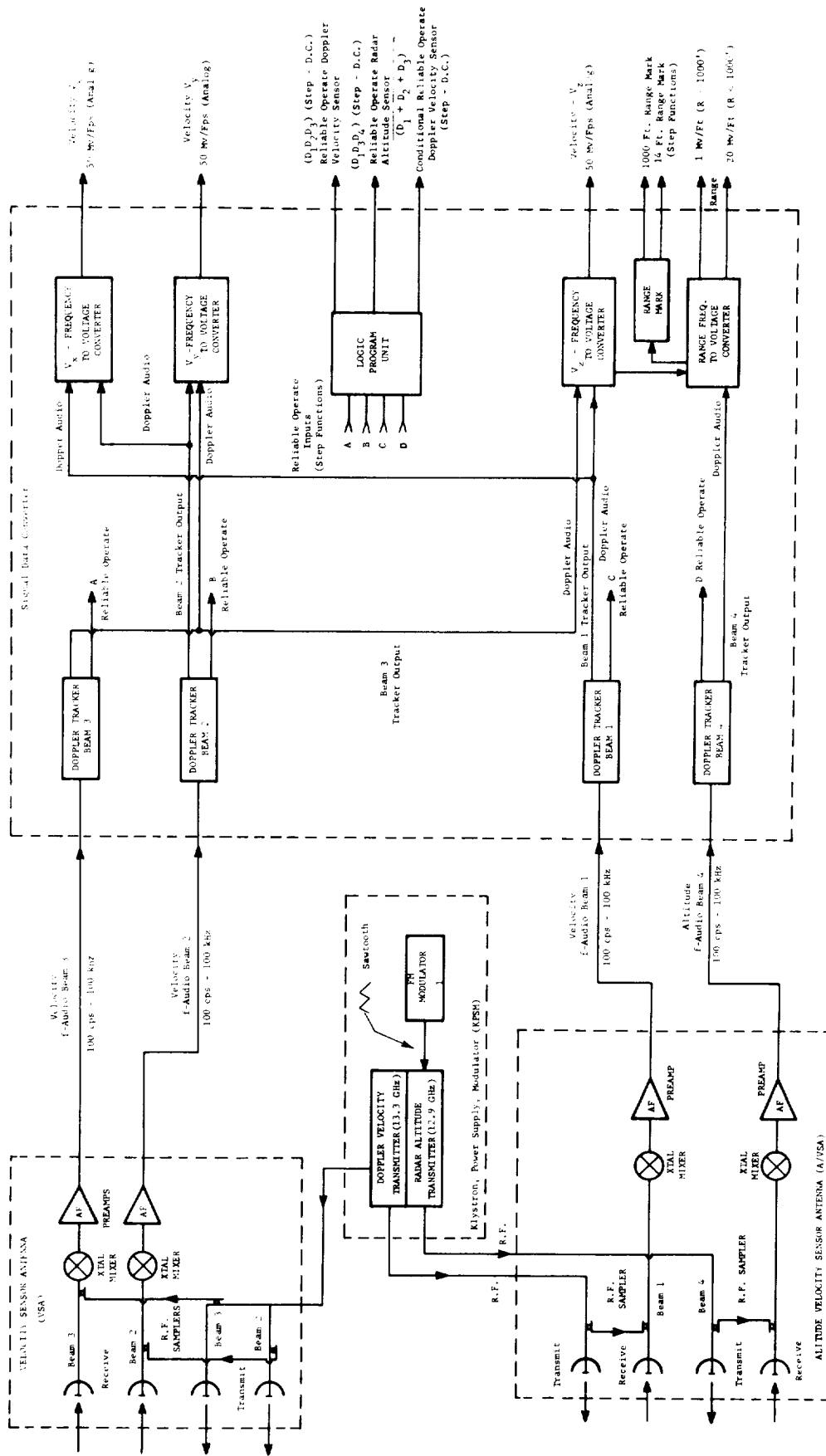


Fig. 3-1. Antenna and beam configuration, RADVS.
 (Z-axis points downward into plane of paper.)



Velocity
Slant Range
Altitude Angle

Operational Characteristics
Velocity Sensor

Altitude Sensor

FIG. 3-2. RAUOS Block Diagram.

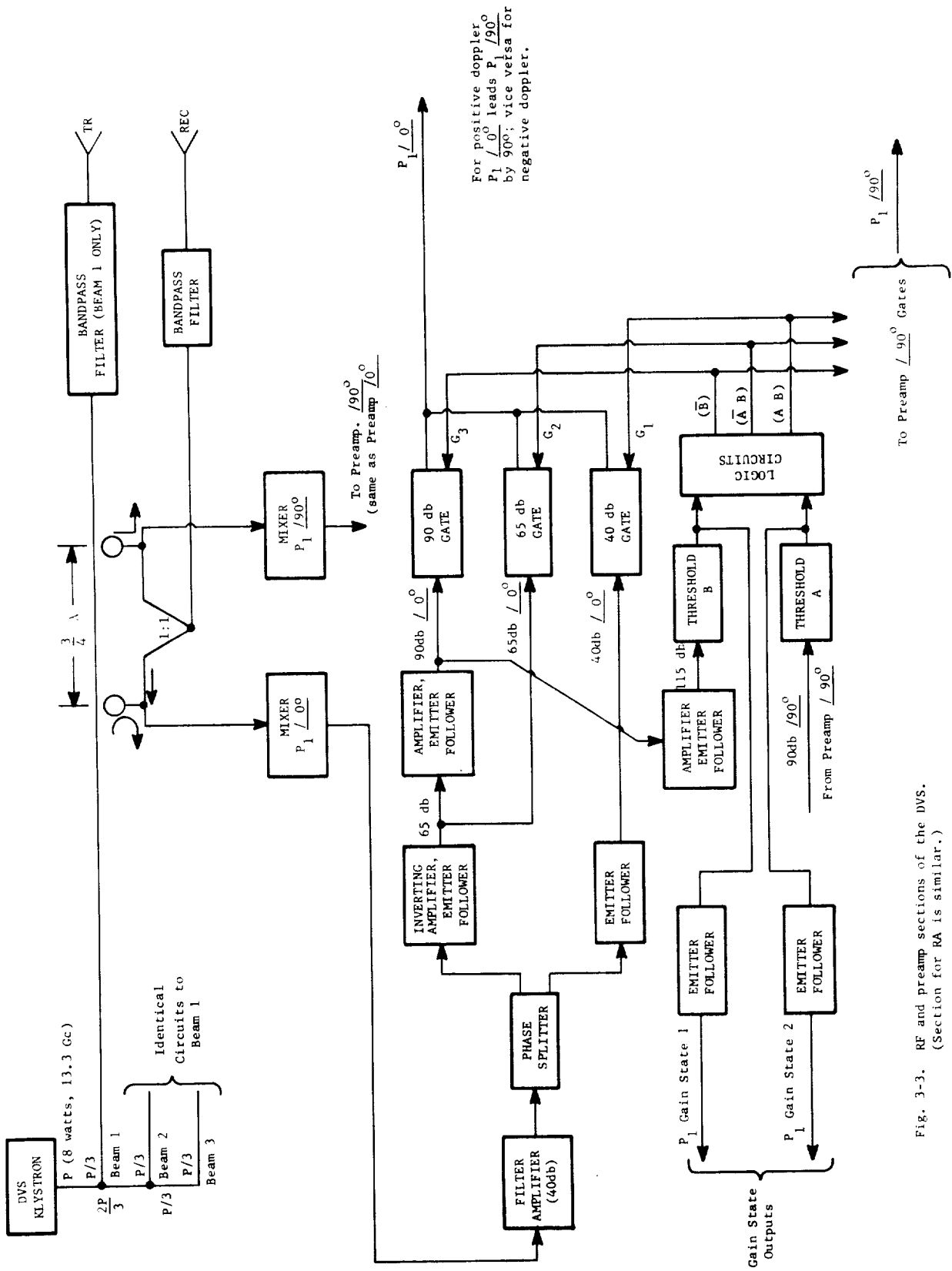


Fig. 3-3. RF and preamp sections of the DVS. (Section for RA is similar.)

Table 3-3. Major characteristics of RADVS
RF and preamplifier

Beam Configuration	— See Fig. 3-1 for antenna-spacecraft relationship
DVS Beams	— 25° off + Z axis
RA Beam	— along + Z axis
DVS Klystron	— 2.0 watts (per beam) 13.3 GHz
RA Klystron	— 250 milliwatts, 12.9 GHz
RF Filters	— To reject spurious components from RADVS transmitters and other on-board equipment. Additional filter in Beam 1 receiver because it shares antenna with altimeter.
Isolators	— One used with each of four mixers to help maintain mixer balance.
Mixers	— Balanced mixers used in altimeter in order to reject local oscillator AM caused by FM sweep; single-ended mixers used in DVS.
Preamplifiers	— Upper cut-off — 100 kHz
Low-frequency roll-off	
Velocity channels — 3 kHz corner frequency, 6 db/octave roll-off in 40 and 65 db gain states; a second corner frequency at 1.2 kHz gives 12 db/octave roll-off in 90 db gain state.	
Altimeter channels — same as above but with 30 kHz and 5 kHz corner frequencies.	
Gain-State-Switches	— Time constant ≈ 0.2 sec Hysteresis ≈ 1 db

One of the DVS frequency trackers is illustrated in Fig. 3-4. The SSBM consists of a pair of balanced modulators phased in such a way that the lower sidebands of outputs 1 and 2 reinforce for positive-doppler inputs and their upper sidebands cancel; negative-doppler inputs produce the opposite effect. This permits rejection of negative-doppler signals during search by use of a limited range of frequency search, as explained below.

The IF amplifier provides a 10 kHz "window" about the VCO frequency; the IF output is used to provide reflectivity data, as well as for frequency tracking. The two quadrature channels between the IF amplifier and the discriminator provide sensing of frequency errors between the input signal spectra and f_c from the crystal oscillator. During the track mode, the discriminator output is applied to an integrator which controls the VCO frequency to drive the tracking error to zero.

The search mode is initiated by application of a 0.1 second "flyback" pulse to the integrator circuit. Discharge of the integrator capacitor sweeps the VCO downward in frequency until the sweep-limit switch is activated at $f_c + 800$ Hz. (The lower limit for the RA is $f_c + 2$ kHz.) Another flyback pulse is then generated which returns the VCO frequency to the upper sweep limit. The important parameters of the sweep operation are (approximately):

Start Sweep Frequencies:

DVS, before burnout:	85 kHz	RA, above 1kft range:	91.5 kHz
after burnout:	26.5 kHz	below 1kft range:	22.5 kHz

Search Rates:

60 kHz/sec for wide sweeps, 15 kHz/sec for narrow sweeps

Search ceases whenever the signal passing through the tracker low-pass filter has sufficient strength to exceed the threshold circuit level. If track continues for at least 0.1 sec., the tracker output is applied to the analog converters by "Doppler Gate" circuits. (The RA tracker does not have this delayed gate feature).

The data conversion section contains additional circuitry for beams 2 and 3 which unlocks either tracker if it appears to be locked onto the same echo as the other (through a sidelobe). This circuitry, which is termed the "cross-coupled lobe logic," was based on the original belief that sidelobe coupling would cause mainbeam signals in one channel to exceed corresponding cross-coupled sidelobe

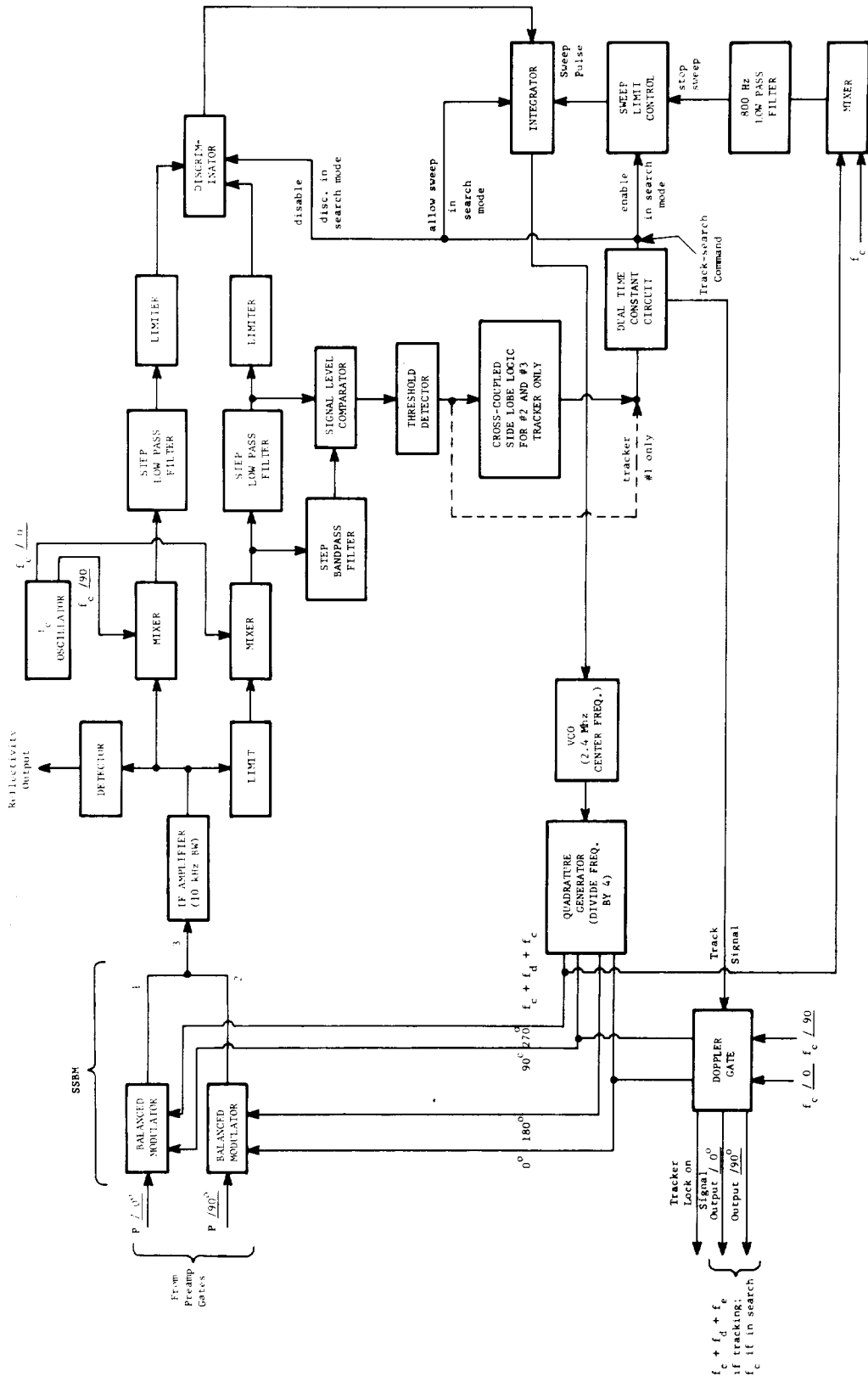


FIG. 3-4. Frequency tracker, simplified block diagram.

signals in the other channel by at least 30 db, and that the two signals would have essentially the same frequency. It was originally employed only between beams 2 and 3 in the belief that no trouble would be experienced between the other beams. Subsequent measurements and analyses have shown this not to be true, and the present approach is to analyze each mission and avoid the difficulty by selection of roll angle, if this proves to be possible. Other solutions are under consideration.

Analog velocity estimates are provided by the following relationships

$$\tilde{V}_x = \frac{\tilde{V}_1 - \tilde{V}_2}{2A} ; \tilde{V}_y = \frac{\tilde{V}_2 - \tilde{V}_3}{2A} ; \tilde{V}_z = \frac{\tilde{V}_1 + \tilde{V}_3}{2B}$$

where $\tilde{V}_i = \frac{\lambda}{2} f_{di} = \frac{\lambda}{2} (f_{VCOi} - f_c)$

$$A = \sin 45^\circ \sin 25^\circ = 0.30$$

$$B = \cos 25^\circ = 0.91$$

These computations are performed in a straightforward manner by using the DVS VCO outputs. Beam 3 VCO output frequency is subtracted from $2f_c$; then the Beam 2 VCO output frequency is subtracted from the resultant to give a digital measure of V_z . A frequency counter, coupled with an appropriate calibration constant, then gives analog V_z . Beams 2 and 3 VCO's are used to obtain V_y ; velocity sense is obtained by using dual quadrature channels, with analog velocity being obtained directly from the sign-sensing circuit. Similarly, Beams 1 and 2 VCO's are used to obtain analog V_x .

Slant range is obtained from Beam 4 VCO. The frequency of this VCO is beat against f_c (sense is always positive), and a frequency-analog conversion is made by a frequency-counting circuit. An analog measure of V_z is subtracted from this output to obtain a measure of slant range.

Other RADVS outputs are summarized in Table 3-4.

D. OUTLINE OF ANTICIPATED RADVS OPERATIONAL PROBLEMS

The major anticipated problems of RADVS operation and testing result from the CW nature of the radar and the unusual environmental conditions arising during lunar descent. Operational problems can arise because of the transmitter-receiver leakage problem, which is inherent to the CW class of radars. A major aspect of this leakage problem is the fact that it would probably cause no serious operational difficulty if it were not greatly aggravated by the environmental conditions existing

Table 3-4. Other RADVS outputs

Range Marks -- 1000 foot mark and 14 foot mark generated by comparing analog slant range and zener references. Altitude scale is changed at 1000 feet by change in FM deviation (4 Mc to 40 Mc) and by 2:1 change in analog circuits.

CRODVS (conditional reliable operate doppler-velocity sensor)-- generated by "or" circuit with Beams 1, 2, and 3 lock-on signals. Used with RODVS into "or" gate to give RODVS output. Once RODVS signal has been generated due to all beams locking, the CRODVS signal is gated out (after one second delay).

RODVS (reliable operate doppler-velocity sensor) -- generated by "and" circuit with lock signals from all three velocity beams, feeding "or" circuit with CRODVS signal. Used to switch system to RADVS control, once the initial cycle of operate under CRODVS has occurred.

RORA (reliable operate radar altimeter) -- generated by "and" circuit with lock signals from Beams 1, 3, and 4.

at the time of lunar descent. The instabilities induced on the transmitters and on the leakage paths by retro and vernier engine vibration and by rocket plumes are the major contributors to the leakage problem. As can easily be imagined, these unusual environmental conditions make it difficult to test RADVS under realistic conditions. The operational problem caused by leakage is one of false-signal lock-on; the false signals arise from modulation on the composite leakage signal entering the pre-amplifier. The most difficult modulation to correct is that on RF leakage paths; however, other sources can introduce serious problems (e.g., vibration effects on the RF mixer which may modulate the leakage signal at frequencies up to several kHz). It is expected that most such spurious signals will fall in the doppler band below 10 kHz.

Other forms of false-signal lock can also occur. One cause could be passage of the ejected retro tankage through one of the mainbeams. Although reflections from this source will have negative doppler, its radar cross section is so large that the negative-doppler rejection capability of the receiver may not be adequate; note that this capability is critically dependent upon the match between the pre-amplifiers of a given channel. A second effect caused by passage of the retro tankage through a mainbeam would be to reduce the gain-state of the corresponding preamplifiers, in effect blinding the particular channel to weaker ground-reflected signals. False lock can also be caused by cross-coupled sidelobe signals. These signals result from transmission on one mainbeam and reception on a sidelobe of an alternate beam. This problem can become very severe for large lunar approach angles.

Another type of problem which can occur is referred to as the "coherence-loss" problem. This problem becomes increasingly serious at the higher altitudes. Frequency modulation of the klystron transmitters will cause a frequency beam between time-delayed echoes and the klystron reference signal to appear on pre-amplifier signals. This beam will cause spectral lines to appear in the doppler band. In addition, serious spectral spreading of the preamplifier signal can result, with subsequent loss in acquisition sensitivity and in frequency tracking ability. Causes of the FM are microphonic vibrations in the klystron resonant structure and ripple on the klystron power supply.

Both AM and FM on the klystron output can pose serious problems. The effects of AM, however, can be removed effectively by the use of balanced mixers. In order for the AM to produce serious spectral spreading of ground-reflected signals, the

depth of modulation must be several per cent; such severe cases would seldom be encountered, and if they were the accompanying FM would usually cause a much more serious effect than the AM.

Another class of problems which should be considered in evaluating this test program is referred to as adaptive control errors. This is concerned with the fact that certain RADVS parameters are programmed as a function of the position in a series of events which make up the landing sequence. For example, at the generation of the 1000 foot mark the RA klystron deviation is changed by a factor of 10. Simultaneously, the analog scale factor is changed. Similarly, the 14 foot mark is used to shut off the vernier engines to permit free fall for the remainder of the flight. Obviously, failure to perform these adaptive measures at the proper time could result in mission failure.

E. OUTLINE OF RADVS FUNCTIONAL DETAILS

Proper operation under various environmental and dynamic conditions requires successful serial/parallel functioning of the many modules within the RADVS units. Consideration of all of the required processes is necessary in any thorough testing program. For completeness of the present study, therefore, modules have been separated into functional groups which are the fundamental elements of operational sequences; these are listed in Table 3-5 along with information necessary to help define tests.

Table 3-5 will be used and analyzed in later report sections, but certain features should be noted here. First, the choice of grouping is not meant to imply that each group functions (or will need to be tested) individually. Instead, the intent is to group important characteristics which must not be overlooked in defining tests. For example, thorough examination of the klystrons' outputs also gives adequate information about power supply and modulator operation; however, the definition of "thorough" must be based upon the characteristics listed for the power supply and modulator sub-units.

It is also important to understand that the numerical values given in Table 3-5 are not necessarily performance requirements. In fact, most of them are adjusted as the system is better understood and refined. The values given in the table are mainly for reference; the only real criterion of successful performance must be based on system functional requirements.

Regular unit connectors are listed as test access points in Table 3-5 whenever possible. Otherwise, module test points (TP) are given. Only unit connector points will be available, however, in most tests.

Abbreviations used in the table are listed below:

BAL	balanced	LVPS	low voltage power supply
BP	band pass	NOM	nominal
BW	bandwidth	QUAD	quadrature
CKT	circuit	RA	radar altimeter
DET	detector	RCVD	received
DISC	discriminator	R/T	receive/transmit
DTC	dual time constant	SDC	Signal Data Converter
DVS	doppler velocity sensor	TKR	tracker
HV	high voltage	VCO	voltage controlled oscillator
KPSM	klystron power supply and modulator	XMT	transmit
LP	low pass		

Table 3-5. Outline of RADVS functional details.

MODULE GROUP	UNIT	MAIN FUNCTIONS	MAIN PERFORMANCE CHARACTERISTICS	TEST ACCESS PTS
1. HV PWR Supply HV Converter; Filament Converter & Reg.	KPSM	1. Apply regulated filament voltage upon turn-on 2. Delay 20 sec. & apply regulated HV to klystrons	1. Ripple & stability of HV & Filament supplies 2. Sufficient delay of HV application to inhibit tube noise	---
	KPSM	1. Provide linear sawtooth modulating voltage for RA klystron. 2. Change sawtooth amplitude upon deviation control signal. 3. Provide blanking signal for altimeter tracker during "Flyback".	1. Sawtooth waveshape stability 2. Sawtooth timing 3. Blanking signal amplitude and timing	---
2. Klystron Modulator	KPSM	1. Provide transmitted signals for RADVS	1. Sweep linearity for RA klystron 2. Short term freq. stability (coherence) 3. Amplitude modulation 4. Other spurious outputs 5. EMI 6. Power output 7. Frequency	---
3. Klystrons	KPSM	1. Provide transmitted signals for RADVS	1. Sweep linearity for RA klystron 2. Short term freq. stability (coherence) 3. Amplitude modulation 4. Other spurious outputs 5. EMI 6. Power output 7. Frequency	mainly at XMT Feed-horns
4. R/T Feedhorns & Reflectors	R/T	1. Transmit & receive RADVS signals	1. Antenna patterns 2. Transmitter-receiver leakage 3. Insertion loss/VSWR	---
5. Dual detectors (balanced for RA); preamps	R/T	1. Mix RCVD signal with XMT signal two places (with 90° phase difference). 2. Filter through difference frequency mixing component. 3. Provide outputs at amplifications 40 db, 65 db, & 90 db for DVS or 40 db, 60 db, and 80 db for RA.	1. Receiver noise figure ~26 to 15 db 2. Balance of gains & phases between / 0° and / 90° branches of each channel 3. Gain stability 4. Passband shape: 100 kHz BW (nominal); 6 db/oct rolloff at 30 kHz for RA; 6db/oct rolloff at 3kHz for DVS; additional 6db/oct at 1.2 kHz for DVS and 5 kHz for RA in highest gain state. 5. Spurious outputs	None Direct --See Group 6

Table 3-5. Continued

MODULE GROUP	UNIT	MAIN FUNCTIONS	MAIN PERFORMANCE CHARACTERISTICS		TEST ACCESS PTS
6. Threshold detectors and Logic; gate matrices	R/T	<ol style="list-style-type: none"> 1. Yield two signal-threshold outputs for each channel, 25 db apart. 2. Logically process threshold outputs to determine signal amplitude state in each channel. 3. Use logic outputs to gate through the preamp output which is in 10 mv-250mv range for each channel. 	<ol style="list-style-type: none"> 1. Threshold accuracy 2. Amplitude & phase 3. Threshold hysteresis 4. Selection of proper outputs 5. Balance of the /0° & /90° branches for each channel 	39/40P01 39/40P01 39/40P01	
	SDC	<ol style="list-style-type: none"> 1. Supply regulated ± 100 VDC and ± 25 VDC to RADVS modules over a supply variation of 16.5 to 26.0 VDC 	<ol style="list-style-type: none"> 1. Regulation 2. Ripple 	37J13 37J13	
8. Balanced Modulators; IF Amplifier	SDC (TKR)	<ol style="list-style-type: none"> 1. Heterodyne the two preamp outputs of each channel with tracking loop VCO's such that range and positive doppler signals contribute only to the lower sideband and the carrier is eliminated. 2. Pass mixing product components in a band about freq. $f_c = 600$ kHz. 	<ol style="list-style-type: none"> 1. Degree of extraneous sideband and carrier elimination 2. Other spurious outputs 3. Passband shape: 10 kHz BW at 600 kHz; max. gain ~ 30 db. 4. Gain stability 	TP-5 TP-5 TP-6 TP-6	
	SDC (TKR)	<ol style="list-style-type: none"> 1. Isolate & detect IF output for telemetry 	<ol style="list-style-type: none"> 1. Gain stability 2. Ripple 	37J06 37J06	
10. IF Gate Generator; IF Gate	SDC (RA TKR only)	<ol style="list-style-type: none"> 1. Cutoff (blank) the IF output during the blanking pulse interval (flyback). 	<ol style="list-style-type: none"> 1. Amount of attenuation during blanking period 2. Stability & linearity during non-blanking period 	None Direct --See Group 11	
	SDC (TKR)	<ol style="list-style-type: none"> 1. "Lower" the IF output in freq. by f_c and divide into two quadrature branches. 2. Filter both branches by LP filters of 1.5 kHz BW, stepped to 300 Hz after retro separation gate (DVS), 2 kHz BW stepped to 300 Hz after deviation signal (RA). 	<ol style="list-style-type: none"> 1. Gain & passband shapes 2. Relative phasing of the two branches 3. Proper filter switching when commanded. 	TP-7/ & TP-8 TP-7/ & TP-8 (37J05, 6-one branch on DVS #2 & #3 only)	

Table 3-5. Continued

MODULE GROUP	UNIT	MAIN FUNCTIONS	MAIN PERFORMANCE CHARACTERISTICS	TEST ACCESS PTS
12. Limiters; Frequency Discriminator	SDC (TKR)	<ol style="list-style-type: none"> Provide a pulse train output at a freq. and polarity determined by the freq. difference between the IF output and f_c when "track" command given. No output during "search." 	<ol style="list-style-type: none"> Symmetry for positive & negative freq. differences. Ability to follow track-search command Bandwidth of operation. Gain stability 	TP-15 TP-15 TP-15 TP-15
13. Sweep Control Switch & Integrator; Sweep Limit Switch; VCO; Quadrature Generator; Isolation Amplifier	SDC (TKR)	<ol style="list-style-type: none"> Provide 4 VCO outputs separated in phase by 90°. In track mode: integrate freq. disc. output & apply to VCO (with dither for RA after deviation signal). In search mode: for DVS, sweep VCO from $f_c + 82 \text{ kHz}$ to $f_c + 800 \text{ Hz}$ before separation signal, $f_c + 22 \text{ kHz}$ to $f_c + 800 \text{ Hz}$ after; for RA, sweep VCO from $f_c + 90 \text{ kHz}$ to $f_c + 2 \text{ kHz}$ before deviation signal, $f_c + 22 \text{ kHz}$ to $f_c + 2 \text{ kHz}$ after. 	<ol style="list-style-type: none"> VCO frequency stability. VCO gain Search sweep starting points and rates Integrator time constant in track mode. 	TP-21 TP-21 TP-9 37J04 5,6,7 TP-21
14. Step BP Filter; Differential Threshold Detector.	SDC (TKR)	<ol style="list-style-type: none"> In med. & low preamp gain states, yield an output when the preamp output is greater than 8 mv. In high preamp gain state: give output when LP filter output exceeds noise sample by about 9 db for DVS, 3 db for RA. Provide noise sample from 2 kHz BW at 6 kHz (for RA), 1.4 kHz BW at 4 kHz before separation signal and 600 Hz BW at 1.4 kHz after separation (for DVS). 	<ol style="list-style-type: none"> Noise sampling filter passband shape & location. Proper filter switching when commanded. Accuracy of threshold det. outputs. 	TP-16 TP-16 37J04, 5, 6 for DVS only
15. Dual Time Constant Circuit; Doppler Gate	SDC (DVS TKR only)	<ol style="list-style-type: none"> Give track command when DTC signal received. Give D-lockon signal (which changes TKR output from f_c to VCO) 0.1 sec. after DTC signal. Remove track command and D-lockon signal 0.2 sec. after DTC signal ceases. 	<ol style="list-style-type: none"> Relative phases of the $/0^\circ$ and $/90^\circ$ outputs of each tracker. Timing of functions. 	37J04, 5,6 TP-22 37J04, 5,6 ---
16. Time Delay Switch	SDC (RA TKR only)	<ol style="list-style-type: none"> Delay signal to change filter BW until 2 sec. after deviation signal is given. 	<ol style="list-style-type: none"> Delay time 	---

Table 3-5. Continued

MODULE GROUP	UNIT	MAIN FUNCTIONS	MAIN PERFORMANCE CHARACTERISTICS		TEST ACCESS PTS	
17. Velocity & Altimeter Converters	SDC	1. Convert the trackers' outputs to analog velocity and altitude signals.	1. Accuracy 2. Linearity 3. Drift Stability 4. Ripple amplitude	} 37J02, 9, 11, 12		
	SDC	1. Generate 13 ft. and 1000 ft. range marks in absence of marker inhibit signal. 2. Provide a deviation control signal at 1000 feet.	1. Accuracy of mark points 2. Susceptibility to false mark.		37P01 37J02	
19. Reliability Circuit; Conditional Reliability Circuit.	SDC	1. Give output (RODVS) initially when at least one DVS lockon signal is given; after they first appear simultaneously for 1 sec., give RODVS only when all 3 are present. 2. Give output (RORA) whenever trackers 1,3, & 4 are locked simultaneously. 3. Give output (CRODVS) from initial lockup until all DVS trackers stay locked simultaneously for 1 sec. 4. Inhibit markers until 3 sec. after RORA. 5. Inhibit RODVS and RORA until 1 sec. after low voltage is applied. 6. Give latched output (separation gate) about 3 sec. after burnout signal.	1. Logic operations 2. Delay times 3. Output Amplitudes	} 37J02 37J09		
	SDC	1. Provide basic f_c freq. at $/0^\circ$ and $/90^\circ$ 2. Provide $2 f_c$ signal	1. Freq. stability 2. Relative phase stability of outputs		37J09 37J09	
	SDC	1. Yield dual time constant (DTC) ckt input signals for trackers #2 & #3 whenever they are tracking doppler signals which either differ in freq. by more than 100 Hz or in amplitude by less than 30 db.	1. Logic operation 2. Threshold accuracy, stability, hysteresis		37J08 37J08	
	SDC	1. Carry transmit signals from KPSM to R/I units. 2. Split power for DVS beams 3. Isolation of beams.	1. Integrity of connections 2. Attenuation 3. Power splitting and isolation performance		XMT Feedhorns	
	20. Reference frequency generator	SDC	1. Provide basic f_c freq. at $/0^\circ$ and $/90^\circ$ 2. Provide $2 f_c$ signal		1. Freq. stability 2. Relative phase stability of outputs	37J09 37J09
	21. Cross-Coupled Lobe Logic	SDC	1. Yield dual time constant (DTC) ckt input signals for trackers #2 & #3 whenever they are tracking doppler signals which either differ in freq. by more than 100 Hz or in amplitude by less than 30 db.		1. Logic operation 2. Threshold accuracy, stability, hysteresis	37J08 37J08
22. Waveguide Assembly	—	1. Carry transmit signals from KPSM to R/I units. 2. Split power for DVS beams 3. Isolation of beams.	1. Integrity of connections 2. Attenuation 3. Power splitting and isolation performance	XMT Feedhorns		

IV. "DESIRABLE" TEST PROGRAM DESCRIPTION

A. PHILOSOPHY OF A "DESIRABLE" TEST PROGRAM

1. Introduction

The following discussion summarizes a testing philosophy, typical of one which might have been generated at the outset of the Surveyor Program. In fact, RTI has attempted to base the testing philosophy on only a knowledge of the RADVS mission requirements and its performance characteristics, while remaining unbiased by a knowledge of the actual test program now in effect. In order to best do this, the write-up was prepared immediately after RTI personnel had finished the initial orientation period at JPL, at which time the team had become familiar with the RADVS system and the mission profile. Although they had been briefly exposed to the general nature of the test program, they had not acquired a detailed knowledge of it. It should, of course, come as no great surprise that the philosophy described below is not greatly different from that of the test program now in effect because the basic principles of a test program are quite fundamental. Differences between the RTI suggestions for desirable tests and those actually being performed are expected to become more apparent as a more detailed description of the former is given.

2. General Considerations

Any test program which does not duplicate exactly the actual operating conditions will always be viewed with suspicion. In fact, all military and space programs allow some margin for unanticipated problems to be encountered during early tests under actual operating conditions. Obviously, the acceptable margin must be weighed carefully against penalties which may result from partial or complete failure. It is an unfortunate fact that any pre-flight test program for space research vehicles cannot be completely realistic. Some degree of risk in the capability of a test program to detect and prevent operational failures of a vehicle must be accepted, not just because of unpredictable part failures but also because of the impracticality of realistic simulation of actual operational conditions.

Although the point made above may be so obvious to appear trivial, it leads to what is believed to be some important conclusions:

- (1) some lack of realism in a pre-operational test program for space vehicles must be accepted;
- (2) numerical estimates of the confidence levels which may be assigned to certain portions of testing programs are rather

meaningless; the relative merits of many aspects of different test programs, or in modifications to a given program, are based on scientific and engineering judgements which are open to debate.

The overall test program philosophy described below in broad terms is intended to represent a good compromise between complete and realistic testing and costs (in dollars and schedule).

For further discussion, it is useful to consider test phases as corresponding to the major divisions of the RADVS delivery program. Such test classifications would be as follows:

- (1) Special tests (design verification)
- (2) Unit tests (unit construction verification)
- (3) Vendor system tests (system assembly verification)
- (4) Buyer system tests on S/C (installation verification)
- (5) Prelaunch system tests on S/C (launch configuration verification)

The first of these phases would consist of special tests to determine whether problems were inherent in the basic system design coupled with the environmental conditions and all of the anticipated descent profiles. The results of such special tests could of course range from re-design, through the imposition of individual test requirements on each RADVS (if tests reveal marginal conditions), to the conclusion that no comparable testing of each RADVS is necessary (if tests reveal that no problems are likely to be incurred). The remaining phases would be fundamental to the preparation of every flight system; they might be termed "flight-readiness" test phases.

3. Special Tests

The basic task of special tests is to yield enough information about system operation to permit much simpler testing of flight systems. This implies functional testing under as realistic conditions as practical. The degree of realism desired is made evident by noting the problems expected for the intended application.

As indicated previously, the interaction between environmental conditions and radiation performance characteristics is particularly strong for CW radar systems. The nature of the transmitter-receiver leakage signal is very much dependent upon the environmental conditions. The need for operation of the velocity and range sensors simultaneously with vernier engine operation poses the most difficult RADVS testing problem, and possibly the most difficult operational problem.

There are several reasons why realistic tests (exclusive of the actual operational flight) involving both environmental and radiating conditions cannot be conducted on spacecraft which are intended to be flown:

- (1) any low altitude operation of the S/C mounted in its upright position would be seriously hampered, and quite possibly invalidated, by the presence of strong ground reflections;
- (2) firing the vernier engines during such tests is quite impractical because of contamination of S/C surfaces and components;
- (3) mounting the assembled S/C in an inverted position, in order to avoid ground effects, is undesirable because of handling problems (with the possibility of damaging the system), and because of difficulties in operating the vernier engines in this position; and
- (4) the vacuum conditions existing on the moon are difficult to simulate in the earth's environment under conditions also permitting firing the vernier engines.

The conclusion to be drawn from these considerations is that realistic testing of the environmental interaction with radiating performance is impractical for an assembled flight spacecraft. This interaction may be very important, however, and it is very desirable that any significant degradation of system performance which it causes be evaluated and corrected, if necessary. It may be possible to do this with a special "one-time" test performed on a mock-up S/C containing a partial RADVS system and one or more vernier engines. Experimental evidence that no serious problem exists because of vernier engine effects on transmitter-receiver leakage would obviously be extremely valuable in establishing a high level of confidence in the capability of the RADVS to play its role in soft landing, without the need for evaluating these effects on each S/C. On the other hand, experimental evidence of the existence of a serious problem, or of a marginal situation, would indicate the need for corrective action; after such action the experimental set up could be used for evaluating its effectiveness.

4. Unit Tests

These tests are defined as those which can be performed on the units of RADVS under laboratory conditions and under simulated environmental conditions (temperature, vacuum, vibration, etc.). Except for large mechanical units and active electromagnetic radiating units, testing under simulated conditions should present no serious problems. The nature of RADVS would indicate that testing the electrical properties of the antennas under realistic environmental conditions would present the major difficulty in the unit tests. It may, of course, be

desirable to forego parts of such tests entirely, checking certain antenna characteristics in conjunction with other units during system tests. For example, for a RADVS antenna which has been proven to be of sound mechanical design, it is believed to be unnecessary to check the antenna pattern characteristics under varying temperature and vacuum conditions. However, it would be desirable to test the antenna match and transmitter-receiver leakage during vibration.

The major purpose of the unit tests should be to establish that each unit fulfills its design requirements and to yield confidence of successful future operation as a system.

5. Vendor System Tests (Ryan)

If the unit tests have been performed very thoroughly, the only requirement of system tests is to assure proper mating of units. Such tests are preferably made at the vendor (Ryan) than at the buyer (Hughes) because it is easier to accomplish fixes at the former. Duplication of these tests with the system installed on the S/C would be desirable, however, for added assurance.

Unfortunately, the possibility of sufficiently thorough unit tests is unlikely because of difficulties in simulating all signals and all environments for each unit. Particular problems are expected to be:

- (1) simulation of structural resonances of the S/C frame in vibration;
- (2) simulation of electromagnetic interference effects without connecting all components to the S/C; and
- (3) simulation of the thermal environment which exists when the only form of heat transfer between the surroundings and the S/C is radiative.

Since none of these environment-simulation problems can be completely solved without installing the system on a S/C, much of the potential usefulness of system tests at Ryan is lost.

Consideration of these different aspects leads to concluding that vendor system tests should be primarily concerned with verifying system performance under ambient environmental conditions.

6. Buyer System Tests (Hughes)

The purpose of these tests is to check out the proper inter-marriages between RADVS and the other parts of the S/C. Full environmental testing should be made to insure proper S/C operation in its assembled state, under the severe environmental conditions to be encountered in space. Special attention should be

paid to testing those units susceptible to interference from other S/C systems (e.g., electrical noise pick-up on the klystron supply voltages).

Although it is very desirable to radiate and receive signals from the RADVS antennas, when the complexities of locating the spacecraft so that these antennas "look" through essentially free-space toward remote targets are considered, it appears that a compromise may be required, or at least may be desirable from cost and schedule standpoints. A first compromise would be to couple the RADVS antennas through feed adapters and waveguide to other antennas which could radiate toward and receive echos from special targets, such as signal repeaters which impose a doppler shift and bandwidth spreading on the re-radiated signals. In this manner, real delay is imposed upon the signals; this is quite important to testing the range measurement and klystron coherence losses. Signal bandwidth spreading is also important from the standpoint of differences in the response of the frequency trackers and the analog output circuits to actual "noiselike" signals rather than to sinusoidal signals. Of almost equal value would be tests for which delay is produced by a long length of transmission line or a delay line (suitably operated at an intermediate frequency). Bandwidth spreading could be imposed by an active circuit inserted at any convenient point in the signal path.

7. Pre-launch System Tests (Cape Kennedy)

The purpose of these tests is to check on the survival and proper operation of the S/C system after shipment and other pre-flight tests. It is desirable that the tests be of a functional nature, rather than environmental, to detect any degradation of components. An overall system test to check sensitivity and tracking is very desirable. Because of time and facility limitations, these should be relatively simple. They should be essentially a back-up of previous tests, with no basically new tests being performed.

B. "DESIRABLE" FLIGHT-READINESS TEST PROGRAM

Consideration of the stated philosophy leads to the design of two complementary testing programs, one of special tests and the other of flight readiness tests. The latter program is chosen for first study because it can be approached more systematically, and it promises to yield greater insight into system operation and testing requirement details.

A complete testing program can be generated from the foregoing information in the following steps:

- (1) inspect the RADVS Functional Details Table, Table 3-5, to determine a list of characteristics which are minimally sufficient at the

- unit level to assure successful operation.* (The practicality of all tests listed need not be considered at this point.);
- (2) do the same for the system level;
 - (3) determine which of the characteristics listed in (1) and (2) are likely to be affected by the environmental conditions described in Section III; and
 - (4) combine the results of the first three steps with considerations of test practicality and desired redundancy (for improved reliability) to obtain a practical, thorough test program. (Further modifications would be likely during actual implementation of the program.)

Assumptions about the extent of test signal realism are required before the steps listed can be undertaken. The most basic is that all units will be exercised with signals resulting from the full range of possible doppler and range signals. Other assumptions are listed below so that they can be referred to numerically as needed:

- (1) range rates, doppler rates, and spectral shapes will be realistically simulated;
- (2) a complete test with negative doppler and range will be performed;
- (3) the range signal will increase a decade in frequency during sweep return;
- (4) delay times corresponding to propagation delay from high altitudes will not be provided during normal signal simulation.

The results of the first three steps, under the above assumptions, are shown in Table 4-1. The first four environments listed are ones during which RADVS is to operate. Most of the characteristics checked in these columns are expected to be influenced by the environment; others are listed to check the system's or unit's "state of health." The last column refers to the nonoperating environment expected at launch and during transit. Requirements checked there are mainly to ascertain general "state of health." Characteristics from Table 3-5 which are not included in Table 4-1 are listed in Table 4-2 along with an indication of why they were omitted from the former table.

The last step in generation of the test program requires a statement of criteria for determining the desirable sequence. These criteria, which are mainly

* For the purposes of this program, testing below the unit level is undesirable because of the difficulty of simulating the many interconnection effects.

derived from the stated program philosophy, are listed below:

- (1) Thorough unit level testing is desirable because the analysis and correction of faults is generally less time consuming there than at the system level.
- (2) Environmental tests should be repeated with the system installed on the spacecraft because simulation of the mission environment is not likely to be very accurate during tests of individual units.
- (3) EMI tests are not likely to be meaningful at the unit level because most problems are due to interconnections and grounding of units.
- (4) Constant acceleration testing of the entire spacecraft is probably not practical.
- (5) There is no basic need for testing the complete system while not installed on the spacecraft except, perhaps, as a final reference test before leaving the vendor; such a test need not be extensive.
- (6) Stability tests are easily handled by performing pertinent tests in every phase and comparing results.
- (7) A brief prelaunch test sequence is desirable to check for damage during transit to the launch site.
- (8) Nonoperating environments are anticipated to be imposed upon the entire spacecraft in the course of testing other systems; no unit level checks are required except for increased insurance of passing later tests.

The resulting "desirable" preflight test program is given in Table 4-3. (The overall system characteristics of "warm-up time" and "power consumption" were added at this point.)

Details of performing the required tests are discussed in Sections VI and VII, where the present program and the "desired" program are compared and modifications are recommended.

Table 4-1. Minimally Sufficient Characteristics to Check during Comprehensive Testing at the Unit Level, System Level, and in the Environments Noted

Characteristics	Minimally Sufficient at the Unit Level Assuming No System Tests Are Performed	Minimally Sufficient at the System Level Assuming No Unit Tests Are Performed	Testing Environments in Addition to Lab Ambient					
			Should Test During Acceleration	Should Test During Vibration	Should Test During Temperature	Should Test During EMI	Should Test For Survival of Non-operating Environment	
KPSM								
1. Frequency Coherence	X	X		X	X		X	
2. Amplitude Modulation	X			X	X			
3. Noise & other Spurious Outputs	X			X	X		X	
4. RA Klystron Sweep Linearity & Rate	X	X		X	X			
5. Powers of Signal Outputs	X	X		X	X			X
6. Frequencies of Outputs	X			X	X			
7. Production of Stray Fields	X	X						
8. Blanking Signal Amplitude and Time	X				X			

Table 4-1. Continued

Characteristics	Minimally Sufficient at the Unit Level Assuming No System Tests Are Performed	Minimally Sufficient at the System Level Assuming No Unit Tests Are Performed	Testing Environments in Addition to Lab Ambient					
			Should Test During Acceleration	Should Test During Vibration	Should Test During Temperature	Should Test During EMI	Should Test For Survival of Non-operating Environment	
R/T UNITS								
9. Antenna Patterns	X	X						
10. Transmitter-Receiver Leakage	X							
11. Insertion Loss/VSWR	X							
12. Noise Figure	X		X	X	X			
13. Balance of Gains and Phases between /0° & /90° branches of each Channel	X				X			
14. Preamp Gain Stability with Time	X					X		
15. Preamp Passband Shape	X					X		
16. Preamp Gain Selection Accuracy & Hysteresis	X					X		
17. Spurious Outputs	X			X			X	

Table 4-1. Continued

Characteristics	Minimally Sufficient at the Unit Level Assuming No System Tests Are Performed	Minimally Sufficient at the System Level Assuming No Unit Tests Are Performed	Testing Environments in Addition to Lab Ambient					
			Should Test During Acceleration	Should Test During Vibration	Should Test During Temperature	Should Test During EMI	Should Test For Survival of Non-operating Environment	
SDC								
18. Reflectivity-output Stability & Ripple	X	X			X		X	
19. Tracker Search Ranges and Rates	X				X			
20. Signal-Tracking Threshold Operation (Sensitivity)	X	X	X	X	X		X	
21. Operation times of DIC ckts in DVS trackers	X	X						
22. Delay time between Deviation Signal and LPF BW change in RA Tracker	X	X			X			
23. Analog Output Accuracy, Linearity, Drift Stability, Ripple & Noise	X	X	X	X	X		X	X
24. Range Mark Accuracies and Susceptibility to False Marks	X	X	X	X	X		X	

Table 4-1. Continued

Characteristics	Minimally Sufficient at the Unit Level Assuming No System Tests Are Performed	Minimally Sufficient at the System Level Assuming No Unit Tests Are Performed	Testing Environments in Addition to Lab Ambient					
			Should Test During Acceleration	Should Test During Vibration	Should Test During Temperature	Should Test During EMI	Should Test For Survival of Non-operating Environment	
SDC (Cont'd.)								
25. Reliability ckt logic operations, delay times, and output amplitudes	X	X	X	X	X	X	X	X
26. Cross-Coupled Side Lobe Logic Operation	X	X	X	X	X	X	X	X
27. Waveguide Assembly Performance	X		X	X				X

Table 4-2. Listing of Characteristics in Table 3-2 for which Tests are Judged Unnecessary because of Items in Table 4-1 Noted. (See Text for Meaning of Special Assumption Numerals:)

Characteristics Not Requiring Separate Examination	Responsible Items in Table 4-1	Special Assumptions Required
<u>Unit & System Level</u>		
a. <u>KPSM</u>		
1. Ripple & Stability of Voltage Supplies	1,2,3,4	
2. Time Delay for HV Turn-on	3	
3. Sweep Voltage Timing	4	
b. <u>R/T UNIT</u>		
4. Separate Gain & Phase Balances for Preamp Stages and Gate Matrices	13	
c. <u>SDC</u>		
5. LVPS Regulation & Ripple	17,18,20,23,24	
6. Carrier & Extraneous Sideband Elimination in SSBM	23,24	1,2
7. Spurious Outputs	23,24	1
8. IF Passband Shape	23	1
9. SSBM & IF Amplifier Gain Stability	18	
10. RA IF Gate Performance	23	3
11. Proper Operation of Tracking Loop Components: Time Constants, Gain, VCO Stability, Bandwidth of Linear Operation	19,23,24	1

Table 4-2. Continued

Characteristics Not Requiring Separate Examination	Responsible Items in Table 4-1	Special Assumptions Required
<u>Unit & System Level</u>		
c. <u>SDC (Cont'd.)</u>		
12. Proper Tracker SLP and BP Filter Operation (Search Mode)	20	1,2
13. Threshold Detector Accuracy in all Preamp Gain States	20	1
14. Relative Phase Shifts of Signals through the Doppler Gates	23	
15. Reference Freq. Generator Stability	23	
<u>System Level Only</u>		
a. <u>KPSM</u>		
1. Amplitude Modulation	23	
2. Noise & Other Spurious Outputs	23	
3. Blanking Signal Amplitude and Timing	23	3
b. <u>R/T UNITS</u>		
4. Transmitter-Receiver Leakage	23	
5. Insertion Loss/VSWR	20	
6. Noise Figure	20	
7. Balance of Gains & Phases	23	
8. Preamp Gain Stability	23	

Table 4-2. Continued

Characteristics Not Requiring Separate Examination	Responsible Items in Table 4-1	Special Assumptions Required
<u>System Level Only</u>		
b. <u>R/T UNITS (Cont'd.)</u>		
9. Preamp Passband Shape	23	
10. Preamp Gain Selection Accuracy & Hysteresis	23	1
11. Spurious Outputs	18,23	
c. <u>SDC</u>		
12. Tracker Search Ranges and Rates	20,23	1
d. <u>WAVEGUIDE ASSEMBLY</u>		
13. Performance	20,23	

Table 4-3. Definition of a "Desirable" Flight-Readiness Test Program for the Surveyor RADVS

CHARACTERISTICS TO BE EXAMINED	Unit Level				System Off S/C (At Vendor)		System On S/C (At Buyer)				Survival	Pre-launch	
	Unit Level				System Off S/C (At Vendor)		System On S/C (At Buyer)						
	Lab. Amb.	Accel.	Vibr.	Temp.	EMI	Lab. Ambient	Lab. Amb.	Accel.	Vibr.	Temp.			EMI
1. XMTR frequency coherence	X	X	X	X						X	X		
2. XMTR amplitude modulation	X	X	X	X									
3. Other spurious outputs	X	X	X	X									
4. RA klystron sweep linearity and rate	X	X	X	X						X	X		
5. XMTR output power	X	X	X	X						X	X		X
6. XMTR output frequency	X	X	X	X						X	X		
7. Production of stray fields	X									X			
8. Blanking signal amplitude and timing	X												
9. Antenna patterns	X												
10. Transmitter-receiver leakage	X												
11. Insertion loss/VSWR	X												
12. Noise figure	X												
13. Preamp branches gain and phase balance	X	X	X	X									
14. Preamp gain stability with time	X												
15. Preamp passband shape	X												
16. Preamp gain selection accuracy and hysteresis	X												
17. Spurious outputs from R/T units	X												
18. Reflectivity-output stability and ripple	X										X		X
19. Tracker search ranges and rates	X												
20. Signal-tracking threshold operation (sensitivity)	X	X	X	X					X				X
21. Operation times of DTC circuits	X												
22. Delay time for filter BW change in RA	X												
23. Analog output accuracy, linearity, stability, noise, ripple	X	X	X	X					X				X
24. Range mark accuracies and susceptibility to false lock	X	X	X	X									X
25. Reliability circuit logic operations, etc.	X	X	X	X									X
26. Cross-coupled sidelobe logic operation	X	X	X	X									X
27. Waveguide assembly performance													X
28. System warm up time									X				X
29. System power consumption									X				X

C. "DESIRABLE" SPECIAL TEST PROGRAM

An anticipation of operational problems and an awareness of testing limitations forms the basis for specification of the special test program. As noted in the foregoing philosophy, checking of certain interactions basic to design and operation is not expected to be feasible or desirable on flight spacecraft. These test areas are better known now, having delineated the flight-readiness program. The purpose of the present section is to itemize the extra tests required to yield high confidence of successful operation.

1. Transmitter-Receiver Leakage Tests

A detailed description of the leakage problem is given in Appendix B. Several possible experiments for measuring the RADVS leakage problem are described and evaluated. Only a brief summary of the results is given here.

In order to avoid degradation of tracker sensitivity, the product of the leakage factor and the leakage power in the tracker-filter bandwidth (normalized to the total leakage power) must be of the order of -160 db. Stated in an alternate way, if this requirement is not met the acquisition sensitivity of the tracker must be reduced in order to avoid locking on the leakage component. This problem is the major difficulty with CW radar systems. The allowable combined effects of leakage and modulation on this leakage are so small that a reasonable estimation as to whether the requirement can be met is made possible only by experience with a given system in the environment in which it must operate. The unusual environment of RADVS during lunar descent poses by far the biggest testing problem.

In an attempt to find a reasonable method for realistic measurement of the leakage problem, several possible experiments were suggested and evaluated. The first experiment to be considered consisted of hanging a spacecraft (or a simulating system) above the earth, firing the vernier engines and observing the transmitter-receiver leakage signal. The difficulty in reducing ground reflections to an acceptable level rules out this method. The second experiment is similar to the first, but the spacecraft is inverted in order to reduce ground reflections to an acceptable level. However, the difficulties encountered in firing the vernier engines upside down discourage the application of this method. Still a third and similar method is to tether a balloon-supported spacecraft above the earth, sufficiently high to reduce ground reflections to an acceptable level, again observing and analyzing the transmitter-receiver leakage. Of the three methods, the latter offers most promise.

All three of the test methods mentioned above have common shortcomings of a serious nature. First, the acoustical air-coupling which exists in the tests, but is not present in the lunar environment, tends to mask the desired results. In theory, this coupling can be reduced to an acceptable degree by various acoustical shielding techniques. An even more serious difficulty is the fact that plume-coupling effects would not be realistically tested by any of the tests because the plume characteristics would be grossly different in the lunar environment than in the test environment because of the atmosphere. This limitation is believed to be sufficiently serious to discourage use of any of the three tests for studying the effects of vernier plume on the transmitter-receiver leakage.

Only brief consideration was given to conducting tests in a vacuum chamber. Overall RADVS system tests with vernier engine operation are impractical. Perhaps a combined analytical and experimental study where relevant plume characteristics are measured and subsequently used to analyze the leakage problem would be very helpful. However, such a program would be lengthy and costly and is believed to be impractical at this point in the Surveyor program.

A completely analytical approach to the leakage problem can be conducted; one such JPL study was performed [67]. However, the uncertainties of plume characteristics and of antenna characteristics (in particular the near-field levels outside the center of major field concentration), require that the computed results be viewed with caution. It is believed, with the present state of knowledge concerning these uncertainties, that a completely analytical approach would have very limited usefulness.

An earth test is described which is believed to be very useful in evaluating vibration effects, but which will not test for plume effects. This consists of a two-step process: measurements of the driving-force vibration characteristics of the retro rocket and the vernier engines; and application of these measured vibration levels to an inverted spacecraft containing RADVS. (A modification would be to use Surveyor 1 vibration data which were obtained during retro fire and vernier engine operation of the lunar descent, rather than the data obtained as described in the first step.) During the second step all preamplifier output signals would be recorded and/or analyzed in order to obtain spectral plots of these signals.

Because these vibration tests do not include plume effects, their value may be questioned. It may be useful to point out that there are several mitigating factors to the plume effects; consequently, those tests described above which do

not include these effects are still quite valuable. The mitigating factors are as follows:

- (1) Plume coupling will be predominantly in the negative doppler band; consequently negative-doppler rejection circuits will provide significant rejection of this coupling.
- (2) It is expected that plume coupling will have a random, thermal-noise-like character with a fairly wide bandwidth; consequently, the noise-developed threshold in the acquisition circuits will provide a significant degree of receiver desensitizing so that false-lock is not as likely to occur as for narrow-band non-thermal noise components; although such desensitization is undesirable, it is preferable to false lock.

Unfortunately, these arguments are not sufficiently conclusive to justify completely ignoring plume effects; lack of knowledge about the degree of coupling and its spectral characteristics is of considerable concern. For example, too much receiver desensitization, although it may avoid false lock, may also prevent correct lock-on to desired signals. (This desensitization is expected to occur only for the lower portion of the doppler band, say, less than 10 kHz.)

The final test studied is an on-board test where spectral characteristics of preamplifier signals are obtained during an actual lunar descent. Two promising methods of obtaining this data are described. One is a simple spectrum analyzer employing a stepped VCO which steps a narrow-band filter through the doppler band. The other simultaneously observes many contiguous spectral bands covering the doppler band of interest by means of banks of doppler filters.

The last two tests described above (the earth-bound vibration test and the on-board test) are believed to be very useful and practical and are considered to be valuable parts of a desirable test program.

2. Flight Tests

It is desirable to conduct a series of flight tests on an early experimental model of the radar in order to verify its operational capability under certain realistic conditions. It is apparent from the foregoing discussion that completely realistic simulation of lunar environmental conditions cannot be achieved. In fact, there appears to be no practical way to simulate realistically RADVS operation during retro and vernier firing. However, RADVS can be tested for high altitude operation to verify its design for proper operation when realistic signals

are present. The major attraction of such tests is that they test the system's capability for acquiring and tracking low-level signals which have realistic fluctuations and spectral characteristics. Klystron frequency instabilities will show up during such tests as a "coherence loss" or, stated another way, as a spectral spreading loss; such instabilities will produce no observable effect during ground tests in which only small delays are imposed on the received test signals. Any anomalies of acquisition, tracking, and signal processing of realistic signals will be discovered during such tests and corrections can be made. Although preamplifier noise signals resulting from transmitter-receiver leakage will not be a good indication of those existing during lunar descent, the reduction of such components to acceptable levels will certainly enhance the RADVS' capability for operating under lunar descent conditions. From the standpoint of such noise characteristics, then, the high altitude tests must be viewed as essentially qualitative in that they highlight trouble spots which require corrective action.

If during the flight tests certain problem areas are discovered which are sensitive functions of environmental conditions, correction of these problems for the flight tests alone may not be sufficient. For example, if during these tests marginal corrections are made for the transmitter-receiver leakage problem, special attention should be given to additional tests which ensure that lunar descent conditions will not seriously aggravate the problem.

The flight tests should be conducted under conditions which are as realistic as possible. Operating altitudes should preferably be as high as 40,000 feet and the antenna should be tiltable from 0° to 70° relative to vertical (i.e., the limits encountered for RADVS descents). The altitude requirement cannot be met by the helicopter; because this is otherwise a good choice it may be desirable to compromise on the altitude requirement. A subsonic, fixed-wing aircraft cannot provide the hover testing of a helicopter, but generally offers a superior "flying laboratory" because of the greater available space (as for example offered by the KC-135). Altitude limitations of some aircraft can be partially compensated by inclusion of flight tests conditions which present low signal level; flights over smooth seas or flat sandy terrain offer one way of satisfying this condition.

The major deficiency of flight tests, as described here, is that lunar descent conditions are not realistically simulated; in particular, retro and vernier firing effects are not present. Therefore, the flight tests cannot be viewed as complete verification of RADVS' capability for controlling lunar descent. In spite of this limitation, such tests are considered as a necessity for radar design verification.

3. Interfering Signal Tests

There will, of course, be undesirable signals appearing in the preamplifier outputs. It is important to determine whether false-lock can occur on such signals, or whether their presence can cause deleterious effects on tracking the correct signal.

One such undesirable signal arises from reflections from the retro-rocket tank. The amplitude and velocity distribution of this signal should be quite predictable, so that realistic simulation of retro tank passage through the antenna beams should be possible. The velocity of this target will be negative; thus, the negative-doppler rejection capability of the circuit will discriminate against it. However, because of the short range and relatively-high strength of the signal, there is a good chance for it to cause difficulty. Possible effects are as follows:

- (1) It might scatter enough transmitted and/or received signal to drop the lunar echo below the tracking threshold; this is considered a normal effect.
- (2) It might back-scatter enough energy to suppress the lunar signal by switching the preamp gain level; this is also an expected result.
- (3) It might back-scatter enough energy so that its positive doppler image is large enough to cause erratic tracker behavior. (Its image might even be tracked in some cases.)
- (4) It might have low enough frequency and high enough amplitude to pass through a tracker's lowpass or bandpass filters at a significantly high level.
- (5) Its presence in mixers with true signals might cause trackable intermodulation components.

Because of these possibilities, very thorough design verification tests should be performed with such signals.

Another source of interfering signals is through cross-coupled sidelobes, which have been shown to present a serious problem (Appendix C). In all practical cases these signals are small relative to the correct mainbeam signal, which is simultaneously present in a given receiver channel. The main concern is lock-on to the incorrect signal, which could have disastrous results. Although analysis

shows quite clearly that the present RADVS will normally lock-on certain cross-coupled sidelobe (CCSL) signals, the effect is important enough that it should be thoroughly tested. For example, the test would show whether there is some natural weak-signal suppression in the receivers and trackers, which is not discovered by analyses assuming linear-circuit operation. Changes are presently being made in RADVS to include CCSL logic for all beam combinations; a very thorough analysis and testing of the resulting system should be made, at least one time, to discover any unanticipated interactions of such multiple-logic circuitry.

The above discussion would indicate that interfering signal tests and complete tests of any CCSL fix should be run as a special, or one-of-a-kind, test. However, tests of negative-target rejection capability could easily be run on each RADVS system. Decision of the extent of testing in the flight-readiness program should be based on operating margins found in special tests. Narrow margins are dangerous because proper operation depends on critical circuit balances to eliminate negative doppler signals in the trackers.

4. Environmental Overtests

The number of systems available for special testing is anticipated to be too small for much statistical significance to be obtained; i.e., rather little confidence could be assigned to any quantities thus determined, such as "mean time to failure." The coupling of overttesting with engineering analysis, however, can contribute useful information without a large number of test samples.

The basis for testing should be a system reliability analysis starting at the component level. Since statistics of component failures can generally be obtained to sufficient confidence, unit and system failure statistics can be computed within useful confidence intervals. Properly instrumented tests would then be used to reveal whether various component interactions were correctly anticipated.

Early results of the program mentioned would indicate design modification needs. Later, they would determine test requirements for the flight-readiness program.

Another phase of environmental overttesting should be employed to help predict the effects of flight-readiness tests on the system. A cycling of the system through the anticipated flight-readiness program a few times would show any degradation that might be expected from testing.

The details of these special tests cannot be listed without knowing the reliability analysis results. Basically, though, all environmental conditions would be varied from a low level to the point where failure became imminent.

V. PRESENT TEST PROGRAM DESCRIPTION

A. OVERALL PROGRAM OUTLINE

The Surveyor test program has four main facets: developmental tests, type acceptance (or approval) tests (TAT), reliability tests, and flight acceptance (or approval) tests (FAT). The first two types of tests differ from the latter in that they do not generally involve flight spacecraft. They both have the basic task of proving the design but differ by their positions in the program sequence. The third, reliability tests, can involve special sequences on either flight or test vehicles but is normally entwined in unit construction and regular FAT. The fourth set is used to determine flight readiness of systems which must actually perform the missions.

An additional test group within the program might be termed "quality assurance tests." This group is actually a part of construction which helps assure passage through other tests; it will not be considered separately in the study. Similarly, reliability tests will not be viewed as a separate group.

B. TEST EQUIPMENT

All of the formal type acceptance and flight acceptance testing by the buyer is performed with use of System Test Equipment Assemblies (STEA's). There are about three STEA's located at the El Segundo facility, two at the Eastern Test Range, and one used at other installations as needed. In addition, the same type of RADVS test equipment assembly is used by the vendor for system FAT. All of these assemblies can be considered to be identical for purposes of the present study.

Details of STEA contents and operation are found in HAC publication 6594500, "STEA Operation and Maintenance Manual," Vol. I and II. For completeness of discussion, an abbreviated diagram of the portion of STEA which provides simulated signals to RADVS is shown in Fig. 5-1. Other STEA connections with RADVS are possible either through adapters placed at the normal module connectors or by use of the spacecraft's telemetry system; the latter requires use of STEA's RF test racks. Through these connections STEA permits examination of preamp outputs, tracker lock indicators, range marks, blanking signals, CRODVS indicator, RODVS indicator, RORA indicator, reflectivity outputs, analog outputs, and preamp gain state signals. An eight channel oscillograph (Brush, mark 200) and a digital voltmeter (Nonlinear Systems, 484A) can be selected to monitor most of the signals. In addition, STEA provides indicator lamps showing the states of the RADVS bilevel-signal outputs.

Provisions for loading and filtering the RADVS analog outputs are also contained in STEA. The purpose of the loading is to simulate the normal spacecraft (Flight Control) terminations whenever the actual connections do not exist. The reason for filters is to simulate the spacecraft response so that effects on operation of analog output noise and ripple can be determined; the filter transfer functions are

$$G(s) = \frac{5}{(2.6 s + 1) (0.11 s + 1)^2}$$

for V_x and V_y ,

and

$$G(s) = \frac{5}{(0.08 s + 1)^2}$$

for V_z [35]. Monitoring can be performed either with or without the filters.

Another capability of STEA is to simulate spacecraft dynamics in closed loop control tests. The simulated signal received by RADVS in these tests is the same as shown in Fig. 5-1 except that the input frequencies are determined by voltage controlled oscillators (VCO's) instead of the sources shown. The VCO's, in turn, are driven by signals obtained from computed spacecraft motion. Therefore, the only real difference to RADVS is that its simulated return signals vary in frequency rather than remain essentially fixed.

An evaluation of the use of STEA will be withheld until evaluation of the entire program. At present it will be pointed out that only the simulated return signal is essentially a single sinusoid which tracks the current transmitted signal with negligible time delay. (Also, see Appendix G.)

C. DEVELOPMENTAL AND TYPE ACCEPTANCE TESTS

1. Vendor Tests *

Type approval tests at the vendor, Ryan, were essentially completed in late 1964; Ryan report 51765-1A was the controlling document for these tests. The specimen tested was the first regular model produced, serial number one (S/N-1).

During the Ryan TAT, the following environmental conditions were applied (separately): vibration, constant acceleration, shock, thermal-vacuum, low temperature storage, and electromagnetic interference (EMI). These phases are briefly described in Table 5-1 with an outline of results as recorded and analyzed in Ryan report 51766-1 [61]. (The poor quality of the captions on the reproduced records precludes complete re-analysis.)

* Documentation of vendor developmental tests was not available for the present study. Available information on type acceptance tests is presented herein.

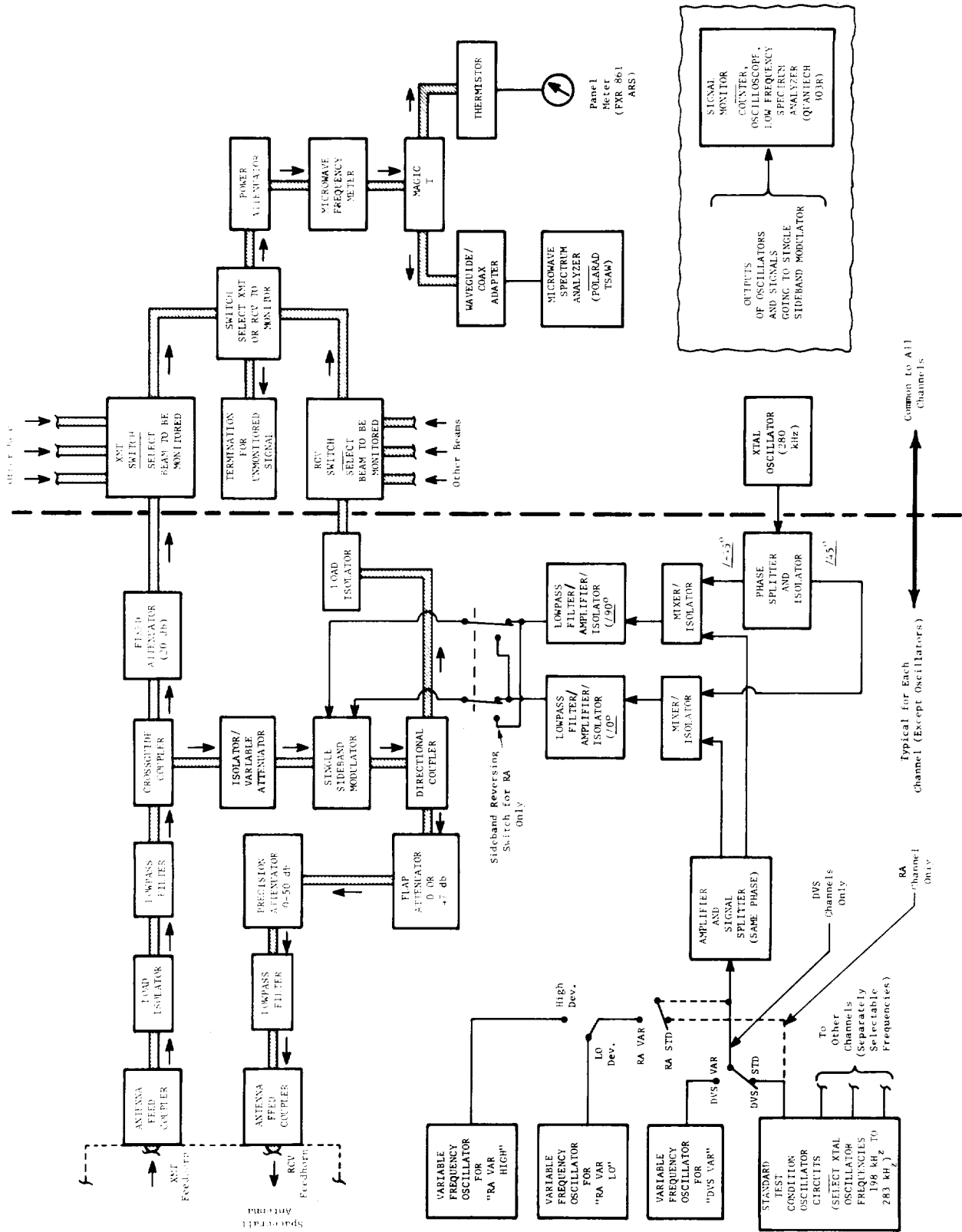


Fig. 5-1. Diagram of the RADUS signal simulation portion of STEA. The channel shown is typical of all DVS and RA channels except as shown.

Table 5-1. Description of the Vendor TAT

UNIT	OPERATING/ NONOPERATING	ENVIRONMENT	NOTABLE RESULTS
ALL	NONOPER.	VIBRATION, SINUSOIDAL: 6 sweeps on 3 axes--5 Hz to 20 Hz @ 0.9 in. peak excursion; 20 Hz to 125 Hz @ 18g p-p; 125 Hz to 1.5 kHz @ 4g p-p plus 4.5 g rms (first sweep) or 2g rms (5 sweeps) of white Gaussian noise, bandlimited 100 Hz - 1.5 kHz.	<ol style="list-style-type: none"> 1. No degradation of performance noted on any unit. 2. Structural resonances of the units were noted in the range of 100 Hz to about 600 Hz.
SDC	OPER.	VIBRATION, SINUSOIDAL: 1 sweep on 3 axes--levels about $\frac{1}{2}$ of above except noise at 2.5g rms.	<ol style="list-style-type: none"> 1. No degradation of performance noted. 2. Structural resonances present.
KPSM	OPER.	VIBRATION, SINUSOIDAL: 2 sweeps on 3 axes--first sweep: 5 Hz to 19 Hz @ 0.5 in. peak excursion; 19 Hz to 125 Hz @ 9g p-p; 125 Hz to 2 kHz @ 2.7g rms white GAUSSIAN noise--bandwidth not specified.	<ol style="list-style-type: none"> 1. Preamp output rose to 40 mv in range around 70 Hz and to 70 mv at about 1.1 kHz during sinusoidal sweep on vertical axis. 2. Similar type of results on horizontal axes except one gradual rise to 160 mv @ 125 Hz noted. 3. Only notable Gaussian-input response was 40 mv at 191 Hz and 20 mv at 1.4 kHz on minor horizontal axis. <p>Note: These levels should be compared with the 10mv to 250 mv range of preamp outputs in normal operation.</p>
RA/VS R/T UNIT	OPER.	VIBRATION, GAUSSIAN: 9 sweeps, 3 axes: 50 Hz to 2 kHz, 0.002g ² /Hz, bandwidth not specified; 3 to 10 sweeps, 3 axes: 100 Hz to 1.5 kHz, 4.5g rms (bandwidth unspecified)	<ol style="list-style-type: none"> 1. First nine sweeps: mechanical resonances appeared @ 350 Hz, 1.2 kHz, and 1.6 kHz to 2 kHz; preamp outputs did not exceed 6 mv. 2. Second set: mechanical resonances similar to above; preamp outputs typically in range 10 mv to 30 mv. <p>Note: preamp outputs recorded from a spectrum analyzer.</p>

Table 5-1. Description of the Vendor TAT. (cont.)

UNIT	OPERATING/ NONOPERATING	ENVIRONMENT	NOTABLE RESULTS
R/T	OPER.	VIBRATION, SINUSOIDAL: 3 sweeps, 3 axes: 5Hz to 20 Hz, 0.45 in. peak excursion; 20 Hz to 125 Hz, 9g p-p; 125 Hz to 1.5 kHz, 2g p-p.	1. No results of preamp outputs given.
DVS R/T UNITS	OPER.	VIBRATION, GAUSSIAN (same as for RA/VIS unit)	1. First nine sweeps: mechanical resonances similar to other R/T unit; some preamp outputs reached 14 mv. 2. Second set: similar to other R/T unit
ALL	BOTH	CONSTANT ACCELERATION: 10 g for 4 min. nonoperating, 5g for 2 min. operating.	1. No degradation or change noted (per Test History)
ALL	NONOPER.	SHOCK, HALF-SINE: 4 times along pos. thrust axis; 2 times each along plus-X, minus-X, plus-Y, and minus-Y axes: 12 to 16g in Z direction, 4 to 8g in others.	1. No change in mechanical or operational characteristics noted.
ALL	BOTH	THERMAL-VACUUM: After about 80 hours of nonoperate (at turnon): pressure = 1.1×10^{-6} torr; R/T temp. = -54 to -57°F; KPSM temp. = -14 to -20°F; SDC temp. = +44 to +46°F. After 6.5 minutes of operation: pressure = 1.9×10^{-5} torr; temperatures about same except KPSM temp = +7 to +43°F	1. VA 264A klystron was redesigned to eliminate arcing first found; KPSM retested at later date. 2. Bad diode found in KPSM filament converter. 3. Bad solder joint in tracker low pass filter in post reference run.
ALL	NONOPER.	LOW TEMPERATURE STORAGE: -45°C stabilized for 5.5 hours with units in shipping containers; afterward connected as system for test.	1. Open transistor in D ₄ tracker considered isolated case. 2. Loss of 1 watt DVS power considered natural because of 50 hour klystron age.
ALL	OPER.	EMI, CONDUCTED & RADIATED: Broadband & narrowband tests	1. Noise increase on analog outputs noted--results not meaningful in present study.

Certain additional features are noted below:

- (1) The vibration environment was applied by driving each RADVS unit separately with an electromagnetic shaker. No attempt was made to simulate the spacecraft's structural characteristics. Instead, the mountings were intended to have a flat response. Monitoring was with accelerometers placed on the mountings. Whenever tests called for the units to be operating, R/T units and the KPSM were used in conjunction but only the unit under test was vibrated; connections were made with damped flexible waveguide. Signals for the SDC were provided by oscillators.
- (2) Constant acceleration was applied to each unit separately with use of a centrifuge. Units were operated during a portion of the test.
- (3) Shock testing was performed on each unit with use of a Barry Sand Drop Machine, model 73. No units were operated during the tests.

2. Buyer Tests

A view of the overall spacecraft special test program by the buyer, Hughes, is useful in understanding the relationships of special RADVS tests. Such a listing is given below; a more detailed description of the portions involving RADVS follows the list.

DESIGN ACTIVITIES:

1. Reduced scale and full scale spacecraft models and mockups, designated M-1 through M-13, were constructed for purposes of obtaining subsystem design compatibility.
2. One-fourth scale and full scale models, MA-1 and MA-2, were used for antenna tests.
3. The MT-1, a full scale spacecraft model with thermally simulated components, was used for evaluation of thermal control provisions.
4. A spaceframe with components simulated by point masses, S-1, was given static and vibration structural tests.
5. A more elaborate spaceframe, S-2A, was tested with vibration, shock, and static loadings. (1963-65).
6. Vernier propulsion system tests were performed using spaceframes S-4 through S-7. The last of these, which employed dummy masses to simulate S/C components, was used to establish vibration levels for FAT and TAT. (Through mid 1965).

7. Spaceframe S-8 was used for flight control/propulsion interaction tests at the Air Force Missile Development Center (AFMDC).
8. The S-8 Spaceframe also was used for RADVS vibration tests in the upsidedown position. (late 1964)
9. The S-10 frame was used to determine thermal performance of all subsystems and qualify the S/C thermal design. (early 1966)
10. The T-1 test vehicle was used for drop tests of the landing gear and for spacecraft/Centaur separation tests.

RELIABILITY AND SYSTEM-TEST ACTIVITIES

1. The T-2H "vehicle" was an installation of the QA-1 RADVS and test equipment on a helicopter to evaluate RADVS performance. (design/development phase: mid 1963; verification phase: mid 1964)
2. The T2N-1/-2 test vehicles were used for RADVS/flight control/vernier propulsion subsystem tests during descents from a balloon. The X-3 and X-4 RADVS was used. (Sept. 1965 through May 1966)
3. The T-21 prototype vehicle, which is essentially identical to flight model spacecraft, was used for the formal System Type Approval Test Program; its purpose was to verify design and to check compatibility with ground equipment at the Eastern Test Range and deep space networks. It used the QA-1 RADVS.
4. Spacecraft SC-1 and SC-2 were used to check noise generation characteristics. (mid 1965 and Jan. 1966, respectively)

As noted, the formal TAT made use of the T-21 vehicle. The portions of this program which affected RADVS were the System Functional Test (SFT), Vibration Test (VT), and Solar-Thermal-Vacuum (STV) Test Phases [13,14,15]. The SFT phase was for system performance verification and calibration in normal laboratory surroundings. The other two phases are outlined in Table 5-2.

All tests were performed using a system test equipment assembly (STEA) similar to that described in report Section V.B.

Table 5-2. Listing of the Environmental Portion of Formal System TAT Using the T-21 Vehicle (with QA-1 RADVS)

ENVIRONMENT	TESTS
1. lab ambient after (launch) VIBRATION: swept sinusoidal, 5-40 Hz @ 2.25 g peak, 40-100 Hz @ 1.20 g peak along z axis (2.0 g peak in lateral directions); swept sinusoidal, 100-1500 Hz @ 2.0 g peak on three axes, PLUS bandlimited 100-1500 Hz random @ 2.0 g rms along z axis for 10 minutes (4.5 g rms in lateral directions for 2 minutes).	1. XMTR power 2. Tracker sensitivities
2. during (descent) VIBRATION: swept sinusoidal, 100-1500 Hz @ 2.8 g peak, PLUS bandlimited 100-1500 Hz random @ 0.2 g rms for 2 minutes on three axes.	1. Closed loop terminal descent test. 2. XMTR power 3. Tracker sensitivities
3. after IONIZATION-layer-simulation in the Solar Vacuum Chamber at pressures between 100 and $\frac{1}{2}$ mm Hg; and after STV of 130 ± 5 watts/ft ² , $-310 \pm 10^{\circ}$ F background, and 1×10^{-6} torr	1. XMTR power 2. Tracker sensitivities

The salient features of other special tests involving RADVS are described below: (For details, see references 13, 14, 16, 22, 33, 34, 35, 38, 42, 43, and 48 in Appendix A.)

1. VIBRATION: An S-8 spaceframe fitted to simulate an A-21 vehicle after retro eject was supported in an inverted position by a shock-cord system. Shakers attached at the three vernier engine points were driven with noise to obtain overall force outputs between 10 and 56 pounds rms with flat spectra bandlimited to the 80 to 2000 Hz range. (An expected mission level of 10 pounds rms was established from engine firing tests.) Preamp outputs were recorded on magnetic tape (10 kHz bandwidth). Analog outputs, preamp gain state number 2, tracker lock signals, RODVS, RORA, and range marks were monitored on a galvanometric recorder. Subsequent plots of the spectral content of the preamp outputs were made using a 50 Hz filter (and one second integration time) on the (looped) tape playback. Significant results were:

- (a) A tracker with a 3 db acquisition threshold was very susceptible to false lockon, but those with a 9 db level had no significant trouble. (The higher threshold greatly increases tracker desensitization to double sideband signals, in the high gain state over frequencies of interest.)

- (b) An antenna without shock mounting and with different surface coating showed appreciable return from foot pads and crushable blocks. The broadband power was sufficient to switch preamp gain states. All DVS trackers were susceptible to false lock from this unit's output at force levels of 28 and 56 pounds.
- (c) Evidence of leakage between R/T units was noted (but not completely analyzed).
- (d) Isolators were found to be required.
- (e) The altimeter was stated to be so insensitive to vibration that no data for it was presented or analyzed.

2. FLIGHT TESTS: The T-2H phase of the T-2 test program flight-tested RADVS with use of a helicopter. The model used in the tests contained all of the main features of flight models. The maximum altitude flown was about 6,000 ft over the terrain. On-board instrumentation consisted of a magnetic tape recorder for preamp outputs, analog outputs, range marks, and reliable operate signals; a recording oscillograph for tracker lock signals in addition to those mentioned; and a camera to record the terrain being viewed by RADVS. This same signal information was also telemetered. Data analysis included spectral analysis of preamp outputs and comparison of analog outputs with optical tracking data from ground installations. Significant results of the 1964 tests were:

- (a) Analog output accuracy was generally within tolerance when the system was tracking normally.
- (b) The 14 ft range mark was frequently triggered by noise at ranges greater than 18 ft.
- (c) In flights over water, trackers 2 and 3 locked onto beam one through a sidelobe. Also, the CCSL logic between trackers 2 and 3 was found to operate properly over water, but no such situation could be imposed over land.
- (d) Noise on the analog outputs appeared to be higher than expected.
- (e) Check of altimeter performance over rough and mountainous terrain showed satisfactory performance. (Accuracy was not checked.)
- (f) The DVS analog outputs were perturbed when preamp gain state switching occurred.

3. DESCENT TESTS: Descent tests were performed with the T2N-1 and T2N-2 vehicles, which are special frames fitted with RADVS, flight control, and vernier engine propulsion subsystems. Main modifications made to RADVS for test purposes included:

- (a) altering the waveguide runs to fit the frame;
- (b) locking the RA in the high deviation mode by bypassing the deviation control SCR;
- (c) disabling the signal-to-noise acquisition mode by disabling all preamp high gain threshold detectors (to mitigate vernier engine noise degradation);
- (d) bypassing the cross-coupled sidelobe logic circuitry;
- (e) restricting DVS operation to the narrow-band mode by applying a permanent burnout signal; and
- (f) restricting RA operation to the narrow band mode by providing a permanent deviation signal to the tracker filters.

Telemetered data included the 14 ft mark, reliability signals (except CRO), analog outputs, 10 fps detector, preamp gain states, some preamp outputs, and tracker lock signal. Tests were run from releases at about 1,450 ft to parachute recovery at about 600 ft and from releases at about 900 ft to landing. Significant results were:

- (a) The D1 tracker locked onto leakage from the RA XMT feed. Problem was diminished by tuning the RA klystron for reduced AM and by adding isolators to the DVS XMT waveguide.
- (b) Transients appeared in analog velocity outputs at preamp gain switching points.
- (c) Mechanical isolation of the klystrons was found to be needed.
- (d) All other operation was considered satisfactory and within tolerances.

D. VERIFICATION AND ACCEPTANCE TESTS

1. Vendor Unit Tests

Unit tests which are performed as part of the vendor construction verification procedure are outlined in the following Ryan documents:

- 51765-9 SDC Test Requirements
- 51765-10 KPSM Test Requirements
- 51765-11 RA/VS Antenna Test Requirements
- 51765-12 DVS Antenna Test Requirements
- 51765-13 Antenna Manufacturing Test Procedures
- 51765-14 Special Temperature Tests
- 51765-16 KPSM Ranging Test Procedures

Unit tests which form part of the buyer's acceptance test procedures are outlined in Ryan documents:

51765-2B, Part III, Unit Acceptance Tests

51765-2B, Part II, Environmental Tests (unit vibration only)

Tests performed are outlined in Table 5-3. Other available details are contained in Appendix D.

2. Vendor System Tests

The vendor system tests consist of operational checks during a sequence of simulated operational conditions. All tests are performed under laboratory ambient conditions. The controlling document is Ryan report number 51765-2B, Part I, [60].

Tests performed are outlined in Table 5-4. The standard test conditions (STC) and other details are contained in Appendix E. The test equipment assembly used is essentially the same as described in Section V.B.

3. Buyer Flight Acceptance Tests

The total Hughes test sequence and requirements are concisely described in HAC document 3023926 A, Surveyor Spacecraft A-21, System Test Specification [31]. For completeness of the present report, the contents of this document which affect RADVS are outlined briefly below. In addition, test requirements relating to RADVS have been reproduced for inclusion in Appendix F.

Flight Acceptance Tests by Hughes are performed only on vehicles which have been (essentially) completely assembled and aligned. All units used must have satisfactorily passed the appropriate lower level (vendor) FAT. The Hughes FAT, therefore, is mainly concerned with verifying the compatibility of units and checking that system functional requirements are met. This is accomplished through a sequence of 8 phases, of which 6 concern RADVS.

The first phase is termed the Initial System Checkout (ISCO) Test Phase. As the name implies, this phase yields initial verification of compatibility of subsystems and gives reference data for future phases. The next 4 phases in which RADVS is exercised are environmental tests. These are the Mission Sequence/Electromagnetic Interference (MS/EMI), Solar Thermal Vacuum (STV) Functional, Vibration (VIB), and Vernier Engine Vibration (VEV) Test Phase. Finally, set of performance verification tests are performed during the Airforce Eastern Test Range (AFETR) Test Phase.

Information from Appendix F has been compiled into Table 5-5 for easier reference. For purposes of this table, the "lab ambient" test listing includes both the ISCO phase tests and any ambient readiness tests for other phases. Another feature to note is that only tests within the VIB phase are listed in the "vibr. survival" column, although tests in other phases usually follow; in particular, all "prelaunch" tests offer verification of survival.

Table 5-3. Outline of Vendor Tests on Flight Units

UNIT	CHARACTERISTIC TESTED	UNIT VERIFICATION		UNIT ACCEPTANCE		
		AMB.	TEMP.	AMB.	VIB.	TEMP.
KPSM	Amplitude Modulation	X			X	
	Other spurious outputs	X			X	
	RA klystron rate	X	X	X		X
	Output powers			X	X	
	Output frequencies	X	X	X	X	X
	Blanking signal amplitude, width, risetime	X				
	Power consumption	X		X	X	
	Warm-up time	X		X		
	HV time delay	X				
	Klystron supply voltages, regulation, ripple	X				
	Modulation inhibit circuit (for test use)	X				
R/T	Antenna patterns	X		X		
	Noise figure	X	X	X		
	Preamp gain & phase balance	X	X	X		
	Preamp gain selection accuracy			X		
	Preamp passband shape & gain	X	X			
	VSWR at XMT & RCV flanges			X		
	Preamp microphonics				X	
	Insertion loss of special test horns	X				
Microwave isolation between feeds	X					
SDC	Reflectivity-output calibration	X				
	Signal-tracking thresholds (sine input)	X		X	X	
	Signal-tracking thresholds (sine plus noise)	X				
	Signal-tracking thresholds (doppler spectrum)	X				
	Response time	X		X		
	Analog output accuracy, linearity (sine input)	X		X		
	Analog output ripple, noise (sine input)	X			X	
	Analog output accuracy, linearity (doppler spectrum)	X				
	Range mark accuracies	X				
	Cross coupled sidelobe logic	X		X		
	Power consumption	X		X		
LVPS outputs & ripple	X					

Table 5-4. Outline of Vendor System Flight Acceptance Test

CHARACTERISTICS TESTED	STC NUMBERS
RA klystron sweep rate	--- (for reference)
XMTR powers	--- (for reference)
XMTR frequencies	--- (for reference)
Preamp gain selection accuracy	---
Reflectivity-output	---
Signal tracking threshold (DVS)	1, 4, 6, 8
Signal tracking threshold (RA)	2, 4, 6
Acquisition time (to RODVS)	1, 4, 6
Acquisition time (to RORA)	2, 4, 6
Analog output accuracy, linearity (velocities)	1, 2, 4, 5, 6, 7, 8, 9, 10
Analog output accuracy, linearity (altitude)	2, 4, 5, 6, 7, 8, 9, 10
Analog output noise & ripple (at S/C filter output)	10
1000 ft range mark accuracy	7
14 ft range mark accuracy	10
Reliable operation indicating circuit operation	combination
Cross-coupled sidelobe logic operation (sine input)	11
Logic signal amplitudes	7
Analog transients due to preamp gain switching	6
Delay time from power-on to RO signals	5
Negative doppler rejection	3
Warm up time	1, 5
Mechanical test & inspection	---
Power consumption	---
Thermal sensor integrity	---

Table 5-5. Listing of the Buyer Flight Acceptance Tests

CHARACTERISTICS TESTED	Operating Conditions						HAC TEST REQ. NUMBER (see Appendix F)	NOTES*
	lab ambient	vibration	temperature	EMI	vibr. survival	prelaunch		
1. Ranging accuracy (waveguide simulator)	X					X	RA 135-1	1
2. Ranging accuracy (freespace simulator)						X	RA 136-1	2
3. RA klystron deviation width (high & low)	X		X			X	RA 116-1	
4. XMTR output power	X		X			X	RA 107/108-1	
5. XMTR output frequency	X		X			X	RA 105/106-1	4
6. Preamp output noise level & spurious outputs	X					X	RA 133/134-1	3
7. Preamp gain state logic & accuracy	X		X			X	RA 111-1/122-1	
8. Preamp gain state signal false output		X	X	X		X	RA 111-2	3
9. Reflectivity-output calibration at one freq.	X						RA 122-1	4
10. Reflectivity-output accuracy & repeatability			X			X	RA 122-2	4
11. Reflectivity-output in quiescent state		X		X		X	RA 122-3	3
12. Signal-tracking thresholds (sensitivity)	X					X	RA 109-1	4
13. Acquisition time						X	RA 124	
14. Analog output accuracy	X		X			X	RA 112-1, -2	4
15. False lock susceptibility and analog zero accuracy	X	X	X	X		X	RA 112-3/104-2	3
16. Analog output noise & ripple	X					X	RA 125/126-1	
17. Range mark accuracies	X		X			X	RA 114/115-1, -2	
18. Range mark false-lock susceptibility		X	X	X		X	RA 114/115-3	3
19. Reliability circuit logic & delay	X		X			X	RA 102/103-1, -3	
20. Reliability circuit false outputs		X	X	X		X	RA 102/103-2	3
21. Cross-coupled sidelobe logic						X	RA 129-1	
22. Waveguide leakage integrity	X				X	X	RA 123-1	3
23. Waveguide grounding	X	X				X	RA 127-1	
24. Warmup time from primary power to TX			X	X		X	RA 121-1	
25. Power consumption over input voltage range	X	X	X	X		X	RA 101-1	
26. Tracker-lock indication by TM	X		X			X	RA 104-1	
27. Unit temperatures indicated by TM	X	X	X	X		X	RA 117+120-1, -2	
28. Negative velocity and range rate rejection						X	RA 130-1	
29. Range mark lockout until 3.7 sec. after BO						X	RA 132-1	

* NOTES:

1. About 600-900 feet.
2. About 1700 feet equivalent free space distance. (both deviation modes)
3. Measured with the simulated return signal level below acquisition.
4. Test conducted with the KPSM undeviated.

VI. EVALUATION OF PRESENT TEST PROGRAM

A. INTRODUCTION

The definitions of various portions of the programs are reiterated below to help avoid possible misinterpretations:

1. Unit Verification Tests are performed on all flight units by the vendor, Ryan, prior to the acceptance tests detailed in Ryan report 51765-2B [60].

2. Unit (Flight) Acceptance Tests (FAT) are performed on all flight units by the vendor, Ryan, under cognizance of the buyer, Hughes, as detailed in Ryan report 51765-2B, parts II and III.

3. Vendor System (Flight) Acceptance Tests (FAT) are performed on all flight systems by the vendor, Ryan, under cognizance of the buyer, Hughes, as detailed in Ryan report 51765-2B, part I.

4. Buyer-Flight Acceptance Tests (FAT) are performed on all flight systems by the buyer, Hughes, at El Segundo and Cape Kennedy as detailed in Hughes report 3023926A [31].

5. "Flight-Readiness Tests" is a name used in this report to encompass all tests performed of flight units or systems; tests listed above are in this category.

6. Type Acceptance (or Approval) Tests (TAT) and Developmental Tests were performed on units or systems not intended for flight (see Section V.C).

7. "Special Tests" is a name used in this report to encompass all tests performed outside of the flight-readiness testing program.

B. COMPARISON OF TEST SPECIFICATIONS WITH MISSION REQUIREMENTS

1. Introduction

The purpose of this section is to determine whether environmental or functional conditions exist for which RADVS is not adequately tested. The study consists of two parts: The first compares environmental conditions simulated during the various test phases with the actual environment to be encountered during the various phases of the mission; no consideration is given to functional requirements RADVS must satisfy. In the second part, the operations to be performed by RADVS are compared with the test requirements.

The main reference for test specifications is the buyer FAT, which is outlined in Section V.D.3. and detailed in Appendix F.

2. Comparison of Simulated and Actual Environments

On the basis of the mission profile (sketched in Section III.B.), the various parts of the mission can be compared with the appropriate test phase.

(a) Pre-Launch (PL) Phase

In this phase, the main environmental condition RADVS has to withstand is the EMI at the launch pad. The S/C in the MS/EMI test phase, sequence three, goes through a real-time simulated flight during which it is commanded through all modes of operation. Therefore, the survival of RADVS to EMI in the PL and in the subsequent launch phase is automatically checked.

According to the HAC test specification, test levels are equal to or greater than those expected from all sources except the Centaur C-band radar transponder. This is of no great consequence to RADVS, however, because tests with the S/C telecommunications transmitter are at higher power density and nearly the same frequency. Furthermore, RADVS contains no pyrotechnic devices or other components that might fail due to low-level RF heating.

(b) Boost Phase

Static acceleration and acoustic environments expected during boost are not simulated in tests. The first of these is discussed in view of descent condition in a later section. The effect of the latter, acoustic pressure, during nonoperating conditions is expected to be less severe than vibration because of attenuation by the shroud and by the long propagation distance from the source. Also, the T-2N test indicates that nonoperating survival of acoustic environments is no great problem.

Boost vibration levels are expected to exceed those of the VIB phase of the buyer FAT. It appears, though, that the vendor unit acceptance tests are sufficient; a direct comparison cannot be made because of the unknown effects of structural resonances.

(c) Transit Phase

During the transit phase, the most severe environmental conditions RADVS must withstand are related to the combination of solar radiation and vacuum. Comparison of actual and test environments is as follows:

<u>Parameter</u>	<u>Actual Expected</u>	<u>Simulated</u>
Temperature of background:	-460 ^o F	-300 ^o F
Pressure:	10 ⁻¹² torr	5 x 10 ⁻⁶ torr
Incident flux:	130 w/ft ²	130 w/ft ² (variable)

The differences noted should have little effect on the temperature reached during transit; therefore, the survival of RADVS is sufficiently checked.

Radiation conditions expected in the Van Allen belt are not imposed in testing. A special test (TAT) should be sufficient for this case because susceptibility is

very unlikely to vary among systems of the same design. (Such a test appears to have been conducted with the T-21 vehicle, but details are lacking in the available documents.)

(d) Descent Phase

The shock and constant acceleration caused by retro-rocket ignition and burning are not simulated in test. The shock environment does not need to be considered separately because the rise time involved is slow compared to the response times of any RADVS components. Static acceleration is important, however, because it stresses every component and connection to a high degree. It is also a factor during boost, as mentioned, but the level during descent is about twice as high. Furthermore, RADVS is required to operate during descent.

The expected wideband vibration level due to all vernier engines is 10 pounds rms, which is much less than the total input of 60 pounds specified in the buyer FAT VEV phase. Relative to the vernier engine level alone, therefore, the VEV phase overtests by a factor of 6. For a typical S/C weight during VEV of 650 pounds, the corresponding acceleration level (roughly) is $60/650 \approx 0.1$ g-rms. Since this closely compares with the 0.2 g level expected during retro burning, the VEV phase probably yields a sufficient test of wideband vibration during descent.

No tests are ever conducted on flight systems in which RADVS operation during sinusoidal vibration is checked. If the HAC environmental specification ([5], Section 3.2.3.4) is realistic, then such a test should be added. An easy place would be in the buyer FAT VIB phase, where levels are near those expected during descent.

Temperature and pressure are essentially the same at the beginning of descent as during transit. After turn-on, RADVS temperatures rise. This condition is realistically tested in the STV-TD phase of buyer FAT.

3. Comparison of Test and Actual Functional Requirements

The JPL Surveyor System Specification (No. 30240) and HAC procurement and detail specifications [1,23] are written in terms of functional requirements. From these, requirements of frequency, spectral width, and power for signals used in simulations must be determined. The computation of frequencies is usually straight-forward, and the determination of spectral width is easily approximated to usable accuracy. The determination of power, although straight-forward, involves the estimation of unknowns; the results, therefore, are not strictly enforceable. Nevertheless, test power levels must be examined.

Computations are based on the following factors:

- (a) transmitter power, DVS: 31.8 dbm

- (b) transmitted power, RA: 24.0 dbm
- (c) antenna gain (one way), both: 28.0 db
- (d) minimum Muhleman reflection coefficient: -7.1 db

Since spread spectra are not generally used in tests, the spectral spreading loss must also be computed. This is accomplished by assuming the spectra to have a Gaussian shape and the filters to have rectangular passbands with widths:

- (a) for DVS before burnout: 3 kHz
- (b) for DVS after burnout: 600 Hz
- (c) for RA before deviation signal: 4 kHz

The 3 db width of the assumed signal spectrum is

$$\Delta f = \frac{2V}{\lambda} (\Delta\theta) \sin\theta \quad (6-1)$$

where V is the velocity magnitude, λ is the free space signal wavelength, $\Delta\theta$ is the two-way antenna beamwidth, and θ is the angle between beam centerline and velocity vector [68].* Representative figures for the angle, θ , can be obtained by assuming an angle of 45° between roll axis and lunar vertical, and 44° between the velocity vector and vertical at start of retro-fire. If the initial velocity is 8,800 fps and if the S/C retains its attitude relative to the lunar vertical throughout retrofire, then results for a beam at the worst roll angle are as shown in Fig. 6-1. (See Fig. 6-2 for relationships assumed.) Initial misalignments of velocity and roll axis a few times greater than the 1° assumed for Fig. 6-1 results in little change for velocities above about 750 fps. Below 750 fps, the change would be noticeable but not great.

a. DVS Beam Power

One of the worst conditions of available power occurs when the return power is lowest and the spectrum is widest. The maximum range for a beam occurs when the vehicle is at the maximum operating slant range of 50 kft and its attitude with respect to the lunar vertical is 45° [1]. The worst-case beam is then at an angle of 70° with the lunar vertical. The return power for this beam is computed as follows [50, and HAC IDC 2253.3/359]:

*Equation 6-1 is a valid approximation for $\theta \geq \frac{\Delta\theta}{2}$ and $\Delta\theta$ less than about 15° .

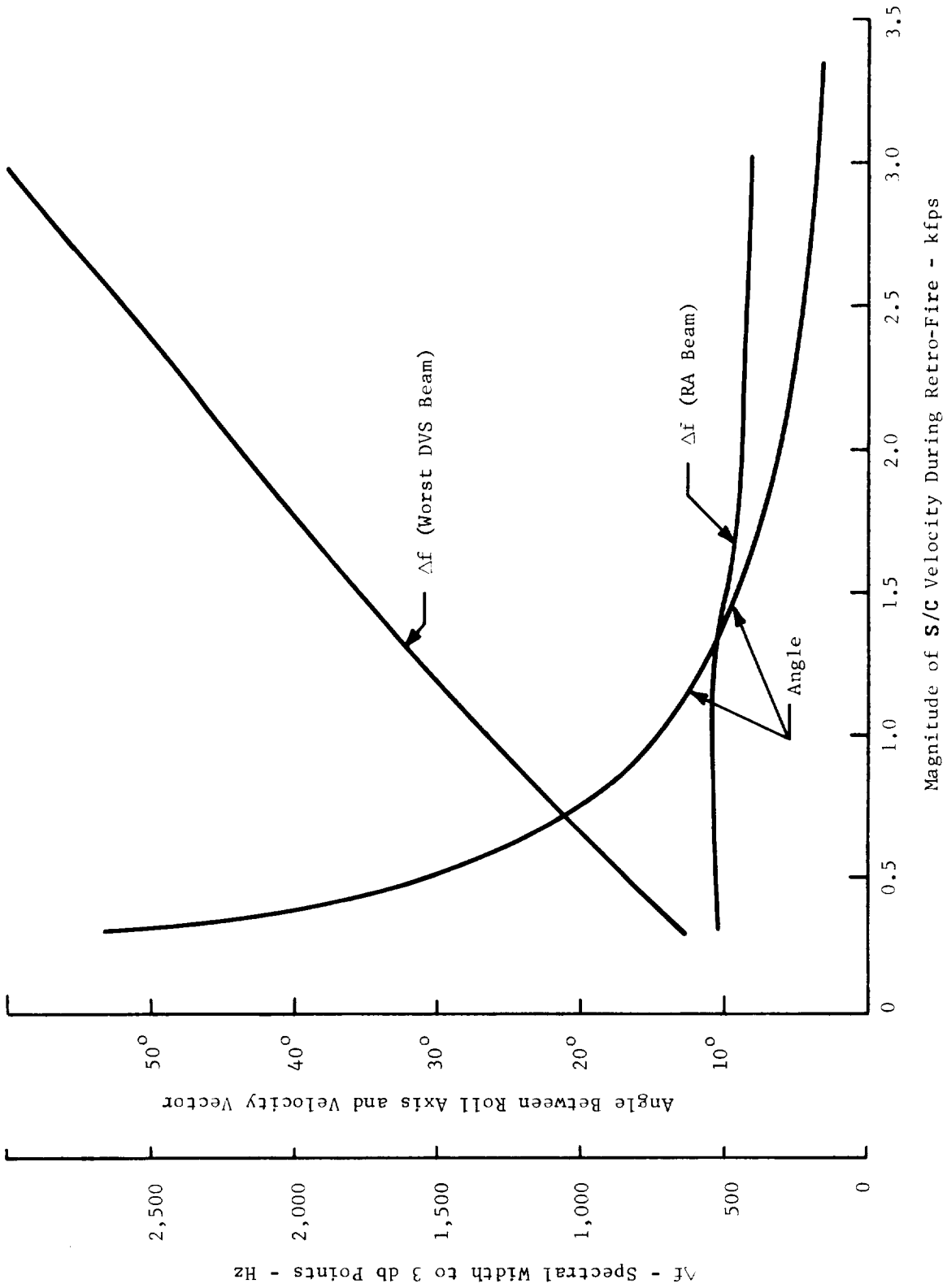


Fig. 6-1. Spectral width and velocity misalignment angle vs velocity magnitude. (See Fig. 6-2 for relationships assumed.)

$\frac{P_t G \lambda^2}{2(4\pi)^2}$	→	+12.1 dbm
$[50 \text{ kft} \cos 45^\circ \sec 70^\circ]^{-2}$	→	-100.3 db
Muhleman reflectivity coefficient	→	-7.1 db
Muhleman reflectivity factor at 70°	→	-13.2 db
<hr/>		
Received power at 50 kft, 45° attitude	=	-108.5 dbm

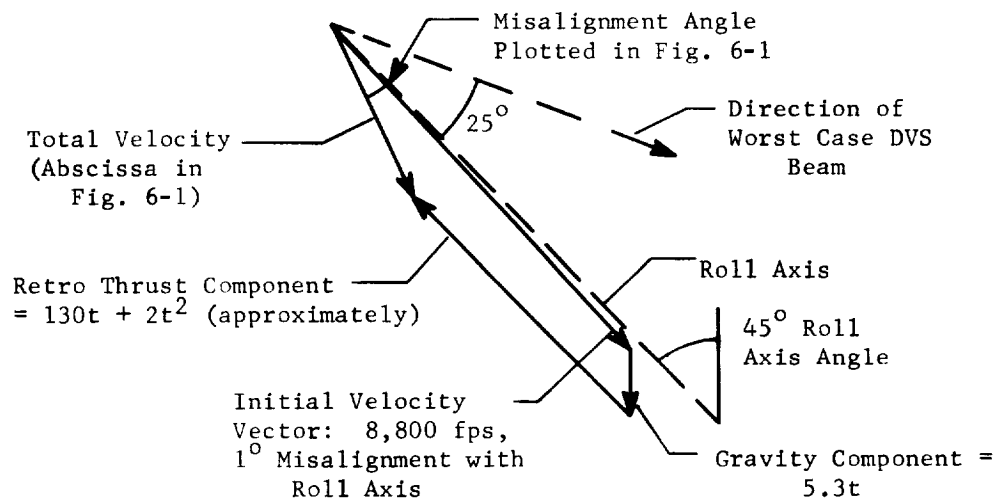


Fig. 6-2. Relationships assumed to computed curves of Fig. 6-1.

Fig. 6-1 shows that the worst case of spectral spreading occurs for maximum velocity. Before burnout, the maximum velocity at which the DVS is to operate is 3,000 fps. This yields a spectral spreading loss of about 1.1 db. After burnout, the maximum velocity requirement is 850 fps. The loss for this case (with the narrower pass-band) is the same, 1.1 db. Therefore, tests with narrow (line) spectra should require operation at -109.6 dbm.

The situation before burnout is simulated in STC 1 at levels of -106 dbm and -111.4 dbm in the vendor and buyer tests, respectively (see Appendices B and F). The condition after burnout is not simulated completely, but no real difference of performance would be expected between the 3,000 fps and 850 fps simulations.

Another problem condition occurs at low frequencies where preamp roll-off causes loss of power. The minimum beam components of velocity for which acquisition ability is required vary linearly from 62 fps at 50 kft to 29.6 fps at 34 kft, and then remain constant at 29.6 fps [1, Section 4.6.3.1.7.2]. Since spreading losses

are negligible here, the representative powers to be simulated are (at 70° angle of incidence):

<u>V_{beam}</u>	<u>R</u>	<u>P_r</u>
62 fps	50 kft	-108.5 dbm
38 fps	40 kft	-106.6 dbm
34.4 fps	38.5 kft	-106.2 dbm (STC 8)
29.6 fps	34 kft	-105.1 dbm

The worst situation is the -105.1 dbm level at 34 kft because the preamp roll off is about 12 db/octave, while the gain due to range reduction is only 6 db/octave. The doppler frequency for 29.6 fps is about 800 Hz. The closest test condition is STC 8, which has beam frequencies at 930 Hz. The maximum range at which this frequency must be acquired is 38.5 kft. Since the difference in preamp gain between 930 Hz and 800 Hz is 3.8 db while the difference in altitude is only 1.1 db, the level for STC 8 should be -108.8 dbm in order to check the worst case due to preamp roll-off. This is to be compared with -104 dbm and -103 dbm for the vendor and buyer test specifications, respectively.

b. RA Beam Power

Fig. 6-1 shows that the maximum spreading of the RA return spectrum (due to doppler shift) remains somewhat less than the wideband acquisition bandwidth. Consequently, it need not be considered.

The high altitude case is computed as follows:

$$\frac{P_t G \lambda^2}{2(4\pi)^2 (40\text{kft})^2} \longrightarrow -87.4 \text{ dbm}$$

Muhleman reflectivity coefficient $\longrightarrow -7.1 \text{ db}$

Muhleman reflectivity factor at 45° $\longrightarrow 12.1 \text{ db}$

Received power at 40 kft, 45° attitude = -106.6 dbm

This figure is to be compared with values in STC 2, which are -104 dbm and -113.3 dbm in the vendor and buyer test specifications, respectively.

The worst case of low frequency acquisition occurs when both range and roll-axis velocity are minimal. Specifications require operation at roll-axis velocities down to +1 fps [1, Section 4.6.4.1.7]. At a 1,000 ft range, the return power would be -74.6 dbm. No test condition approaches this combination of range, velocity, and power; a more realistic check is made in STC 7 with $V_z = 100$ fps, however.

c. Returns from Retro-tankage

The relative velocity between S/C and ejected retro-tankage can be computed for a number of vernier thrust profiles if the tankage is assumed to be in free-fall. For this case, the main problem is the assignment of power density levels in possible situations involving near field and/or minor lobe structures. The effort of such an analysis, however, would not be justified because of the doubtfulness of the free-fall assumption.

One reason for questioning this assumption is because of the momentary unlock of beam 3 during the descent of Surveyor 1. (If the tankage had been in free-fall, the chance of breaking a DVS beam prior to appreciable attitude correction would have been virtually zero.) The fact that unlock occurred so soon after retro eject makes it appear that the two events are correlated. However, quantization of the telemetered data seems to preclude complete knowledge of what happened and an analysis of how it happened. For example, if retro entry into the beam 3 did indeed cause the unlock through shadowing or gain-state switching (which might have been missed in the telemetered signal), then how did the retro-tankage enter the beam so shortly after eject (a matter of about two seconds). This might be explained if the retro engine thrust was still "tailing" off. For such a condition, it appears that computation of a velocity-power profile for retro signals into a given beam would be very difficult, and probably would have to be of a Monte Carlo type.

The foregoing discussion shows that the adequacy of present flight-readiness tests cannot be meaningfully evaluated from the available information. Consequently, the situation is reconsidered in view of the special test program in Sections VI.B.3 and VII. Pertinent tests in the current flight-readiness program are listed below for reference.

Vendor Tests

DVS: -59 fps beam velocity (-1.6 kHz),
-50 dbm (ref: STC 3)
RA: -3.5 kHz, -113 dbm (ref: STC 3)

Buyer Tests

DVS: opening velocity of 65 fps
or less, -50 dbm or less (ref: RA130-1)
RA: receding target of 3.5 kHz or
less, -113 dbm or less (ref: RA130-1)

4. Summary of Comparisons

The significant discrepancies found between mission requirements and test requirements are collected together in Table 6-1; other conflicts have already been discussed and discarded. Further discussion of Table 6-1 is withheld until Section VII, where recommendations are made.

Table 6-1. Listing of Significant Discrepancies Between Mission Requirements and Test Requirements

MISSION REQUIREMENT	TESTING DISCREPANCY
1. Survive Van Allen belt radiation.	1. Details of the T-21 test need be reviewed to determine the need for a special test.
2. Survive static acceleration of boost; operate during static acceleration of retro-fire.	2. No test in flight readiness program.
3. Operate during vibration during retro-fire.	3. Wideband vibration tests are performed; narrow band vibration per HAC spec. 224800 is not checked.
4. Operate on available return power for all situations within specification.	4. Possible return levels of low frequency signals are not simulated.
5. Operate in presence of retro rocket tankage separation.	5. Possible conditions are questionable.

C. COMPARISON OF PRESENT AND "DESIRABLE" PROGRAMS

1. Introduction

Objective evaluation of the present program can be accomplished by comparing it with the "desirable" program generated in Section IV; although the "desirable" program might have defects of its own, it is complete enough to afford a thorough analysis. Comparison is performed in two steps;

- (a) Overall contents of the programs are compared under the assumption that all tests listed are adequately performed.
- (b) Each point of comparison is reviewed to determine adequacy of meeting requirements.

The first step mainly consists of juxtaposing tables and details from Sections IV and V. The second requires examination of the assumptions behind developments in IV, consideration of the actual test configurations in V, and notice of the comparisons in Section VI.B.

2. Flight-Readiness Test Programs

Step (a) of the flight-readiness program comparison is handled by overlaying Tables 5-3, 5-4, and 5-5 on Table 4-3; the consolidated effect is presented in Table 6-2. Apparent inconsistencies are easily recognized in this display. Their interpretation, however, requires the analysis outlined as step (b) of the comparison.

Preliminary to step (b) the STEA signal simulation technique, which is used in almost all flight-readiness tests, was examined. The basic finding was that previously assumed characteristics of proper spectral shape are not fulfilled in such tests. (Details are given in Appendix G.) This factor must be considered in determining test adequacy.

The detailed review completing step (b) is listed below. Some of these items will be elaborated upon in Section VII, Suggested Test Modifications.

ENTRY NO.	DISCUSSION
1.	XMTR frequency coherence: Coherence problems are not very evident at low altitudes and completely disappear in the STEA technique, as discussed in Appendix G. No pertinent tests have been or are being performed in the Surveyor program.
2.	XMTR amplitude modulation: Unit level tests in vibration and temperature were placed in the desirable program for convenience but can be waived in lieu of thorough system tests.

ENTRY
NO.

DISCUSSION

-
3. Other spurious outputs from KPSM: This item is adequately checked in unit testing and will be implicit in system performance tests.
- 4a. Klystron sweep linearity: As noted in Appendix G, sweep non-linearity effects are altitude dependent. The current ranging tests might give some indication, but more extensive tests are desirable. STEA tests do not check sweep linearity.
- 4b. Klystron average sweep rate: Rate measurement is included in the desired vibration and acceleration tests because rate is not otherwise indicated. The extra three tests under lab ambient conditions are not necessary because rate is directly indicated by analog output accuracies.
5. XMTR output power: Measurement is called for during unit environmental tests because no other gross indication of proper klystron operation is obtainable. The unit temperature test missing in the present program can be waived in lieu of the system temperature test. The two extra lab ambient tests in the current program are totally redundant.
6. XMTR output frequency: Average frequencies read on a wave meter indicate little about operation, except large changes can be expected to have concomitant decreased analog output accuracy (in actual use), lowered power levels, and increased spurious sideband generation. The characteristic most sensitive to shift of average frequency, analog output accuracy, is completely insensitive in STEA simulations because true propagation is missing. Consequently, frequency should be checked in all environments except EMI, which is not expected to change average values a noticeable amount. The current extra lab ambient tests are redundant; the prelaunch test is reasonable, though, because it is so simple.
7. Production of stray fields: In the overall program no requirement is placed on EMI generation. Therefore, testing might be deleted with the assumption that action would be taken if noticeable problems would occur.
8. Blanking signal characteristics: These tests were desirable at the unit level for convenience only. Acquisition tests with a realistic range signal will test the effect of blanking.
9. Antenna patterns: Present testing appears to match the "desired" program.

ENTRY
NO.

DISCUSSION

-
10. Transmitter-receiver leakage: This portion of the program is as intended. Tests with both antennas on an assembled S/C still must be considered.
11. Insertion loss/VSWR: Problems could occur during different environments but they would appear as lower power levels or lower sensitivity. Therefore, the unit test is sufficient.
12. Noise figure: The effects of noise figure normally show up in sensitivity measurements. A measurement during acceleration is desired, though, because this environment probably can be imposed only at the unit level.
13. Preamp branches gain and phase balance: Present tests are sufficient because effects are also indicated in analog accuracy and false lock measurements.
14. Preamp gain stability with time: This test is implicit in the frequent checking of reflectivity calibration and system sensitivity.
15. Preamp passband shape: Unit level tests are adequate because sensitivity tests at various frequencies accomplish system level checks.
16. Preamp gain selection accuracy: If accuracy and sensitivity tests were run at many different power levels, separate system level gain selection tests would be superfluous. Since this probably won't be the case, environmental testing of this item should be complete.
17. Spurious outputs from R/T units: The outputs, in themselves, are secondary to their effects on false locks, analog accuracy, and sensitivities. Since these effects are to be checked at the system level, there is no need to check for spurious outputs beyond the unit level.
- 18a. Reflectivity-output calibration (stability): The present test program essentially matches the desired one.
- 18b. Reflectivity-output ripple: No direct specification of ripple exists. Since large values will be evident to the test operator when measuring with the DVM, this phase need not be added to the program.

ENTRY
NO.

DISCUSSION

19. Tracker search range and rate: These items might be covered in thorough acquisition tests at the system level. Nevertheless, since they should be easy to perform and they indicate the time constant of the tracking loop integrator, their addition to the unit test program is reasonable.
20. Signal-tracking threshold operation (sensitivity): Only the lab ambient unit verification tests use spread spectra in the present program. All other tests either apply sinusoids or no signal; the latter is the case in the system environmental tests. Consequently filter bandwidths, threshold circuit operation, klystron AM effects, preamp gain and phase balance, preamp gain selection operation, tracker search range, and blanking circuit operation are not checked in system environmental simulations.
21. Operation times of DTC circuits: These delay times are not explicit system requirements, but they appear to be necessary for proper operation with real signals. (No documented test exists in which they are checked.) Temperature might affect timing without being otherwise evident. Other environmentally induced defects will be easily discernable in other tests.
22. Delay time for filter BW change in RA: A delay between deviation signal and bandwidth change of the low pass filter in the RA tracker was evidently found necessary to help insure proper operation in real use. No documented test of this characteristic exists. A check for large variations with temperature would be reasonable.
- 23a. Analog output accuracy: The main discrepancy is the lack of a vibration test and an EMI test in the present program. Accuracy tests indicate whether spurious signals and/or noise tending to offset the center of the spectrum being tracked are present. Accuracy also indicates the tracking loop gain value. The fact that realistic spectra are not used in most tests means that converter circuitry is not fully checked for response range.
- 23b. Analog output noise and ripple: Environmental tests are lacking except for the unit FAT vibration test. All tests should be run with spread spectrum simulation because this checks the tracking loop bandwidth and converter response range.

ENTRY
NO.

DISCUSSION

- 24a. Range mark accuracies: Range mark accuracy indicates proper operation of the mark circuitry and shows whether noise is appearing on inputs. Therefore, all environments should be imposed. Extra lab ambient tests do not seem to add much information as long as analog accuracy is being checked.
- 24b. Range mark susceptibility to false mark: These tests are performed with no signal input in the present program. Tests with spread spectra would impose realistic conditions for checking environmental effects on the mark circuitry.
25. Reliability circuit logic operations: The present program is in basic agreement with the desired program, except for the EMI test; logic circuitry might be quite susceptible to EMI. A check during acceleration would test integrity of the circuitry.
26. Cross-coupled sidelobe logic operation: Environmental tests of the cross-coupled sidelobe discrimination circuitry are missing from the present program. The many gates and threshold detectors should be checked during the operating environments. Operation of the circuitry making the frequency test should be tested with spread spectra.
27. Waveguide assembly performance: The two test programs essentially agree.
28. System warmup time: No reason for checking warmup time during the EMI test is evident.
29. System power consumption: Extra tests in the present program appear to be superfluous except, perhaps, to help assure that connections to STEA are correct.
- 30.-
37. Miscellaneous: The first four tests in this group are fitting assurance checks at the vendor level. The others were considered to be included in other tests already listed.
38. Ranging tests: The procedure used in the present ranging tests generally excludes checking blanking signal effectiveness. The distances used are not great enough to make frequency coherence problems evident. Problems due to AM would be no more apparent than STEA tests. Some information about sweep rate and linearity is obtained, however. This topic will be further discussed when considering test modifications.

ENTRY
NO.

DISCUSSION

-
39. Power supply transits: Although some tests are run at the extremes of supply voltage levels, no checks are made of transients effects.
-

3. Special Test Programs

Each area of the special test programs is compared separately as follows:

a. Transmitter- Receiver Leakage Tests

The discussion of Section IV concluded that testing of plume effects on leakage is probably not feasible, except in actual flight. The favored earth-bound alternative was decided to be an upsidedown vibration test. This latter type of test was performed using the S-8 vehicle.

The S-8 tests simulated vernier engine vibration levels based on available information. Levels used in the "desired" test would either be based on S/C-1 flight data or at least on more recent data. It appears that levels during retro fire should also be simulated if operation during this phase is desired.

Processing of the S-8 data appears to coincide with the "desired" test procedure. Subsequent analysis of S-8 test data seemed to lack determination of the desensitization caused. Margins by which the trackers avoided false lock also were not readily available.

Finally, the differences between the test equipment and present flight equipment should be reviewed.

b. Flight Tests

The desired flight test described in Section IV appears to have been fulfilled in the T-2H program. A small amount of additional knowledge was gained from the T-2N descent tests, but these tests were of main value to the flight control and vernier engine systems.

c. Interfering Signal Tests

Thorough testing in this area was specified in the "desirable" test program. No such effort in the present program is evident from the available documentation. The only related tests are:

- (1) The CCSL circuitry was caused to operate in the T-2H tests in flights over water.
- (2) A single negative doppler simulation is performed in vendor and buyer system FAT (see Appendix E, STC-3; Appendix F, test RA 130-1).

Table 6-2. Comparison of Present and "Desirable" Flight-Readiness Test Programs

Legend: = entry in "Desired" program. = tested in system FAT.
 = tested in unit verification tests. = major inconsistencies of programs. (see test of comparison, step b).
 = tested in unit FAT.

CHARACTERISTICS	Unit Level				System Off S/C (At Vendor)		System On S/C (At Buyer)			Survival	Pre-launch	
	Lab Amb.	Accel.	Vibr.	Temp.	Lab Amb.		Lab Amb.	Vibr.	Temp.			EMI
1. XMTR frequency coherence	<input checked="" type="checkbox"/>	<input checked="" type="checkbox"/>	<input checked="" type="checkbox"/>	<input checked="" type="checkbox"/>			<input checked="" type="checkbox"/>					
2. XMTR amplitude modulation	<input checked="" type="checkbox"/>	<input checked="" type="checkbox"/>	<input checked="" type="checkbox"/>	<input checked="" type="checkbox"/>			<input checked="" type="checkbox"/>					
3. Other spurious outputs from KPSSM	<input checked="" type="checkbox"/>	<input checked="" type="checkbox"/>	<input checked="" type="checkbox"/>	<input checked="" type="checkbox"/>			<input checked="" type="checkbox"/>					
4a. Klystron sweep linearity	<input checked="" type="checkbox"/>	<input checked="" type="checkbox"/>	<input checked="" type="checkbox"/>	<input checked="" type="checkbox"/>			<input checked="" type="checkbox"/>					
4b. Klystron average sweep rate	<input checked="" type="checkbox"/>	<input checked="" type="checkbox"/>	<input checked="" type="checkbox"/>	<input checked="" type="checkbox"/>			<input checked="" type="checkbox"/>					
5. XMTR output power	<input checked="" type="checkbox"/>	<input checked="" type="checkbox"/>	<input checked="" type="checkbox"/>	<input checked="" type="checkbox"/>			<input checked="" type="checkbox"/>					
6. XMTR output frequency	<input checked="" type="checkbox"/>	<input checked="" type="checkbox"/>	<input checked="" type="checkbox"/>	<input checked="" type="checkbox"/>			<input checked="" type="checkbox"/>					
7. Production of stray fields	<input checked="" type="checkbox"/>	<input checked="" type="checkbox"/>	<input checked="" type="checkbox"/>	<input checked="" type="checkbox"/>			<input checked="" type="checkbox"/>					
8a. Blanking signal amplitude, width, risetime	<input checked="" type="checkbox"/>	<input checked="" type="checkbox"/>	<input checked="" type="checkbox"/>	<input checked="" type="checkbox"/>			<input checked="" type="checkbox"/>					
8b. Blanking signal timing	<input checked="" type="checkbox"/>	<input checked="" type="checkbox"/>	<input checked="" type="checkbox"/>	<input checked="" type="checkbox"/>			<input checked="" type="checkbox"/>					
9. Antenna patterns	<input checked="" type="checkbox"/>	<input checked="" type="checkbox"/>	<input checked="" type="checkbox"/>	<input checked="" type="checkbox"/>			<input checked="" type="checkbox"/>					
10. Transmitter-receiver leakage	<input checked="" type="checkbox"/>	<input checked="" type="checkbox"/>	<input checked="" type="checkbox"/>	<input checked="" type="checkbox"/>			<input checked="" type="checkbox"/>					
11. Insertion loss/VSWR	<input checked="" type="checkbox"/>	<input checked="" type="checkbox"/>	<input checked="" type="checkbox"/>	<input checked="" type="checkbox"/>			<input checked="" type="checkbox"/>					
12. Noise figure.	<input checked="" type="checkbox"/>	<input checked="" type="checkbox"/>	<input checked="" type="checkbox"/>	<input checked="" type="checkbox"/>			<input checked="" type="checkbox"/>					
13. Preamp branches gain and phase balance	<input checked="" type="checkbox"/>	<input checked="" type="checkbox"/>	<input checked="" type="checkbox"/>	<input checked="" type="checkbox"/>			<input checked="" type="checkbox"/>					
14. Preamp gain stability with time	<input checked="" type="checkbox"/>	<input checked="" type="checkbox"/>	<input checked="" type="checkbox"/>	<input checked="" type="checkbox"/>			<input checked="" type="checkbox"/>					
15. Preamp passband shape	<input checked="" type="checkbox"/>	<input checked="" type="checkbox"/>	<input checked="" type="checkbox"/>	<input checked="" type="checkbox"/>			<input checked="" type="checkbox"/>					
16. Preamp gain selection accuracy	<input checked="" type="checkbox"/>	<input checked="" type="checkbox"/>	<input checked="" type="checkbox"/>	<input checked="" type="checkbox"/>			<input checked="" type="checkbox"/>					
17. Spurious outputs from R/T units	<input checked="" type="checkbox"/>	<input checked="" type="checkbox"/>	<input checked="" type="checkbox"/>	<input checked="" type="checkbox"/>			<input checked="" type="checkbox"/>					
18a. Reflectivity-output calibration (stability)	<input checked="" type="checkbox"/>	<input checked="" type="checkbox"/>	<input checked="" type="checkbox"/>	<input checked="" type="checkbox"/>			<input checked="" type="checkbox"/>					
18b. Reflectivity-output ripple	<input checked="" type="checkbox"/>	<input checked="" type="checkbox"/>	<input checked="" type="checkbox"/>	<input checked="" type="checkbox"/>			<input checked="" type="checkbox"/>					
19a. Tracker search ranges	<input checked="" type="checkbox"/>	<input checked="" type="checkbox"/>	<input checked="" type="checkbox"/>	<input checked="" type="checkbox"/>			<input checked="" type="checkbox"/>					
19b. Tracker search rates	<input checked="" type="checkbox"/>	<input checked="" type="checkbox"/>	<input checked="" type="checkbox"/>	<input checked="" type="checkbox"/>			<input checked="" type="checkbox"/>					
20. Signal-tracking threshold operation (sensitivity)	<input checked="" type="checkbox"/>	<input checked="" type="checkbox"/>	<input checked="" type="checkbox"/>	<input checked="" type="checkbox"/>			<input checked="" type="checkbox"/>					
21. Operation times of DTC circuits	<input checked="" type="checkbox"/>	<input checked="" type="checkbox"/>	<input checked="" type="checkbox"/>	<input checked="" type="checkbox"/>			<input checked="" type="checkbox"/>					
22. Delay time for filter BW changes in RA	<input checked="" type="checkbox"/>	<input checked="" type="checkbox"/>	<input checked="" type="checkbox"/>	<input checked="" type="checkbox"/>			<input checked="" type="checkbox"/>					
23a. Analog output accuracy, linearity, stability	<input checked="" type="checkbox"/>	<input checked="" type="checkbox"/>	<input checked="" type="checkbox"/>	<input checked="" type="checkbox"/>			<input checked="" type="checkbox"/>					
23b. Analog output noise and ripple	<input checked="" type="checkbox"/>	<input checked="" type="checkbox"/>	<input checked="" type="checkbox"/>	<input checked="" type="checkbox"/>			<input checked="" type="checkbox"/>					

Table 6-2. Continued.

CHARACTERISTICS	Unit Level				System Off S/C (At Vendor)		System On S/C (At Buyer)				Survival	Prelaunch	
	Lab Amb.	Accel.	Vibr.	Temp.	Lab Amb.		Lab Amb.	Vibr.	Temp.	EMI			
24a. Range mark accuracies	/	/	/	/	/	/	/	/	/	/	/	/	/
24b. Range mark susceptibility to false mark	/	/	/	/	/	/	/	/	/	/	/	/	/
25. Reliability-circuit logic operations, etc.	/	/	/	/	/	/	/	/	/	/	/	/	/
26. Cross-coupled sidelobe logic operations	/	/	/	/	/	/	/	/	/	/	/	/	/
27. Waveguide assembly performance	/	/	/	/	/	/	/	/	/	/	/	/	/
28. System warmup time	/	/	/	/	/	/	/	/	/	/	/	/	/
29. System power consumption	/	/	/	/	/	/	/	/	/	/	/	/	/
30. KPSM HV time delay	/	/	/	/	/	/	/	/	/	/	/	/	/
31. Klystron supply voltage level, regulation, ripple	/	/	/	/	/	/	/	/	/	/	/	/	/
32. Response time of system to input step	/	/	/	/	/	/	/	/	/	/	/	/	/
33. LVPS output amplitudes and ripple	/	/	/	/	/	/	/	/	/	/	/	/	/
34. Analog transients due to preamp gain switch	/	/	/	/	/	/	/	/	/	/	/	/	/
35. Negative doppler rejection	/	/	/	/	/	/	/	/	/	/	/	/	/
36. Range mark lockout until after B0 (delay)	/	/	/	/	/	/	/	/	/	/	/	/	/
37. Preamp gain state signal false output	/	/	/	/	/	/	/	/	/	/	/	/	/
38. Ranging tests	/	/	/	/	/	/	/	/	/	/	/	/	/
39. Power supply transients	/	/	/	/	/	/	/	/	/	/	/	/	/

Unless further tests are uncovered, the present program must be regarded as deficient in this area.

d. Environmental Overtesting

Although environmental overttesting took place in both vendor and buyer TAT, no statistical significance appears to be ascribable to the results. Levels used seem to be based on estimated flight conditions rather than being varied to determine operational dependences. The amount of instrumentation seems to have been minimal for assuming that complete failure would be recognized.

Fatigue-type testing is lacking in the present program according to available documentation.

D. DOCUMENTATION ADEQUACY

At all levels of testing (unit verification, unit flight acceptance, and system flight acceptance), it appears that the testing requirements are clearly defined and documented. However, the test procedures and equipment setups are not completely documented. With regard to systems tests, it appears that this shortcoming is being remedied (Hughes is in the process of preparing test procedures). A more serious deficiency appears to be in the documentation of procedures and equipment setups for the unit tests; this documentation is believed to be important because the unit test equipment and setups are not consolidated into permanent assemblies as completely as equipment for systems tests.

E. TESTING CONSISTENCY

It has been found that testing at the various levels is generally consistent. One exception appears to be in the method of specifying radar acquisition sensitivity. The system specification to the vendor is given in terms of altitude performance over a range of entry angles. This method leaves open a number of possible questions, such as choice of the lunar reflectivity model and extremes of attitude and velocity during entry. A more precise specification would be a simple curve of acquisition sensitivity versus doppler frequency derived from current knowledge of the lunar surface and anticipated mission requirements. Since sensitivity numbers appear to be in a state of flux, it is believed that the suggested method of specification should be employed and documented at an early date.

VII. SUGGESTED TEST MODIFICATIONS

A. FLIGHT-READINESS PROGRAM

1. Changes in Content

Suggested modifications to the flight-readiness test program are based mainly on the discussions of Section VI. In particular, Table 6-1 provides a listing of important factors. The significant entries of this table are recast into Table 7-1 to show which actions are suggested in the specific cases. A number of these results are discussed further below; for additional comments, Section VI should be consulted.

a. Unit Constant Acceleration Test

In the present program the only appreciable mechanical stress imposed upon the system while operating is due to wideband random vibration. No operating tests are performed during the narrow-band vibration or constant acceleration conditions listed in the environmental conditions specification [5, Sections 3.2.3.3 and 3.2.3.4]. Determination of which condition creates the greatest stress of each component or connection must be based on the mechanical transfer functions between the input points and the element in question. Although such specific information is not available, the nature of the response characteristic might be reasoned as follows: Since the paths between the input forces and any given element are made up of many components of different sizes and materials, the associated transfer functions would be expected to have poles and zeros spread over a wide frequency range. At the same time, the variation of damping constants would not normally be great for solid components. Consequently, because functions with the characteristics described do not have sharply defined resonances, both narrow-band and wideband inputs would be expected to have effects which are mainly dependent on their total power levels. When applying this reasoning to consideration of the retro descent phase, constant acceleration appears to be the most severe; the levels specified are:

constant acceleration @ 10.8 g \rightarrow $117g^2$
sinusoidal vibration @ 1.4 g rms \rightarrow $2g^2ms$
wideband vibration @ 0.2 g rms \rightarrow $0.04g^2ms$

(Driving point impedances must be considered before definite statements of power levels can be made, but it is unlikely that a large difference will be noted.)

The foregoing discussion shows that the constant acceleration environment might easily induce the greatest mechanical stress on components and connections. For this reason addition of such a test to the flight-readiness program is suggested.

Table 7-1. Listing of Suggested Changes to the Present Flight-Readiness Test Program

Legend: a = suggested test addition
 d = suggested test deletion
 d* = deletion is suggested, but retention would have little effect on program
 r = suggested test revision for added realism

CHARACTERISTICS TO BE EXAMINED	Unit Level				System Off S/C (At Vendor.)		System On S/C (At Buyer)				Survival	Prelaunch	
	Lab Amb.	Accel.	Vibr.	Temp.	EMI	Lab Ambient	Lab. Amb.	Accel.	Vibr.	Temp.			EMI
1. XMTR frequency coherence	a	a	a	a									
4a. Klystron sweep linearity & width	a	a	a	a									
4b. Klystron sweep rate						d						d	
5. XMTR output power						d*							
6. XMTR output frequency						d*							
12. Noise figure													
16. Preamp gain selection accuracy						d						d	
17. Spurious outputs from R/T units												d	
19. Tracker search ranges and rates													
20. Signal-tracking threshold operation (sensitivity)	a	a	r	r									
21. Operation times of DTC circuits	r	a	r	r								r	
22. Delay time for filter BW change in RA	a												
23a. Analog output accuracy	a			a									
23b. Analog output noise and ripple													
24a. Range mark accuracies													
24b. Range mark susceptibility to false mark													
25. Reliability circuit logic operations						d						d*	
26. Cross-coupled sidelobe logic operations													
28. System warmup time													
29. System power consumption						d							
39. Power supply transients						a							

Furthermore, operation during the imposed environment is preferred because certain likely faults would tend to be present only during the acceleration; an example would be failures due to faulty circuit board connections.

A centrifuge would be a natural choice for performing the suggested test. In fact, the test was indicated at the unit level in the "desirable" program to minimize the requirements on the centrifuge. If a large enough centrifuge to carry the whole RADVS system and test jig is available, however, a system test would be preferred.

The obtaining of KPSM RF outputs during a centrifuge test would be impractical. As an alternative, power and frequency could be measured by mounting a power meter (with DC output) and a wavemeter on the centrifuge arm. Sweep linearity measurement could not be accomplished in this case, but sweep rate could be determined by detecting amplitude modulation (probably with a little added circuitry).

A simple, accurate method of checking preamp gain selection is not evident. Other operations of the R/T units could be checked, however, by mounting a KPSM (or other source) on the centrifuge arm. Modulation could be applied to give a sinusoidal AM output, which would permit quantitative testing of the preamplifier output during constant acceleration.

Full operational testing of SDC units is possible assuming that slip ring noise could be made negligible.

b. Other Test Additions

Most of the suggested test additions are concerned with more complete system environmental testing. These items were probably omitted from the present program because their measurement was not compatible with use of the S/C telemetry link. Nevertheless, they cannot be ignored if a reasonable confidence of success is desired (See Section VI).

In the case of temperature (STV) and EMI (MS/EMI) tests, RF access is already provided. The addition of extra hardline to handle the added test requirements would not be expected to affect the simulations appreciably. (An alternative would be addition of an on-board recorder.)

The existing vibration (VEV) test does not provide RF access to RADVS. Addition of this access through flexible waveguide appears quite feasible, however. Alternatively, much of this testing could be transferred to the unit level. The desired result could be obtained by "equalizing" the shaker drive to simulate the presence of the spacecraft.

The purpose of certain additions (items 19, 21, 22, and 39 of Table 7-1) is to fill apparent gaps in the existing program. No special problems are anticipated in fulfilling these requirements. The addition of klystron coherence and sweep linearity measurements (items 1 and 4a, Table 7-1) is to fill gaps caused by the inability of providing true time delay in the present signal simulation equipment.

The effect of this deficiency, which is fully discussed in Appendix G, is to ignore problems causing false locking and reduced sensitivity at high altitudes. Associated implementation requirements are described in Section VII-A-2, below.

c. Test Deletions

The test deletions noted in Table 7-1 are suggested because no added confidence appears to be gained from them. (See Section VI for more specific reasons.) The main purpose for them in the present program is believed to be for convenience of the assembly and testing personnel. Therefore, these suggestions should only be regarded as items for review by such personnel. None of the tests cause any harm to the system, but the time they take might be better spent elsewhere. (Especially simple tests are marked with asterisks in Table 7-1 to indicate that very little time would be saved by their deletion.)

d. Test Revisions for Added Realism

The specific revisions suggested are:

- (1) Use of simulated return signals with realistic doppler (spread) spectra;
- (2) Use of simulated range signals with "flyback" effects present;
- (3) Use of the full range of possible frequencies and power levels to match the functional specification; and
- (4) Use of more realistic retro tankage return signal simulation.

The main need for spread spectra testing is for items 20, 23b, 24b, and 26 of Table 7-1. In particular, it is required for checking tracker filter bandwidths, tracking loop performance, analog converter performance, possibility of false range marks due to fluctuating levels, and operation of cross-coupled sidelobe circuitry. Another important reason is to determine whether present analog noise and ripple specifications are adequate for proper flight control in terminal descent. (Implementation is described in Section VII.A.2, below.)

The requirement for more realistic range signals is to check the effectiveness of the blanking circuitry. Simple acquisition tests in each environment should be sufficient.

The requirement of a complete range of input frequencies and associated power levels relates to the discussion on Section VI-B-3. In particular, situations involving preamp roll-off must be examined.

The problem of retro-tankage return signals is discussed in view of special tests in Section VII-B-2, below.

2. Changes of Test Equipment

a. Frequency Coherence and Deviation Linearity Measurement Facility

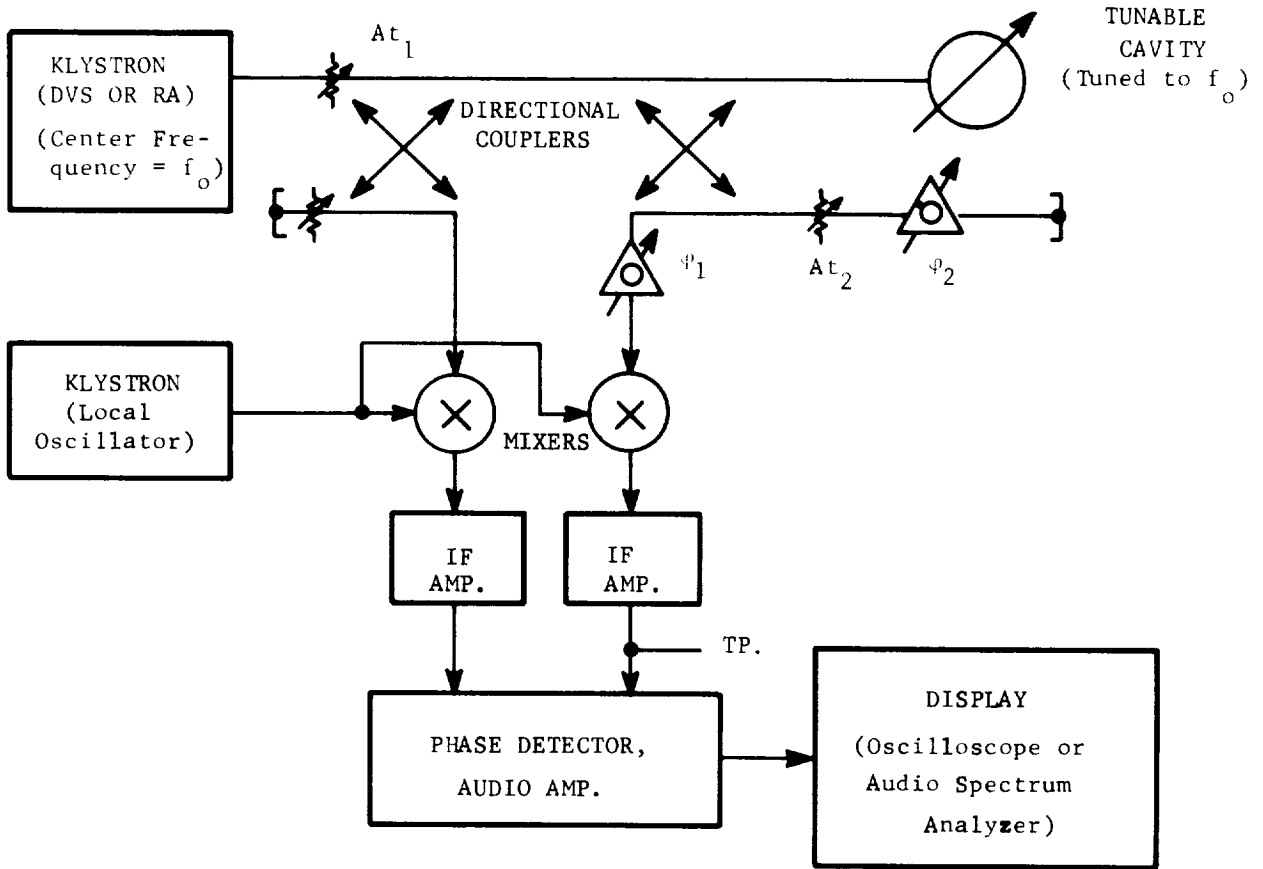
There are several methods of measuring frequency stability. One approach is to measure the frequency spectrum directly, as is done in microwave and low-frequency spectrum analyzers. For the present application the microwave analyzer is inadequate because of its limited resolution, which is normally of the order of a few kHz. The low-frequency, or audio, analyzer does have sufficient resolution; however, to translate the klystron signals down to audio frequencies, a second microwave signal generator must be used with a short-term stability an order of magnitude better than that of the klystron.

Another approach to frequency-stability measurement is to measure the instantaneous frequency by means of a microwave discriminator. This technique, which is suggested for the present application, is also applicable to the measurement of frequency-deviation linearity and the accompanying AM for the RA klystron.

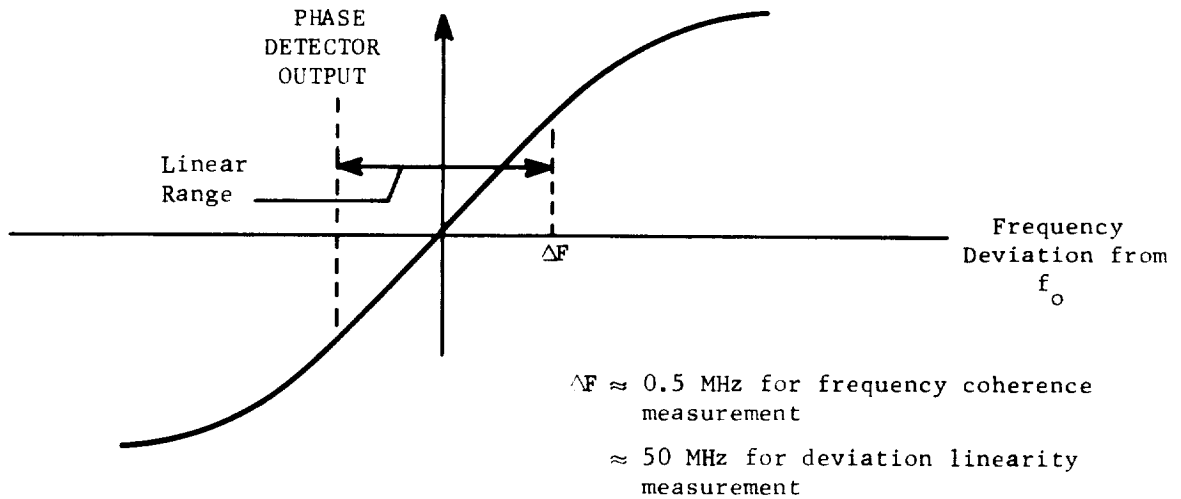
The basic microwave discriminator method of frequency-stability measurement is shown in Fig. 7-1a. The major difference between measurement of klystron coherence and deviation linearity is the required width of the discriminator curve, as shown in Fig. 7-1b. To achieve this difference the loaded Q of the tunable cavity must be changed in inverse proportion to the required width. The width of the narrow-band discriminator curve must be sufficient to respond to the maximum frequency deviation to be measured or to the maximum modulation frequency, whichever is greater. The wideband discriminator curve must be wide enough to provide a highly linear region over at least 40 MHz, which corresponds to the RA wide-deviation mode.

The basic circuit used for the measurement system in Fig. 7-1a is described and analyzed in reference [69]. Proper adjustment of ϕ_1 , ϕ_2 and At_2 permits achieving the discriminator curve in Fig. 7-1b; ϕ_1 is set for maximum discriminator slope, while At_2 and ϕ_2 are set for minimum carrier component at the mixer input. For a discriminator bandwidth of approximately 1 MHz and an audio bandwidth of 10 kHz the minimum measurable frequency increment is approximately 0.14 Hz*; this represents the case of frequency-stability measurement. A discriminator bandwidth of 100 MHz and an audio bandwidth of 10 kHz gives a minimum measurable frequency increment (or deviation from linearity) of 14 Hz*; this is representative of the measurement of deviation-linearity.

* Based on thermal noise limitations in a typical system; see reference 69, equation 8.



a. Discriminator circuit, block diagram.



b. Discriminator curve, for balanced condition.

Fig. 7-1. Stability and deviation-linearity measurement circuit.

The measurement capabilities given above are well within the requirements of the desired application. In fact, the simpler system shown in Fig. 7-2 will probably have adequate sensitivity. The fact that this system operates with a "zero" IF carrier means that its sensitivity will be the order of 30 db worse than that described for the first case.* Thus, the minimum measurable frequency increment for the frequency-stability measurement would be of the order of 4 Hz and for the deviation linearity measurement would be limited to about 400 Hz. Although further analysis and experimental work is desirable to verify this conclusion, it appears that the simpler system is adequate for the desired application.

Interpretation of the discriminator output requires consideration. First, this output must be calibrated in order to obtain the proportionality factor between output voltage and input frequency deviation. Calibration can be achieved by using a klystron standard which has very low FM in its unmodulated mode. Data for a curve of klystron frequency versus electrode voltage (i.e., the reflector voltage if a reflex klystron is used) can be obtained by standard voltage and frequency measuring techniques. A sinusoidal modulating voltage of known amplitude is then applied to the klystron, and the calibration curve used to translate this to a frequency modulation of known deviation. Measurement of the discriminator output modulation then permits completion of the calibration.

Analysis of the discriminator output can take one of several forms. A simple form would be to observe the peak-to-peak frequency deviation and require that this be less than some pre-computed specification. Another would be to apply the discriminator output to an rms voltmeter, similarly requiring that the rms frequency deviation be less than a specified amount. A more precise criterion would be based on a spectrum analysis of the discriminator output (i.e., the spectral content of the frequency modulation). The resulting spectrum could be compared with a specified upper-acceptable curve, which in turn has been derived by an extension of the type of analysis described in Appendix G.

b. Spread Spectrum Simulator

With regard to implementation of the spread-spectrum tests, the following factors are of uppermost importance:

- (1) the signals should be realistic with regard to the amplitude and phase modulation of ground-reflected signals; and
- (2) the implementation should require a small amount of additional equipment to the present STEA and should easily interface with STEA.

*Typical figure based on other experience.

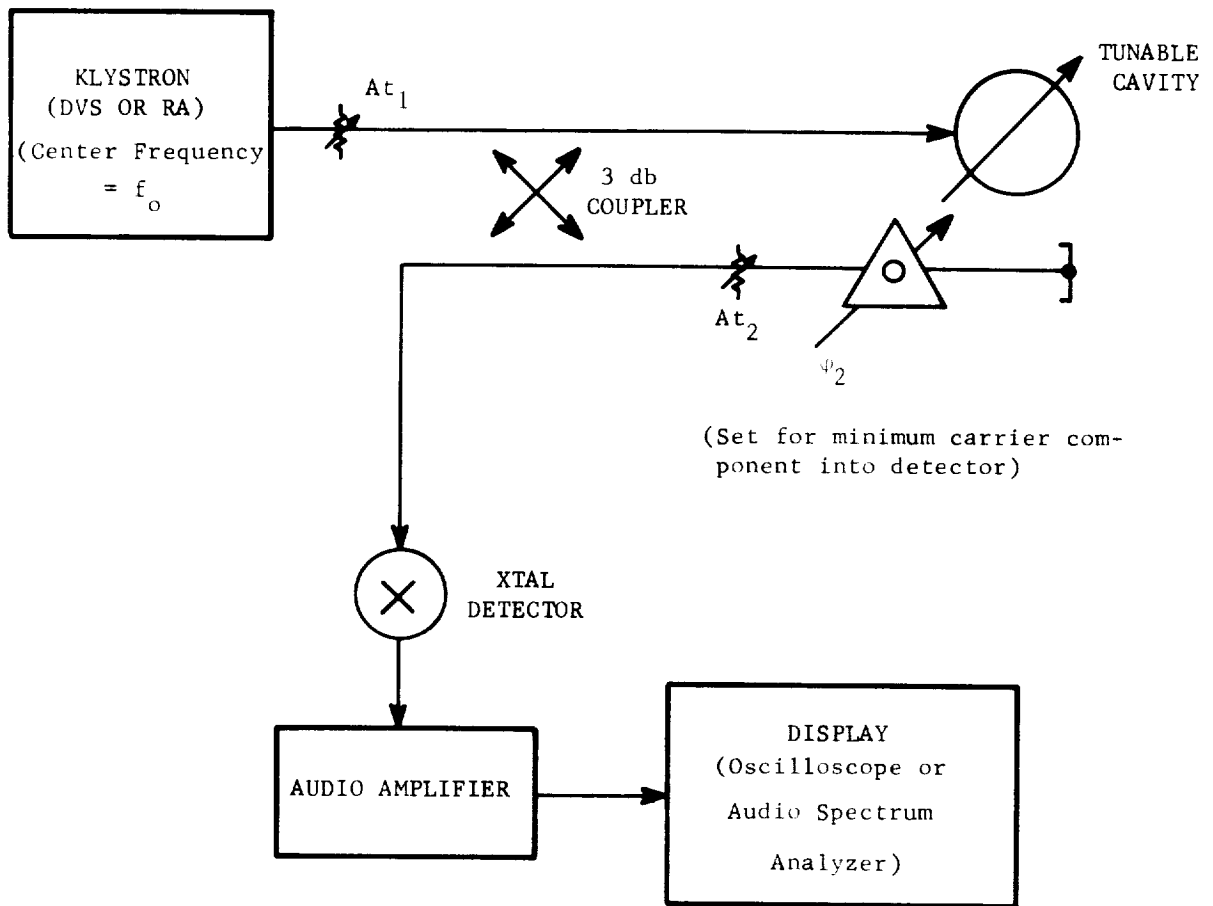


Fig. 7-2. Simplified version of discriminator circuit using audio detection and amplification.

To satisfy the first requirement, the simulating signal should have an adjustable center frequency and bandwidth. The actual ground-reflected signals have a band-limited noise-like characteristic. The generally-accepted model of these signals is based on the assumption that the beam illuminates an area containing a large number of relatively-small scatterers [68]; the surface is assumed to be sufficiently rough to cause reflections from these scatterers to add in a random manner (i.e., the phase density function is uniform over 0-2 π radians). For this idealized model, it is easily shown that the instantaneous value of the resultant signal can be represented by

$$E_d(t) = x(t) \cos 2\pi (f_o + f_d) t + y(t) \sin 2\pi (f_o + f_d) t$$

where

f_o = frequency of the microwave carrier

f_d = center doppler of signal

and $x(t)$ and $y(t)$ are independent random functions having gaussian density functions with zero means and bandwidths equal to that computed for the required doppler signal $E_d(t)$, as computed from velocity and beamwidth considerations.

It follows from these conditions that the amplitude of $E_d(t)$ has a Rayleigh density function [70].

Although the signal described above sometimes differs markedly from ground-reflected signals, it is probably the best model which can be used. The major shortcoming of this representation is that it does not account for the relatively-slow changes in signal characteristics which correspond to slow changes in terrain characteristics. Thus, while the long-term statistics of the simulating signal represents the true signal quite well, its short-term characteristics may be appreciably different from those of the true signal.

The form of $E_d(t)$ given above suggests a method for synthesizing the simulating dopper signal. A method of modifying the present STEA equipment to permit selection between single-line and spread spectra is shown in Fig. 7-3. Referring to this figure, the phase splitter output is fed in quadrature into two pairs of balanced modulators. These modulators are also fed by two independent noise sources representing $x(t)$ and $y(t)$ of the above equation. The spectral characteristics of the resultant signal is determined by the response curves of the shaping filters.

To give the desired outputs, the balanced modulators must have a linear response to $x(t)$ and $y(t)$; that is, their outputs need to be the product terms making up the two components of $E_d(t)$. Consequently, the nonlinear elements in the two halves

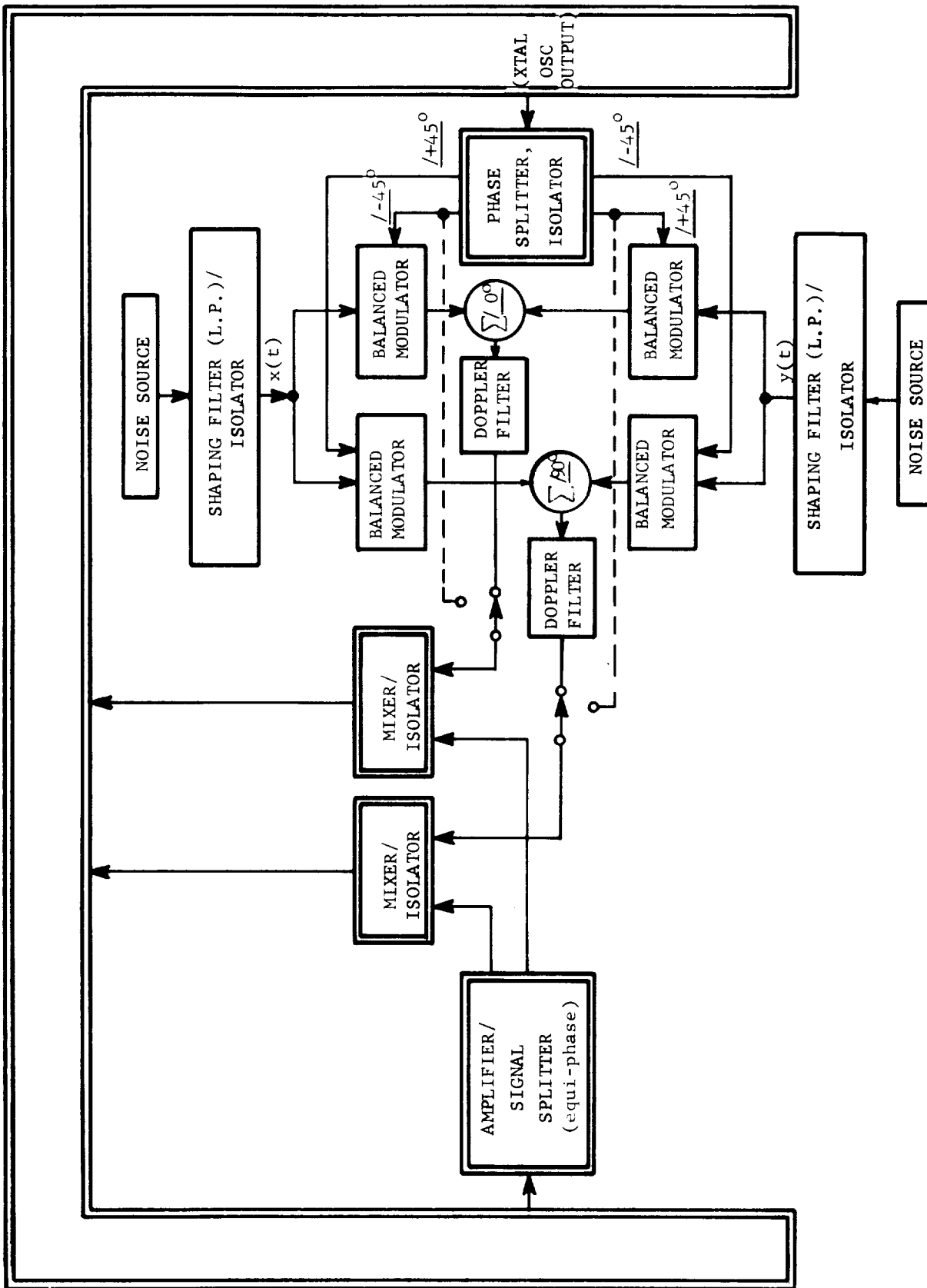


Fig. 7-3. Addition to STEA for implementing spread-spectrum testing. Blocks shown in double lines are existing system; dotted lines from phase splitter to switches show existing mode; switches are in spread-spectrum position.

of each modulator should be well balanced and should be operated at the best bias points and signal levels to minimize unwanted mixing components. (These spurious components, of course, will be present due to higher-order curvature of the I-E curves of the nonlinear elements.)

Considering the interface with STEA, reference is again made to Fig. 7-3. The portion of this figure inside the double lines are components in the existing system. The outputs of the summation circuits are noise spectra, centered about the frequency feeding the phase splitter, 280 kHz. These signals serve the same purpose as the two phase splitter outputs, $/-45^{\circ}$ and $/+45^{\circ}$, except that they have spread spectra. Therefore, they can be substituted directly for the phase splitter outputs, as shown by the two switches. The two outputs are then fed into the Mixer/Isolator pair, from which they feed the STEA single-sideband modulator (see Fig. 5-1). The output of this single sideband modulator is the desired K-band doppler signal, where the added circuitry described above permits selection of either single-line or spread spectrum from all doppler sources now present in STEA.

During the test program review, it was noticed that Ryan has performed spread-spectra testing on SDC units (see Appendix D). Details of the equipment used for these tests have not been reviewed; however, it is quite possible that this equipment can be interfaced into STEA in a similar manner to that described above.

B. SPECIAL-TEST PROGRAM

1. Transmitter-Receiver Leakage Tests

a. Vibration Tests

A conclusion of the discussion in Section IV-C-1 is that two types of tests are desirable in order to further evaluate the transmitter-receiver leakage problem. One type of test, the vibration test, consists of hanging a spacecraft upsidedown and imposing realistic vibration levels at the three points of vernier engine mounting. One such set of tests has been made [38], and may prove to have been adequate. At the time these tests were made, however, no data from an actual lunar descent were available.

It is suggested that the S-8 tests be reviewed with the objective of comparing the test conditions with the vernier engine vibration levels measured during Surveyor 1 descent. (This was not done during the present study because a simple comparison does not appear possible; the instrumentation for the S-8 test and the Surveyor 1 descent was not the same.) It is also desirable to explore the possibility of extrapolating the results of the S-8 tests to conditions existing during retro-engine operation.

In event that the S-8 inputs were far different from the Surveyor 1 excitations, a new upsidedown test would be suggested. Similarly, if it were not found that at least one S-8 system configuration and absorbing material placement was the same as on current flight spacecraft, a retest would be suggested. Such retests would have to be weighed in comparison to the on-board tests described in the next section.

b. On-Board Tests

The second test suggested for further evaluation of the transmitter-receiver leakage problem is an on-board test during actual lunar descent of a future spacecraft. A possible form of the added circuitry required is illustrated in Fig. 7-4. One of the preamplifier outputs is fed into a balanced modulator, identical to those used in RADVS frequency trackers. The other input is a reference signal from a voltage-controlled oscillator; this VCO is stepped synchronously in frequency with the telemetry commutators. Thus, the VCO steps a doppler gate of bandwidth B_s through the band of interest.

Making the detector output time constant comparable to the commutator sampling time permits averaging each sample value over the period. In this case rapid discharge of the detector output at the end of a sample period to reset it for the next sample would be desired. A somewhat shorter time constant would probably be sufficient, however.

Alternate forms of the spectrum analyzer are of course possible. If desirable from a standpoint of required data capacity of the telemetry channel, only one or two preamplifier outputs could be sampled. Various sampling rates are also possible as long as they are appropriately synchronized with the basic telemetry sampling rate.

A study of the circuit shown in Fig. 7-4 shows that the added equipment for performing the suggested experiment is relatively simple; this is especially true if only one or two preamplifier outputs are sampled. The required circuits are conventional and in most cases identical to ones presently in use in the RADVS system.

Further studies of implementation possibilities and problems associated with the spectrum analyzer (including considerations of space and power availability) are required in order to determine the total feasibility of performing this on-board experiment.

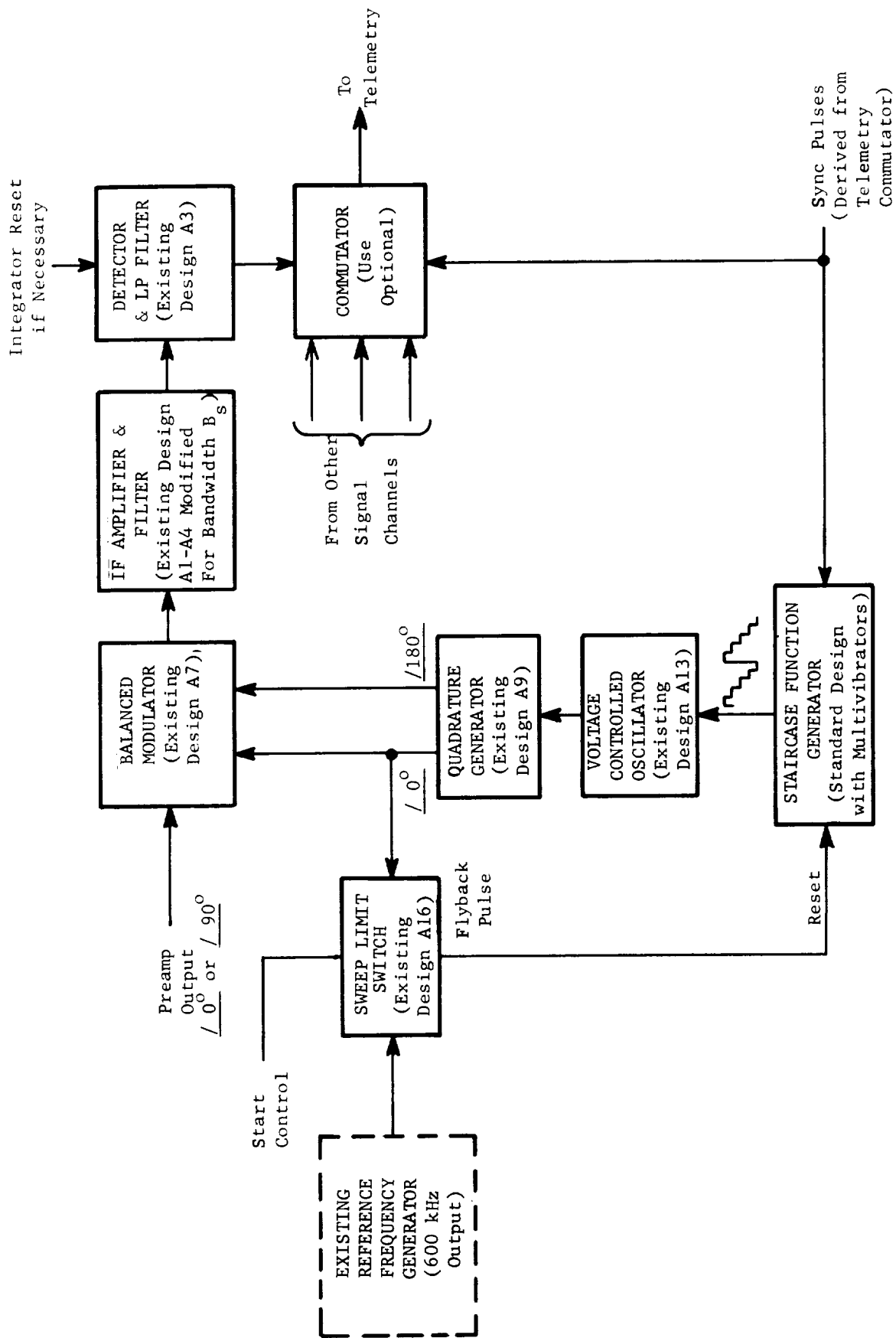


Fig. 7-4. Block diagram for an on-board spectrum analyzer.

2. Interfering Signal Tests

a. Retro Tankage Signals

If it is assumed that the retro tankage is ejected along the spacecraft z-axis and that it has no residual thrust, then the probability of its entering any of the DVS mainbeams is quite small; changes in spacecraft attitude could result in such entry, but the range of entry would probably be sufficient to cause signal rejection because of the target's negative velocity. For the assumed ejection conditions the retro tankage would enter the RA mainbeam at a range of 40-60 feet. Therefore, if these ejection conditions were to apply and if only mainbeam effects are considered, then it would be easy to compute a profile of retro-tankage signal characteristics (i.e., variation of range, doppler, and signal level versus time). This profile could then be used for evaluating the adequacy of the current test program and/or for recommending modifications.

Unfortunately, consideration of retro-tankage effects is not as simple as described in the above paragraph. Review of Surveyor 1 performance during lunar descent shows that DVS Beam 3 unlocked shortly after retro-tankage ejection (within approximately two seconds); re-lock was achieved within about two more seconds. One explanation suggested for this effect was that the retro tankage passed through all or a part of Beam 3, in this way shadowing the lunar surface and causing signal loss. It is somewhat puzzling how the ejected retro-tankage could have acquired a sufficiently large transverse-velocity component to have entered and passed through the beam so rapidly. One possible explanation is that the retro engine was still burning at a low level and that a non-axial thrust component caused a transverse-velocity component. It appears that a conclusive analysis of what actually happened cannot be made because of the inavailability of adequate data. It might even be reasonable to suppose that the retro-tankage had nothing to do with Beam 3 unlock; for example, this unlock could have been caused by an electrical transient which might or might not have been associated with retro-tankage ejection.

Retro-tankage effects could be quite serious. First, if the tankage passes through the mainbeam, a number of things could happen:

- (1) a sufficiently strong retro signal could cause a pre-amplifier gain-state switch, which would cause unlock from the lunar signal, or delayed lock-on;
- (2) The lunar surface could be shadowed, with similar results to (1); and
- (3) Lack of sufficient negative-doppler rejection might permit lock-on to the retro tankage.

Actually, it may be possible for (1) and (3) to occur even if the retro tankage does not pass through a mainbeam, but passes through relatively high sidelobes. Although there is a good chance for the spacecraft to recover from any of these events and make a successful landing, they are nevertheless of serious concern.

The suggested follow-on evaluation consists of the following steps:

- (1) Study of retro-tankage separation paths--ideally, a probability density function should be developed to describe the range of separation velocities and signal levels to be encountered. (Possibilities of post-ejection thrusts caused by retro-engine "tail-off" after ejection and for induced turning moments on the tankage would be considered.)
- (2) Using the results in (1) reasonable estimates of signal level and spectral characteristics should be made. (These estimates would be of a statistical nature.)
- (3) The results of (2) should be used to determine the simulation conditions for checking the reaction of RADVS to retro-tankage signals. (These checks would include both experimental and analytical approaches. Attempts would be made to estimate the probability of landing degradation and failure caused by tankage effects.)
- (4) Based on above results, modifications to the flight-readiness test program should be made. (Also, feasible RADVS modifications to correct any serious deficiencies would be recommended.)

b. Cross-coupled Sidelobe Signals

Previous justification has been given for further studies of CCSL signals (see Section IV-C-3 and Appendix C). Special tests are suggested for determining the effects of two signals simultaneously present in a given DVS channel. Various ratios of the signals would be selected and tests performed over the dynamic signal range of interest. Any inherent suppression of the smaller signal would be observed.

Still another test is suggested in order to determine whether the CCSL logic circuit will perform under all conditions likely to be incurred. Effects of fluctuating, spread-spectrum signal testing would be evaluated to determine whether anomalous effects can occur (e.g., whether slow signal fades can cause errors in the CCSL decision outputs).

Results of these special tests and tests on suggested circuit modification (Appendix C) would be used for planning any necessary modifications to the test program to ensure sufficient testing of CCSL rejection capability.

3. Environmental Overtests

A renewal of the TAT program to provide the features discussed in Section IV-C-4 is suggested. To reiterate, the main objectives are determination of operational margins and analysis of the fatigue effects caused by the flight-readiness test program.

Difficulties of arranging such extensive new tests within the program time limitations are anticipated. Undertaking these tests in parallel to the current flight program, however, might save time in analyzing possible flight failures. The fact that this testing would be important to other systems besides RADVS serves as additional justification.

APPENDICES

APPENDIX A
BIBLIOGRAPHY OF DOCUMENTATION
AND LIST OF REFERENCES

Listed below are documents from Highes Aircraft Co. (HAC), the Jet Propulsion Lab (JPL), and Ryan Aeronautical Co. (RAC) reviewed during the RADVS test study program. Other references are listed following the bibliography of documentation.

	<u>Document Source</u>	<u>Document Number</u>	<u>Rev. Ltr.</u>	<u>Revision or Release Date</u>	<u>Document Title</u>
(1)	HAC	224510	E	1/6/66	Detail Spec., Surveyor System Functional Requirements
(2)	HAC	224550	B	1/26/66	System Spec., Standard Transit Sequence of S/C Operations
(3)	HAC	224665	E	12/17/65	A-21 FAT RADVS Group (Inc. Aux. Procedures) Test Procedure
(4)	HAC	224681	F	12/8/65	A-21 FAT, FC, AMR, RADVS TCM Integration Test Procedure
(5)	HAC	224800	A	7/31/64	Detail Specification Environmental Conditions Surveyor Spacecraft
(6)	HAC	224810	E	4/22/65	Environmental Requirements, Surveyor TAT, Subsystems and Assemblies
(7)	HAC	224820	F	1/18/65	Environmental Requirements, Surveyor FAT, Subsystems and Assemblies
(8)	HAC	224822	A	3/10/65	A-21 System FAT Spec., Mission Sequence-Electro Magnetic Interference Test
(9)	HAC	224847	B	3/1/65	A-21 Model Description
(10)	HAC	224898-1	D	2/3/66	S/C to RADVS STEA Reference Data Test Procedure
(11)	HAC	224909-3	F	4/6/66	Terminal Descent, Closed Loop, FAT
(12)	HAC	224947	B	8/23/65	S/C to STEA Calibration Procedure - RADVS STEA
(13)	HAC	225019	B	6/22/65	Master Test Spec. Surveyor A-21 System TAT
(14)	HAC	225021	B	3/3/65	Test Specification T-21 Vibration Test Phase
(15)	HAC	225026	A	3/31/65	A-21 Type Approval Solar Thermal Vacuum Functional Test Phase
(16)	HAC	225462	A	10/14/65	T-2N Tethered Test Plan, Vol. I
(17)	HAC	227156	A	12/13/65	M/S Patchboard Schedule Test Procedure

	<u>Document Source</u>	<u>Document Number</u>	<u>Rev. Ltr.</u>	<u>Revision or Release Date</u>	<u>Document Title</u>
(18)	HAC	227157	A	2/10/66	RADVS Calibration of RA and DVS Analog Output Signals - #55A and 14 ft. Range Mark Signal Special Test #78 Test Procedure
(19)	HAC	227206	A	3/16/66	RADVS Waveguide Leakage Integrity Test Procedure - Special Test No. 90A
(20)	HAC	227331	D	7/66	A-21 PVT-3, System Flight Verification
(21)	HAC	227741	A	8/66	A-21 PVT-5, Final SCF System Test
(22)	HAC	228103		4/30/65	T-2N Vehicle System Functional Test Plan Vol. I
(23)	HAC	232902	K	6/7/65	Procurement Spec., RADVS
(24)	HAC	232916	A	2/9/64	Detail Spec. RADVS TA & FA Tests
(25)	HAC	239014		7/25/66	Structural Design Criteria and Structural Loads, Surveyor A-21 S/C
(26)	HAC	239524	E	4/15/66	Functional Description, Vol. I
(27)	HAC	239524	E	5/1/66	Functional Description, Vol. II
(28)	HAC	239524	E	5/1/66	Functional Description, Vol. III, Telemetry Functionals
(29)	HAC	239524	E	4/28/66	Functional Description SC-2 Supplement (Preliminary Release)
(30)	HAC	287238		9/15/65	S-7 TAT (Vernier Propulsion System)
(31)	HAC	3023926	A	9/1/66	Surveyor S/C A-21 System Test Specification
(32)	HAC	6594500		1/15/66	STEA Operation and Maintenance Manual, Vol. I and II
(33)	HAC	2254/204		5/65	T-2N Model and Functional Description
(34)	HAC	2254/273		6/66	T-2N-1 Surveyor Test Vehicle Descent Test No. 6 Mission Report
(35)	HAC	2254.6/410		11/10/64	Final T-2H Test Phase Report QA-1 Model RADVS Testing on the Bell 47G Helicopter
(36)	HAC	2254.7/ 232.11.1		7/15/66	A-21 Flight Acceptance MS/EMI Test Phase, Vol. II, Pt. 2A

	<u>Document Source</u>	<u>Document Number</u>	<u>Rev. Ltr.</u>	<u>Revision or Release Date</u>	<u>Document Title</u>
(37)	HAC	A21 FT2.7		8/66	Field Test, Acquisition Sensitivity, Preamp Noise Level Tests--Plugs in/out-- and Calibration of Lunar Reflectivity and Analog Outputs
(38)	HAC	SSD 5216R		5/65	Surveyor S-8 SC/Doppler Radar Performance Evaluation During Simulated Multiple Vernier Engine Random Vibration Excitation, Final Phase Report
(39)	HAC	SSD 64146R		3/25/66	Surveyor Special Noise Test Report
(40)	HAC	SSD 68030-6		2/9/66	System Functional Test Results for RADVS Subsystem, SC-1
(41)	HAC	SSD 68031-6		6/28/66	System Functional Test Results for RADVS Subsystem, SC-2
(42)	HAC	SSD 68149R		7/66	T2N Surveyor Test Vehicles. Tether and Descent Test Series Final Report
(43)	HAC	SSD 68154I		6/66	T-2N Surveyor Test Vehicle Mission Report Descent Test No. 8 - T2N-1 Descent No. 5
(44)	HAC	SSD 68163R		8/66	Surveyor Mission B Final Preflight Maneuver Analysis Report
(45)	HAC	SSD 68164R		8/66	Appendix A of Surveyor Mission B Final Preflight Maneuver Analysis Report
(46)	HAC	SSD 68223R		10/66	Surveyor I Flight Performance Final Report, Vol. III
(47)	HAC	66H-0580/ 6567		1/6/66	Proposal for Additional RADVS System Testing (Upside-down Test)
(48)	HAC	--		11/11/65	T-2N-1 RADVS Problems, Special Review at AFMDC
(49)	HAC	--		--	AM-4 Test Results
(50)	HAC	--		3/24/66	Post Mission Analyses Involving Radar Data (Draft Report by R.A. Dibos)
(51)	HAC	--		6/15/66	Quick Look Report SC1 Radars (by R.A. Dibos)
(52)	HAC	--		9/9/66	RADVS Cross-Coupled Sidelobe Study (by R.A. Dibos)
(53)	JPL	32-1023		8/31/66	Surveyor I Mission Report Pt. 1 Mission Description and Performance

	<u>Document Source</u>	<u>Document Number</u>	<u>Rev. Ltr.</u>	<u>Revision or Release Date</u>	<u>Document Title</u>
(54)	JPL	POM273-B-225		1/20/65	RADVS Testing
(55)	JPL	PD-97		6/30/66	Surveyor I Preliminary Results (NASA) Five-Day Science Rept.
(56)	RAC	400553	B	4/63	Spec. Control Drawing Klystron-Velocity Sensor (Type RE-105)
(57)	RAC	517-001		1/65	Quality Assurance Plan
(58)	RAC	51764-1, Sec.IV		--	System Checkout Procedure
(59)	RAC	51764-1A		9/66	Operation & Maintenance Inst. for RADVS
(60)	RAC	51765-2B		8/1/66	Change 12 to Acceptance Test Procedures for RADVS Ryan Model 517
(61)	RAC	51766-1		10/28/64	Report on TAT, RADVS Model 517, S/N 1
(62)	RAC	51769-9		12/65	RADVS Final Draft of System Parameter Inputs for AM-1, AM-2, AM-3
(63)	RAC	51769-14		6/66	Surveyor RADVS Cross-Coupled Sidelobe Measurements and Potential Solutions
(64)	RAC	--		7/22/65	TAT on S/N 1 KPSM
(65)	RAC	--		6/66	Design Review Data for Double Sideband Discrimination Trackers (ECP-10)
(66)	RAC	--		10/66	Technical Review Data for Cross Coupled Sidelobe Discrimination by all DVS Trackers (ECP-23)
(67)	Kelly, A.J., <u>Analysis of the Interaction of the Surveyor RADVS System and Vernier Thrust Chamber Plumes</u> , (JPL IOM to G.R. Russell), Dec. 17, 1965.				
(68)	Berger, F.B., "The Nature of Doppler Velocity Measurement," <u>IRE Trans. on Aeronautical and Navigational Electronics</u> , Vol. ANE-4, No. 3, Sept., 1957, pp. 103-112.				
(69)	Grauling, C.H., Jr., and D.J. Healey III, "Self-Calibrating and Self-Checking Instrumentation for Measurement of the Short-Term Frequency Stability of Microwave Sources," <u>Proc. of the IEEE-NASA Symposium on the Definition and Measurement of Short-Term Frequency Stability</u> , Goddard Space Flight Center, Nov. 1964, pp. 253-263, (NASA-SP-80).				
(70)	Davenport, W.B., Jr., and W.L. Root, <u>An Introduction to the Theory of Random Signals and Noise</u> , McGraw-Hill, New York, 1958, pp. 158-161.				
(71)	Smith, P.G., "AN/APN-118 Radar, Operation and Theory," Rept. No. CJ2290-1529, Sperry Gyroscope Co., Sunnyvale, Cal., May 5, 1961.				

- (72) Emerson, W.H., and F.P. Brownell, "State-of-the-Art Anechoic Backscatter Ranges," (Rome Air Developmental Center Rept. RADC-TOR-64-25, Vol. 1), Proc. of the Radar Reflectivity Measurements Symposium, Apr. 1964.
- (73) "A Study of Microwave Propagation through Retro-Rocket Plumes During the Control Phase of Lunar and Planetary Landing," Informal Proposal to Hughes Aircraft Co. by the Cornell Aeronautical Laboratories, Buffalo, N.Y., Nov. 5, 1962.
- (74) Dibos, R.A., "Radar Performance Evaluation," paper presented at the Surveyor I Design and Performance Symposium, JPL, Aug. 31, 1966.
- (75) Skolnik, M.I., Introduction to Radar Systems, McGraw Hill, New York, 1962.
- (76) Berkowitz, R.S., (Ed.) Modern Radar, John Wiley, New York, 1965.

APPENDIX B

RADVS TRANSMITTER RECEIVER LEAKAGE

I. DESCRIPTION OF PROBLEM

Fig. B-1 illustrates the RADVS leakage problem. The total leakage is made up of a number of components resulting from different paths, as illustrated. For convenience a single symbol, L, will be used to represent the part of the transmitter power leakage (unintentional coupling) into the receiver. Thus, the receiver leakage power is expressed as

$$P_{\ell} = P_t L \quad (\text{B-1})$$

where P_t = transmitter radiated power.

If the leakage component were a single-line spectrum at the transmitter carrier frequency, it would cause no difficulty. This can be illustrated by the following reasoning. First, such an unmodulated carrier would mix with the identical carrier component which is intentionally coupled into the receiver "front-end." The resulting mixer output would be a d-c component, which would not be passed by the following amplifier circuits and would thus cause no false lock-on problems. However, if the leakage component is too high -- say, comparable to the intentional transmitter coupling -- the mixer crystal will be over-biased, with the possibility of a degradation in noise figure. Because the intentional transmitter coupling is in the order of 0.5 mw, the undesirable leakage component should be held to less than 0.1 mw, requiring a leakage factor of

$$L < \frac{10^{-4} \text{ watts}}{8 \text{ watts}} = 1.2 \times 10^{-5} \cong 49 \text{ db.} \quad (\text{B-2})$$

This is a fairly easy requirement to meet, and will be shown to be much less stringent than those imposed by other considerations.

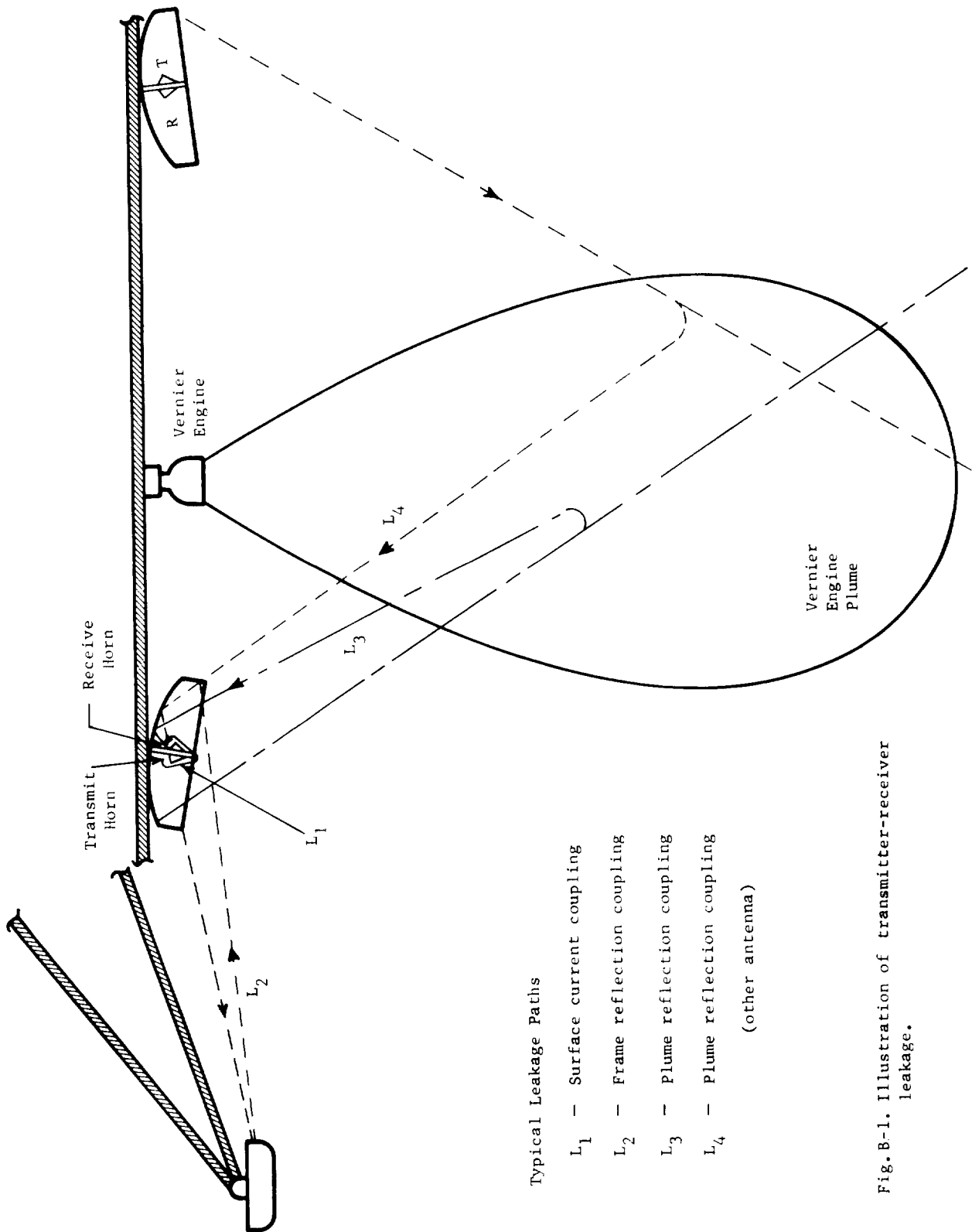
Actually, of course, the leakage signal does not consist of a single-line spectrum. Sidebands on this signal are the major source of difficulty. Such sidebands are caused by

- (a) random noise on klystron output signal
- (b) sidebands induced by vibration of klystron elements (usually periodic in nature)
- (c) sidebands induced by modulation of leakage paths illustrated in Fig. B-1

These components will now be discussed in turn.

The random noise on a klystron output can be estimated with reasonable accuracy. Data were taken on three two-cavity, 13.2 Gc klystrons during a previous doppler radar development [71]:

Varian VA-503	-- 980 volt mode, 300 mw output
Sperry SOU-201	-- 750 volt mode, 500 mw output
Sperry SOU-242	-- 980 volt mode, 300 mw output



Typical Leakage Paths

- L₁ - Surface current coupling
- L₂ - Frame reflection coupling
- L₃ - Plume reflection coupling
- L₄ - Plume reflection coupling
(other antenna)

Fig. B-1. Illustration of transmitter-receiver leakage.

The noise power density was measured as a function of frequency off-set from carrier. Within about 3 db, the resultant curves were identical and followed a 1/f law out to a frequency off-set of 100 kc; higher frequency off-sets resulted in a leveling off of the power density. Using these curves for frequencies below 100 kc results in the leakage noise power density being expressed by

$$N_{\ell}(f)_{\text{dbw}} = P_t(\text{dbw}) + L(\text{db}) - 130 \text{ db} - 10 \log f(\text{kc}) \quad (\text{B-3})$$

where the third term represents the empirically-derived constant and the fourth term the 1/f behavior. In order to determine whether this random noise component is likely to cause trouble, we must consider the inherent sensitivity of the receiver. This sensitivity is determined by the receiver noise level. In the absence of transmitter leakage, this noise level is determined primarily by crystal noise. This latter noise is expected to also have a 1/f behavior in the doppler band below 100 kc. Assuming a noise figure of 20 db at 10 kc, the crystal noise density (referenced to the RF input to the crystal) would be

$$\begin{aligned} N_c(f)_{\text{dbw}} &= 10 \log k T_{\text{ambient}} + 30 - 10 \log f(\text{kc}) \\ &= -204 + 30 - 10 \log f(\text{kc}) \\ &= -174 \text{ db} - 10 \log f(\text{kc}) \end{aligned} \quad (\text{B-4})$$

In order to avoid excessive degradation of the receiver's inherent sensitivity

$$\begin{aligned} N_{\ell}(f)_{\text{dbw}} &< N_c(f)_{\text{dbw}} \\ P_t(\text{dbw}) + L(\text{db}) - 130 &< -174 \text{ db} \\ P_t(\text{dbw}) + L(\text{db}) &< -44 \text{ db} \end{aligned} \quad (\text{B-5})$$

For $P_t(\text{dbw}) = 9$ (i.e. 8 watts from all three beams)

$$L(\text{db}) < -53 \quad (\text{B-6})$$

Here again, the random noise component on the klystron does not impose severe requirements on the leakage factor, because it is believed that between 60 and 70 db decoupling can be achieved rather readily.

Considering the second source of leakage sidebands, both AM and FM sidebands will be induced by vibration of klystron elements. In general, the power in these sidebands will be small relative to that in the carrier. Therefore, the effects may be considered independently and superposition may be employed to determine the combined effects. Considering first the FM sidebands alone, it can easily be shown that they will cause no difficulty for this particular system. This result follows from the fact that the FM appears on both the local oscillator signal, which is intentionally coupled from the transmitter into the receiver, and on the leakage component. Because the delay of the leakage component relative to that of the intentional coupling is very small relative to the period of any frequency in the

doppler band, the beat between the local oscillator signal and the leakage component is essentially zero for all leakage FM sidebands below 100 kc. Thus, the mixer output spectrum would be essentially a d-c component, in spite of FM on the transmitter output.

Unfortunately, FM components on the klystron output can be changed to AM components, by coupling paths which exhibit frequency sensitivity. AM sidebands on the leakage component can cause serious problems in the tracker circuits, because they are translated directly onto the mixer output. Thus, both AM and FM sidebands on the klystron output can cause difficulty (the latter through the process of being changed from FM to AM). The two effects will therefore be treated together, where consideration will be given to the allowable AM sideband power, coupled into the receiver input mixer. The following analysis applies to AM sidebands on both types of coupling listed above in (b) and (c).

Ideally, all sidebands on the mixer output would be below those caused by the mixer random noise component, $N(f)$, as defined previously. Actually, the receiver lock-on threshold is set considerably higher than the noise level, in order to avoid locking onto noise bursts. Thus, it is probably permissible to allow the spurious leakage sidebands to be 6 db above the receiver noise level, without serious difficulty with false lock. Based on this criterion, the allowable AM sideband power in the tracker bandwidth would be

$$P_{AM}(f)_{dbw} \leq [N_c(f)_{dbw} + 10 \log B_i] + 6 \text{ db}, \quad (B-7)$$

or

$$P_{AM}(f)_{dbw} \leq -168 - 10 \log f(\text{kc}) + 10 \log B_i$$

where f = center frequency of the leakage component, relative to the transmitter carrier component, and B_i = tracker pre-detection bandwidth (1500 cps and 300 cps before and after retro burn-out respectively). But this power can also be expressed as

$$P_{AM}(f) = L P_t S_{AM}(f_d) \quad (B-8)$$

where $S_{AM}(f_d)$ = power on transmitter leakage component centered at f_d from transmitter carrier, in bandwidth B_i , and normalized to P_t . Thus, for $P_t = 8$ watts,

$$\begin{aligned} L S_{AM}(f)_{db} &\leq -177 - 10 \log f \text{ (kHz)} + 10 \log B_i \\ &\leq -145 - 10 \log f \text{ (kHz)} \text{ before burn-out} \quad (B-9) \\ &\leq -152 - 10 \log f \text{ (kHz)} \text{ after burn-out} \end{aligned}$$

For example, at 10 kHz center frequency

$$\begin{aligned} L S_{AM}(10 \text{ kHz})_{db} &\leq -155 \text{ db} \quad \text{before burn-out} \\ &\leq -162 \text{ db} \quad \text{after burn-out} \end{aligned} \quad (B-10)$$

Although the above requirement was derived for AM sidebands on the leakage component, it also applies for those PM sidebands which result from differential pathlength modulation between the leakage path and the intentional coupling path. Thus, a similar equation can be written

$$\begin{aligned}
 L S_{PM}(f)_{db} &\leq -145 - 10 \log f(\text{kHz}) && \text{before burn-out} \\
 &\leq -152 - 10 \log f(\text{kHz}) && \text{after burn-out}
 \end{aligned}
 \tag{B-11}$$

where $S_{PM}(f_d)$ = power on transmitter leakage component, centered at f_d from transmitter carrier and in bandwidth B_i , normalized to the transmitter output power.

The above numbers illustrate the major difficulty with CW radar systems. We see that the combined effects of leakage and modulation sidebands must be of the order of -160 db, in order to avoid degradation of tracker sensitivity. The allowable combined effects are so small that a reasonable estimation as to whether the requirement can be met can be made only by experience with a given system. For example, one might with confidence estimate that a value of $L \leq -70$ db can be achieved. However, without experience for a particular configuration, he cannot confidently estimate the interval of L which can reasonably be achieved; for example, one cannot generally say whether L will be or will not be less than some specified amount (say, -90 db). One can say with certainty that the margin between L and the required value of $L S(f)$ will be considerable, so that the stability requirement on the leakage component is extreme. In the absence of vernier or retro engine operation, the leakage path will be extremely stable; the chances of meeting the leakage requirement are excellent under this condition, and tests on this capability are rather easily performed. However, under engine operational conditions the leakage problem is seriously aggravated by vibration and by possible plume coupling; unfortunately, leakage tests under these conditions are very difficult to perform.

In light of the above consideration, it is believed to be important that the combined factors L and $S(f)$ be known in order to predict whether the spurious leakage components will cause difficulty with false lock-on. An experiment to determine this effect would simulate lunar conditions as realistically as possible. The information of interest is the spectrum of the RF mixer output when the system depicted in Fig. B-1 is operating (both vernier engines and radar, and is effectively "looking" into free space. The difficulties of performing the experiment are prodigious, and such an experiment could only be justified in terms of the high cost of the Surveyor Program and of the importance of achieving success on as many missions as possible. It is also important to remember that the later Surveyor missions impose more severe requirements on RADVS than the early missions. At this point in the program, such an experiment would have to be looked on as a back-up to the existing program. In view of the outstanding success of Surveyor 1, the remaining program should not be paced by the suggested experiment; the outcomes of the next few shots will obviously influence the attitudes taken with regard to the experiment.

II. CONSIDERATION OF TRANSMITTER-RECEIVER LEAKAGE EXPERIMENTS

A. Introduction

The principal objective of transmitter-receiver experiments is to obtain data on the characteristics of the transmitter-receiver leakage signal when operating under conditions realistically simulating those existing during lunar descent. Because the RADVS is activated while the retro-rocket is still firing, it would be desirable to obtain data on this leakage signal during this time. However, the

high thrust nature of the retro-rocket appears to rule out the possibility of obtaining such information by any conceivable, and reasonable, near-earth tests. Therefore, in so far as earth tests are concerned, the best that can be done to simulate this period of retro-fire will probably be to measure the vibration characteristics imposed by the retro-rocket and then, in a separate vibration test, to apply this level of vibration to an operating RADVS in an upside-down position, observing the transmitter-receiver leakage signal during this test.

Most of the following discussion will consequently be directed toward possible methods of obtaining the power-density spectra of the transmitter-receiver leakage signal which is present in the pre-amplifier, as it would exist during operation of the vernier engines only. One possible test is an on-board Surveyor test which would obtain data during both retro and vernier engine operation. The practical approach would be to record the actual pre-amplifier signal during the test, and subsequently perform a spectral analysis by standard laboratory techniques. Such a recording would also be useful for playback into a tracker, to test whether it would lock onto any of the spurious leakage components.

B. Ground-Based Experiment, Upright

The leakage problem described above in Part A highlights the desirability for an experiment to evaluate the leakage problem. As pointed out previously, such an experiment is difficult to perform and may even prove to be impractical. Consideration will be given below to possible means of performing a useful experiment.

First, it does not appear feasible to use an actual spacecraft for the type of experiment which is desirable. Factors mentioned previously in Section IV.A such as surface contamination prevent this; additionally, spacecraft availability would not allow the use of an assembled spacecraft, because of the careful and time-consuming effort needed to perform the tests. Therefore, the tests would have to be performed by using a simulating spacecraft structure, on which the critical parts are mounted.

One possible configuration would be to hang the simulating spacecraft from a boom so that it is suspended about 25 feet from the ground. It would probably be sufficient to use one vernier engine, although three engines would be preferred in order to balance the applied torques to the spacecraft. It would be desirable to use two antennas in order to include the coupling path between the transmitter of one and the receiver of the other. Such a configuration is illustrated in Fig. B-2. Only one antenna would be connected to the transmitter, in order to minimize the problem of ground and support-structure reflections. Ground reflections would be further minimized by the use of absorbing material, located over the ground area being illuminated. As shown in a report on anechoic chambers [72], tilting this material away from normal incidence will reduce the back-scatter in the transmitter source direction considerably. This reference tabulates reflectivity data from three operating anechoic chambers. An apparent radar cross-section of these chambers was defined and values computed from measurements. The apparent radar cross-section results primarily from back-scatter from the rear wall. These data would indicate that the minimum apparent cross section of a wall located 25 feet from the transmitting source would be about 75 db below one square meter. Assuming that this value could be achieved with an outdoor range, the ratio of echo to transmitter power, in the absence of other targets, would be

$$\frac{G_t G_r \sigma \lambda^2}{(4\pi)^3 R^4} \quad (B-12)$$

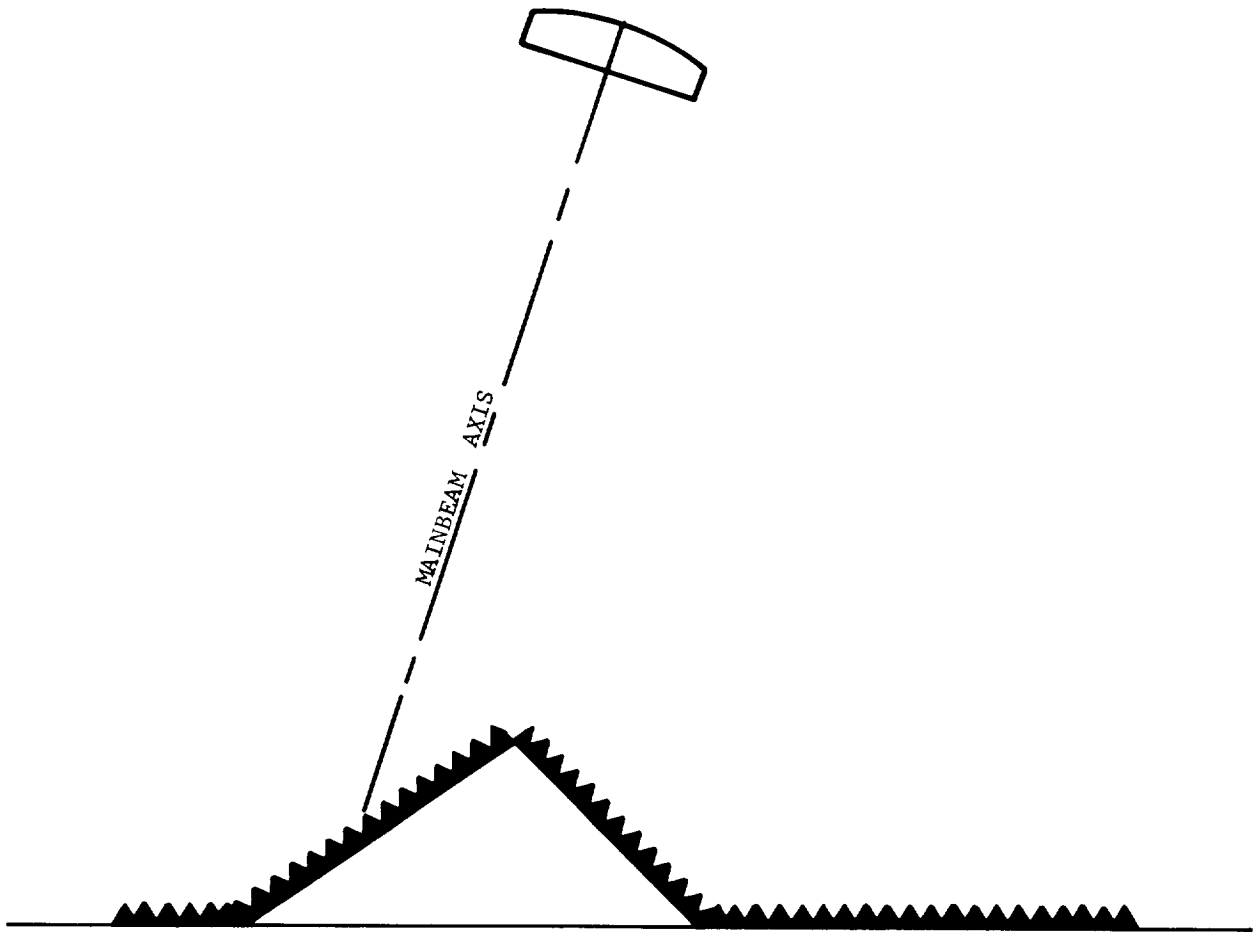


Fig. B-2. Illustration of experimental configuration. Antenna shown is a part of the system illustrated in Fig. B-1.

For the worst-case condition, where both transmit and receive beams of a given channel are pointing at the apparent source of reflection, G_t and G_r will be the peak antenna gain. For RADVS this gain is approximately 29 db. Thus,

$$\frac{P_r}{P_t} \approx \frac{6 \times 10^5 \times 3 \times 10^{-8} \times (0.023)^2}{(4\pi)^3 \times (25/3)^4} \approx 1.1 \times 10^{-12} \quad (\text{B-13})$$

Referring to the previous discussion of the leakage problem, it was shown that the product of the leakage factor and the power distribution of the leakage signal in the receiver bandwidth must be of the order of -160 db. Thus, in order for the echo power calculated above to have negligible effect on the simulated free-space measurement, the modulation sidebands must be

$$S_{\text{AM or PM}}(f) < \frac{10^{-16}}{1.1 \times 10^{-12}} \approx 10^{-4} \quad (\text{B-14})$$

That is, the sideband power in any band centered at f and contained in the tracker pre-detection bandwidth must be less than 10^{-4} of the total reflected power. This obviously would be a difficult requirement to meet. With the vernier engines operating, vibration of the spacecraft and perturbations in the propagation path might easily cause sidebands which exceed this requirement. Unfortunately, there is no convenient way of distinguishing between sidebands on the ground-reflected signal and those on the leakage component which would exist with the spacecraft "looking" into free space.

C. Ground-Based Experiment, Upside Down

Although it would be preferable to conduct an experiment with the spacecraft right-side up, as described above, the practical problems in doing so are very difficult and it is questionable whether this can be done.

An alternate approach is to turn the simulated spacecraft, as described above, upside down in order to minimize the ground-reflection problem. Although this approach is less realistic than the one described previously, it has been considered because of the severe difficulty in performing the test described in Part 2 above. The two important effects to be tested are: (1) the coupling between transmitter and receiver caused by plume reflections; and (2) the modulation imposed on the transmitter-receiver coupling caused by spacecraft vibration and acoustical coupling.

In mounting the spacecraft upside down, the reversal of the gravity vector will certainly modify the plume shape. However, the relatively high exit speed of the exhaust gases would be expected to cause the gravity reversal to have a relatively small effect on this shape. A greater effect on the plume shape is the presence of the earth's atmosphere, which is unavoidably present for any reasonable earth test, and this will be discussed later.

If the vernier engines can be operated properly in the inverted position, and if the spacecraft is properly supported, the vibration characteristics of the spacecraft frame are not expected to be changed materially from those existing during lunar landing. This follows from the fact that a properly-designed spacecraft support can counteract the steady gravitational vector, while not appreciably affecting the vibration components likely to cause spurious leakage sidebands in the doppler band. In any event, any ground testing of the spacecraft, such as described here, should attempt to separate acoustical coupling from spacecraft frame coupling because the acoustical air coupling is absent during lunar descent.

The biggest problem in performing this test appears to be the upside-down operation of the vernier engines. There appear to be differences of opinion in this regard; however, the fact that some propulsion experts think that such operation would be dangerous (from a standpoint of engine operation) would probably rule-out this type of test.

D. Balloon-Supported System

The above considerations indicate that the two experiments described above would probably not be feasible. Still another possibility would be to hoist the simulating structure to an altitude of about 2,000 feet by balloon and tether it to the ground. Much of the present T-2N system could be used for this purpose. The spacecraft frame would preferably be the same as used in Surveyor, because of the desirability for realistic simulation of the vibration transfer function from each vernier engine to the RADVS antennas. This would also mean loading the spacecraft frame with weights, to simulate the major components which would affect the transfer function. The desirability for keeping the overall weight less than that of the actual spacecraft, because of balloon size requirements, may make it desirable to modify the structure in order to produce an equivalent transfer function with less overall weight.

Two major questions are involved in evaluating the feasibility and desirability of this test. The more fundamental question is that concerning the relationship between the plume characteristics for the test and those existing during lunar landing. The second question concerns the presence of air-coupled acoustical coupling during the earth tests, which would of course be absent during lunar descent.

A review of plume characteristics as a function of air pressure is given in two documents. A study of these results indicates that there will be gross differences between the vernier-engine plume which exists during lunar descent and that which will occur during near-earth testing. In fact, these differences are sufficiently great to discourage comparison of plume-coupling behavior between the two different sets of conditions.

With regard to the second question, there appear to be methods by which the air coupling can be reduced to negligible levels or separated from the structural coupling; therefore, this problem does not appear to be as fundamental as that of the plume characteristics. However, the process of reducing this coupling would require rather elaborate experimental setups and testing. In view of the lack of realism in simulating plume characteristics under lunar conditions, it does not appear worthwhile to attempt solution to the air-coupling problem.

In summary, it appears that the balloon-supported system does not permit realistic testing of plume effects. Consequently, it offers very little conclusive information that cannot be obtained by separate measurement of the spacecraft vibration caused by the vernier engines, followed by an upside-down test where this vibration is imposed by shake tables while the leakage-signal characteristics in the pre-amplifiers are studied.

E. Vacuum Chamber Tests

Although the ideal test would be to place the surveyor spacecraft in a vacuum chamber and simulate RADVS-controlled lunar landing, there are several reasons why such tests are not feasible. First, the problem of chamber reflections would be orders of magnitude worse than for the experiment described in B above. Second, firing the vernier engines in a vacuum chamber would probably present extremely difficult problems. A proposal was submitted to HAC by the Cornell Aeronautical Laboratories to perform a combined analytical and experimental study of plume

effects, [67,73] where plume studies would be made in a vacuum chamber. Although such a study would have considerable merit, it is too late in the Surveyor Program to start such a long and costly program.

F. Analytical Approach

A purely analytical approach to the effects of the vernier engines on transmitter-receiver leakage would at first sight appear to be very attractive, in view of the difficulties and questionable value in performing any of the tests described above. However, in attempting to set up the problem, one is immediately confronted with many imponderables. For example, the precise characteristics of the plume under lunar conditions are unknown. The dynamic electrical characteristics of the plume, coupled with vibration effects of the vernier engines, are very important factors to be taken into account in a useful analytical treatment. Equally difficult and uncertain is the electromagnetic interaction problem. Much of the critical interaction can be expected to occur within the Fresnel (near) zone of the antenna, largely outside the cylinder of major field concentration. Precise computation of this interaction cannot be made, and the actual interaction can depend strongly upon antenna parameters which vary considerably from one antenna to another (e.g., those parameters which determine the far-out sidelobe structure).

If calculations were made under the uncertainties described above, the results would have to be used with caution. Unfortunately, previous calculations, based on a much simpler model than is believed desirable, show that the interaction effects can be borderline [67]. Thus, only lengthy computations based upon accurate models would be of value to evaluation of plume effects on the transmitter-receiver leakage problem. It appears at this time that the necessary accuracy of model construction cannot be achieved.

G. Vibration Tests

Because of the difficulty of performing completely realistic earth tests, including realistically-simulated lunar environmental conditions, the best practical earth tests appear to be those which exclude testing for plume effects. Useful earth tests can be performed for which realistic vibration effects are thoroughly tested. These vibration effects are obviously very important, perhaps more so than plume effects, and should be tested.

One approach to these tests is to obtain vibration characteristics of the operating retro-rocket; it would be treated as a driving source, and its spectral and impedance characteristics would be measured. The spacecraft containing RADVS would then be mounted in an inverted position so that vibration tables could simulate retro-rocket and vernier-engine driving sources. The RADVS pre-amplifier outputs would be recorded and analyzed under both simulated retro firing and vernier-control phases. Although it would not be necessary to use a complete operating system, including frequency trackers, if trackers are available their susceptibility to false lock on spurious leakage components could be tested. The important data to be obtained is the recording of actual pre-amplifier noise signals. These stored signals can then be played-back for spectral analyses and for testing tracker susceptibility to false lock.

Additional tests of this type could be performed where the vibration levels used for the tests are set equal to those measured on actual surveyors, during their retro and vernier descent phases.

H. Surveyor On-Board Test

The preceding discussion indicates the serious difficulties in performing transmitter-receiver leakage tests in near-earth conditions. In fact, it appears that completely suitable earth tests cannot be devised. For this reason, it is believed desirable to consider the possibility of performing an on-board test on one of the surveyor spacecraft. One such test is described below.

Relaying the un-processed pre-amplifier signals back to earth is clearly out-of-question because of the bandwidth required to do this. Therefore, some degree of processing of the raw signals must be accomplished on-board the spacecraft. The most meaningful processing is a spectrum analysis, because this can be done with a small amount of circuitry.

A good basis for the planning of an on-board experiment is that the normal system operation be completely unaffected by the experiment. For example, the frequency trackers can be made to perform spectral analyses by disabling their lock-on function and allowing them to scan the doppler band. The tracker filter output may then be detected and telemetered back to earth; simultaneous of the scan-cycle timing would permit construction of the power-density spectrum. However, none of the frequency trackers can be made available for this purpose, and there are inherent dangers in attempting to time-share a tracker. Therefore, the spectrum analyzer function should be performed by added circuitry. Two methods of implementing an analyzer are described briefly below and are discussed more fully in Section VII.

The most promising method appears to be to provide an additional VCO and the necessary circuitry to cause it to scan a narrow-band filter through the doppler band. This would be similar to the use of a frequency tracker, as described above. However, the scan rate, bandwidth coverage, fly-back frequency, and other parameters could be optimized for the spectrum analysis. It appears that stepping the VCO frequency, in synchronization with the telemetry rate, would be preferable to continuous scanning for several practical reasons (e.g., control of the step levels could be very precise, giving accurate indexing of the frequency of a given point).

An alternate spectrum analyzer would be a simultaneous processor; that is, a number of adjacent bandpass filters would be used to observe simultaneously all portions of the doppler band which are of interest. In this case the filters could operate at audio frequencies, or the pre-amplifier outputs could be translated to a higher frequency in order to reduce the filter sizes.

It would be desirable to perform spectral analyses on all three beams; however, if telemetry capacity does not permit this, information obtained on one or two beams would be very useful. For multiple-beam processing, the first analysis method described above clearly becomes the more attractive because the same VCO can be used for the frequency-scan function.

III. APPLICATION OF DATA

Section II was concerned with methods for obtaining data on the spectral and time-behavior characteristics of RADVS pre-amplifier signals. This part describes the value of such data to RADVS design and test.

In analyzing the performance of a CW system, it is necessary to know the characteristics of the noise which limits the tracker acquisition and tracking sensitivity. If this noise were predominately random thermal noise arising in the RF mixer, then its characteristics could be measured in the laboratory; analysis of tracker sensitivity would be straightforward in this case. On the other hand,

other noise components such as transmitter-receiver leakage are often very difficult to evaluate; first, the process of obtaining complete statistical descriptions of these components can be very difficult, as indicated in Part B above; also, the slow variations of the characteristics of these noise components during an operation, or their lack of repeatability from one spacecraft to another, considerably complicates the analysis of their effects and the optimization of tracker design. Thus, for the non-thermal noise components, no general rules can be stated as to how the spectral data would be used to change the testing, or to make necessary modifications to the tracker design. However, availability of good information on noise characteristics does permit studies to be made which lead to optimum performance by design changes and/or changes in operating modes.

As an example of the use of noise spectral data, assume that reliable information is obtained which indicates that serious non-thermal noise components are present only at frequencies below 10 kHz. Because of the importance of early acquisition of all RADVS beams, it is desirable to perform frequency search during retro fire. However, it may be quite useful to limit the frequency search to the band above 10 kHz prior to burnout, because lock-on could occur in most cases (i.e., signal frequencies would exceed 10 kHz in most cases), while false lock on the spurious noise components would be avoided.

Another example of the usefulness of spectral data would be to set the acquisition thresholds at a high enough level to avoid false locks. Although such reduction in acquisition sensitivity is certainly undesirable, it is preferable to false lock, with the resulting erroneous information which would be fed to the control system.

The important point being made here is that a knowledge of the problem, as posed by non-thermal noise components in the pre-amplifier outputs, is essential to finding solutions to it. Lack of such information will cause uncertainties in performance estimation, as well as inability to achieve optimum design.

APPENDIX C

SIDELOBE EFFECTS AS RELATED TO RADVS TEST PROGRAM REVIEW

I. INTRODUCTION

In order to determine the test requirements imposed on RADVS by antenna sidelobe effects, a study has been made of the cross-coupled sidelobe (CCSL) false-lock problem, and of the effects of the simultaneous presence of a main-beam signal and a CCSL signal in the bandwidth of the tracker filter.

Of primary importance to the study are estimates of the relative levels of the correct signal (i.e., mainbeam) and of CCSL signals in a given velocity channel. The latter signals result from mainbeam transmission on each of the other two RADVS beams and sidelobe reception on the receive beam of the particular channel under consideration. Estimates of these relative signal levels are given in Part II for two cases, corresponding to Surveyor Missions A and B.

The main purpose of Part III, CCSL Suppression Possibilities, is to determine whether fortuitous suppression might occur with the present RADVS design, meaning that the problem may have been exaggerated. This consideration also permits answering the question as to whether such suppression might be induced by minor changes in circuit design. Although the answer to the first possibility is negative, the study has led to a suggestion which appears to have considerable promise as a CCSL suppression technique and which is believed worthy of further consideration.

Applicable references are numbers 63 and 45; the second of these has been particularly helpful to this analysis, and some of the conclusions in Part V are based on results contained in this reference.

II. ESTIMATES OF SIGNAL LEVELS

The ratio of mainbeam to CCSL signal levels in channel j is determined primarily by five factors: (1) an antenna gain factor,

$$G_{ij} = \frac{G_{\text{trans. ant. } j}(\text{j beam axis}) \times G_{\text{rec. ant. } j}(\text{j beam axis})}{G_{\text{trans. ant. } i}(\text{i beam axis}) \times G_{\text{rec. ant. } j}(\text{i beam axis})} ;$$

(2) a factor depending upon lunar-reflectivity variation with incidence angles of beams i and j and upon slant range, expressed as a function of spacecraft approach angle ϕ and roll angle ρ ,

$$R_{ij}(\phi, \rho) ;$$

(3) a pre-amplifier roll-off factor which occurs for doppler frequencies less than about 3 kHz

$$A_{ij}(V_x, V_y, V_z) ;$$

(4) a spread-spectrum loss factor

$$L_{ij}(V_x, V_y, V_z, B_t) ,$$

where the V terms represent velocity components (functions of time), and B_t is the tracker bandwidth; and (5) a terrain factor which varies randomly with time, depending upon the particular patches of lunar surface being illuminated.

The above description shows that precise predictions of the ratio of mainbeam to CCSL signal levels are not possible; the spread of this ratio for a given descent can be quite large, partly due to deterministic variables such as φ and ρ , and partly due to random variables such as burnout velocity components and terrain variations. Computation of the probability distribution of the signal ratio is very involved. The results of a Monte Carlo computation including the above factors for a 25° approach angle (Mission B) are reported in [45]. Although similar results for a vertical descent (Mission A) may be available, they have not been included here because each of the factors listed above, except the antenna gain factor, has considerably less influence on the spread of signal ratios for the 0° approach than for the 25° approach.

Case 1 Vertical Approach to Lunar Surface (Mission A)

For this case, the ratio of average signal levels between mainbeam and CCSL signals is determined primarily by the antenna patterns. The $R_{ij}(\varphi, \rho)$ factor will be essentially unity, except for small random variations caused by variations of the spacecraft z axis from lunar vertical.

For consideration of the pre-amplifier roll-off factor and the spectrum loss factor, the dispersion of velocity components along the three DVS beam axes must be considered. Differences in these velocity components are caused by: (1) a random lateral velocity component caused by misalignment between the retro-thrust axis and the velocity vector at initiation of retro-fire; and (2) by the introduction of a lateral velocity component caused by lunar gravity, when the spacecraft z axis is tilted away from the lunar vertical. For vertical approach, only the first factor is important. Data in reference 45 indicate that the 3σ dispersion of lateral velocity caused by the first factor will be approximately ± 150 fps. At retro burnout, the minimum value of V_z is expected to be approximately 240 fps. Translating these numbers into doppler components and spectral bandwidths gives the following results:

For roll angle giving smallest velocity along beam axis

center doppler	=	4,150 Hz
bandwidth	=	300 Hz

For roll angle giving largest velocity along beam axis

center doppler	=	7,560 Hz
bandwidth	=	40 Hz

Therefore, the pre-amplifier roll-off and spread-spectrum effects should be negligible for this case.

Data in reference 45 show that the effects of terrain differences should be small for this case, probably no more than ± 3 db for the ratio of mainbeam to CCSL signals.

These results are summarized in Table C-1, where the nominal values are determined from the antenna gain patterns, as given in reference 63.

Table C-1. Case 1 signal levels

	<u>Antenna Number</u>		<u>Mainbeam Signal</u> CCSL Signal	
	Transmit	Receive	Nominal Value	Variation (terrain effects)
S/N 1	1	2	28 db	} ± 3 db
	2	1	37 db	
	1	3	44 db	
	3	1	46 db	
	2	3	32 db	
	3	2	36 db	
S/N 10	1	2	27 db	
	2	1	46 db	

Case 2 25° Approach (Mission B)

The numerical estimates given in Table C-2 were taken from reference 45. Although all factors contributing to the signal ratio, as described above, were taken into account, observation of the results do not permit attributing various amounts of the dispersion in signal ratio to the different effects. It is of interest, however, to consider the pre-amplifier roll-off and the spread-spectrum loss factors. As was done for Case 1, consideration of the two factors leading to differential dopplers in the three beams gives the following estimates (based on 3σ lateral velocity dispersion at retro burnout of ± 150 fps):

For roll angle giving smallest velocity along beam axis

center doppler = 2,850 Hz
bandwidth = 420 Hz

For roll angle giving largest velocity along beam axis

center doppler = 9,000 Hz
bandwidth = 180 Hz

Thus, it appears that pre-amplifier roll-off effects at retro burnout are also quite small for this case. Spread-spectrum effects will be appreciable in the narrow-band mode ($B_t = 300$ Hz) and the loss should be less than 1 db for this case.

Table C-2. Case 2 signal levels

Roll-Angle	<u>Mainbeam Signal</u> CCSL Signal (db)	
	Transmit 1, Receive 2	Transmit 2, Receive 1
0° (near optimum)	35-39*	35-39
30°	38-42	31-34
60° (near optimum)	35-38	34-37
80°	29-32	40-43
125° (near worst)	14-18	54-58
240°	18-21	51-54

* Spread of values in table account for dispersion in burnout velocity. Additional spread caused by terrain effects is not included; if the same factor given in Table 1 is used to account for these effects, a ± 3 db factor should be added to the range of values given in this table.

III. CROSS-COUPLED SIDELobe SUPPRESSION

Two possibilities exist in the RADVS system by which a strong signal can suppress weaker signals: (1) circuit non-linearities in receiver stages preceding the tracker filter; and (2) by operation of the gain-state circuits. The former can occur, for example, by limiting action in a circuit, but the form of the non-linearity is unimportant to the following discussion.

A. Circuit Non-Linearities

Consider first the possibilities for, and the implications of, circuit non-linearities. The significant circuit stages are: RF mixer, pre-amplifier, single-sideband modulator, IF amplifier, and IF mixer. In order for one signal to suppress another by non-linear action of a circuit, it must be significantly larger than the sum of all other signals present; otherwise, it will be suppressed by the other signals, and this is a situation which clearly cannot be tolerated. Thus, for each stage to be considered, the signal-to-noise ratio of the mainbeam signal must be larger than unity, say by at least six db, in order for CCSL suppression to occur.

The RF mixer will operate essentially as a linear device to the input signals, because these signals will always be small relative to the transmitter reference signal. Furthermore, the noise from this mixer is so wideband that if signal suppression were attempted, the input signals would be the ones to suffer suppression.

The preamplifier is also relatively wideband, compared with the signal bandwidth. The ultimate tracker sensitivity is determined by the tracker-filter bandwidth; this is the effective pre-detection bandwidth of the RADVS receiver. Immediately after burnout, this bandwidth is 300 Hz; because this time interval is of considerable interest, a 300 Hz bandwidth will be taken for illustrative purposes. Although an oversimplification, it is assumed that the preamplifier noise density is uniform from 0-100 kHz; for doppler signals in the vicinity of 10 kHz (which is roughly the case near retro burnout), the preamplifier signal-to-noise ratio (SNR) obtained in this manner is approximately equal to that obtained by a more precise analysis (say, assuming 1/f noise behavior in the preamplifier passband). This SNR may then be expressed as

$$\text{SNR}_{\text{pre-amp}} \approx \frac{P_s}{10^5 N_o} \quad (\text{C-1})$$

where P_s/N_o = ratio of signal power to noise density (at 10 kHz) at the output of the preamplifier. The tracker-filter output SNR is given by

$$\text{SNR}_{\text{tracker}} = \frac{P_s}{2B_t N_o} \quad (\text{C-2})$$

where B_t = tracker-filter bandwidth; the factor of 2 results because of the "fold-over" effect in the IF mixer. Thus, the ratio of SNR's is

$$\frac{\text{SNR}_{\text{tracker}}}{\text{SNR}_{\text{pre-amp}}} \approx \frac{10^5}{2B_t} = \frac{10^5}{600} = 170 \equiv 22 \text{ db} \quad (\text{C-3})$$

In order for the mainbeam signal to cause significant suppression of smaller sidelobe signals in the preamplifier, the tracker-filter SNR must be greater than 28 db (i.e., $\text{SNR}_{\text{pre-amp}} + 6 \text{ db}$). For an acquisition threshold of 10 db above the rms noise level, and allowing a 6 db margin to account for short-term fluctuations in signal amplitudes, the margin between mainlobe and sidelobe signals must therefore be at least 24 db, in order for sidelobe signal suppression to occur (either incidently or intentionally, assuming the circuits are designed to prevent significant noise suppression of mainlobe signals). Unfortunately, the data in Tables C-1 and C-2 show, that for the two landing approaches thus far analyzed, the 24 db margin cannot be achieved. There are other reasons why it would be undesirable to attempt intentional suppression in the preamplifier. First, the two preamplifiers (0° and 90° phases) for a given tracker must be well-matched over their entire dynamic range in order to provide good negative-doppler rejection; and second, the following discussion shows that there are more effective ways of obtaining CCSL signal suppression. Therefore, it is believed that CCSL suppression does not exist to an appreciable degree in the preamplifiers, and that no attempts should be made to obtain suppression in these stages.

The mixers in the single-sideband modulator will be operated at a relatively high level of the VCO reference (essentially an on-off switch). Therefore, the signal transfer function is essentially linear and no sidelobe signal suppression by the mainbeam signal can occur.

With regard to the IF amplifier, the bandwidth ratio of this amplifier and the tracker filter is somewhat more favorable than for the preamplifier. That is,

$$\begin{aligned} \frac{\text{SNR}_{\text{tracker}}}{\text{SNR}_{\text{IF}}} &\approx \frac{10,000}{3,000} = 3.3 \equiv 5.2 \text{ db, wideband mode} \\ &\approx \frac{10,000}{600} = 16 \equiv 12 \text{ db, narrow-band mode} \end{aligned} \tag{C-4}$$

Thus, mainbeam signals having $\text{SNR}_{\text{tracker}} > 11 \text{ db}$ (narrow-band mode) and 18 db (wideband mode) could be allowed to cause suppression of weaker signals in this amplifier. It is extremely unlikely that any non-linearities in the present circuit, which would be unintentional, could cause significant sidelobe signal suppression. However, if signal suppression capabilities were designed into this circuit to the limit derived above, sidelobe signal suppression might be quite effective. For example, assume that the IF amplifier rarely limits on noise, but limits heavily on signals about 6 db greater than noise. To be consistent with the foregoing discussion, assume that the tracker acquisition threshold is 10 db above noise and that a 6 db margin is allowed in order to account for short-term signal fluctuations between the mainbeam and CCSL signals. Thus, CCSL signals would be prevented from rising above the acquisition threshold provided they are more than 7 db (wideband mode) and 14 db (narrow-band mode) below the mainlobe signal. This requirement appears more reasonable than those derived previously, as can be seen from the data in Tables C-1 and C-2. In Part IV it is shown that dispersion of burnout lateral velocity can cause differences of doppler frequencies between mainbeam and CCSL signals as large as 8 kHz. Therefore, in order for the IF amplifier bandwidth to include both signals, its bandwidth would have to be widened, or its center frequency shifted. In this way the stronger signal would always be available to produce sidelobe suppression in the IF amplifier.

Finally, the IF mixer which precedes the tracker filter will operate in a similar manner to the mixers in the single-sideband modulator, and no effective sidelobe-signal suppression can be expected.

B. Gain-State Switching

The second possibility for sidelobe signal suppression (i.e., mainbeam signal switching of preamplifier gain-state) will now be discussed. The question is basically as follows: will the ratio of mainbeam signal to sidelobe signal always be greater than the dynamic range between the tracker acquisition threshold and the signal level which causes a switch to the next lower gain state? If this condition is satisfied, we see that both signals cannot simultaneously fall within this dynamic range; the stronger signal would always manage to switch the preamplifier to a lower gain-state before the sidelobe signal rises above the acquisition threshold. Because the same dynamic range applies approximately to all gain states, it would thus be assured that the stronger signal would always adequately suppress the weaker signal. Unfortunately, it turns out that this requisite signal spread cannot be depended upon, as will now be shown. For RADVS, the dynamic range expressed above has a maximum value of 33 db (allowing for dispersions of threshold, gain-state switches, etc.)[45]. Although it might be argued that this spread could be reduced, the ratio in (C-3) shows that in order for the mainbeam signal to control the gain-state, the value of SNR_{tracker} must be well above 22 db (narrow-band mode, after burnout). If the acquisition threshold is 10 db above noise, if a 6 db margin is allowed to account for short-term signal fluctuations, and if another 3 db is allowed to account for variations in the gain-state trip power relative to preamplifier noise, the 33 db range could probably be reduced to about 21 db. However, if this were done, more gain-states would be required and this would be undesirable for a number of reasons. Furthermore, the improvement would not be sufficient to ensure adequate suppression of CCSL signals. We, therefore, have the answer that CCSL signal suppression cannot be obtained by mainbeam control of the gain-state, because the ratio of mainbeam signal to sidelobe signal will often be less than the dynamic range between the acquisition threshold and the gain-state trip value (33 db for the present RADVS, and about 21 db for a modified system).

IV. SUGGESTED APPROACH TO CORRECTION OF CCSL SIGNAL PROBLEM

A. Description of Technique

The study described above has resulted in a suggestion for correcting the CCSL signal problems. It would appear that the method described below would have considerable promise for solving the problem, and would require only minor modification to existing circuitry.

Fig. C-1 shows a block diagram of the suggested solution. Actually, this is just a simplified block diagram of a portion of the present tracker. The only modification is that the bandpass filter has been widened, as shown in Fig. C-2. Also, the circuit shown in Fig. C-1 should be used for all gain-states, rather than just the 90 db state, as for the present system. The lower cut-off of the bandpass filter is equal to the upper cut-off of the tracker filter ($B_t = 300$ Hz in the narrow-band mode and 1500 Hz in the wideband mode). Its upper cut-off frequency is determined by the maximum doppler differences between all three DVS beams, which in turn is determined by the maximum lateral-velocity dispersion to be encountered during RADVS operation. This value of required upper cut-off frequency must be determined by analysis of the planned missions; preliminary estimates of this frequency are given below in order to illustrate the circuit's capability.

Referring to Figs. C-2 and C-3, the case illustrated is for the CCSL signal present in the low-pass tracker filter, while the correct mainbeam signal is contained in the bandpass filter. The detector circuits are assumed to have equal gain. For low values of P_M and P_{CCSL} (i.e., low SNR's) these signals will have little effect on the average values of E_b and E_t . However, as the power in each signal

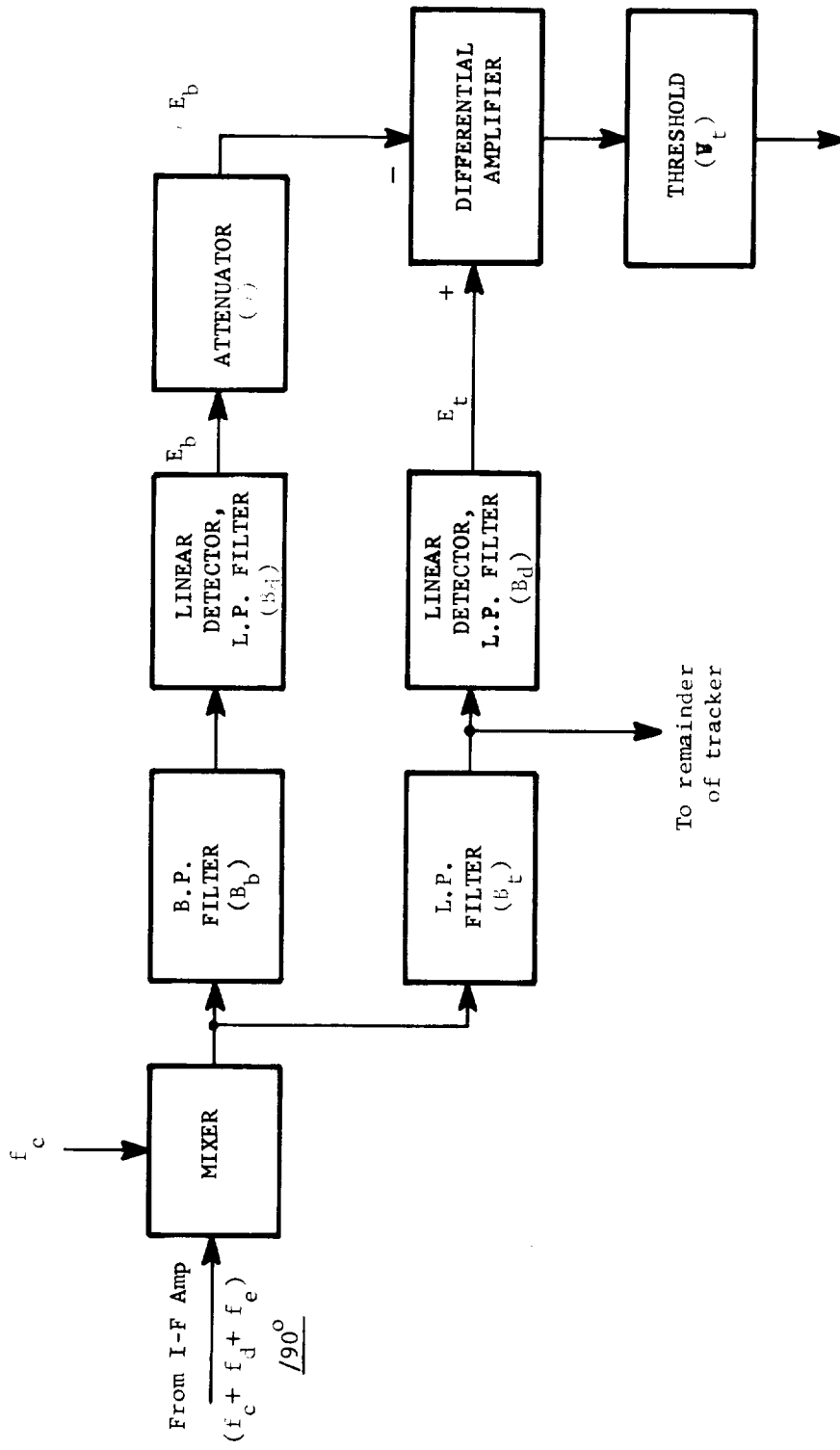


Fig. C-1. Acquisition circuit, block diagram.

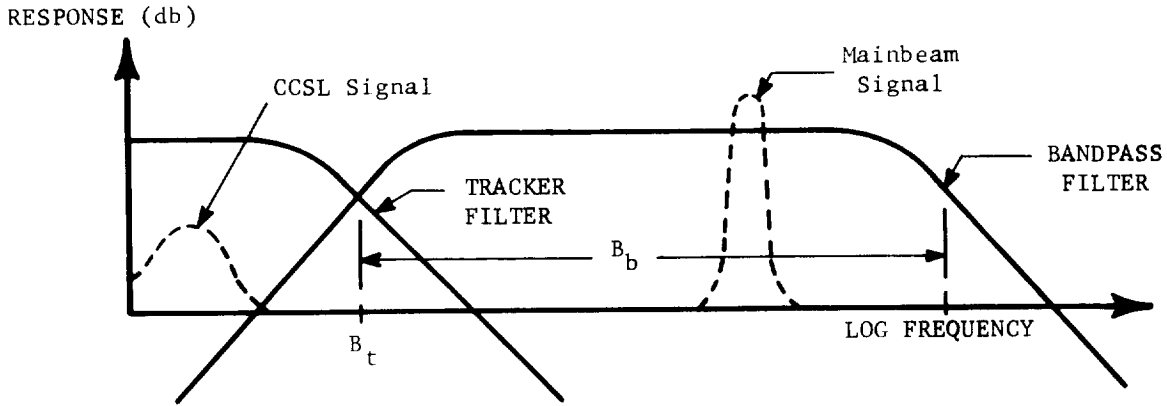


Fig. C-2. Response curves of lowpass and bandpass filters in Fig. C-1.

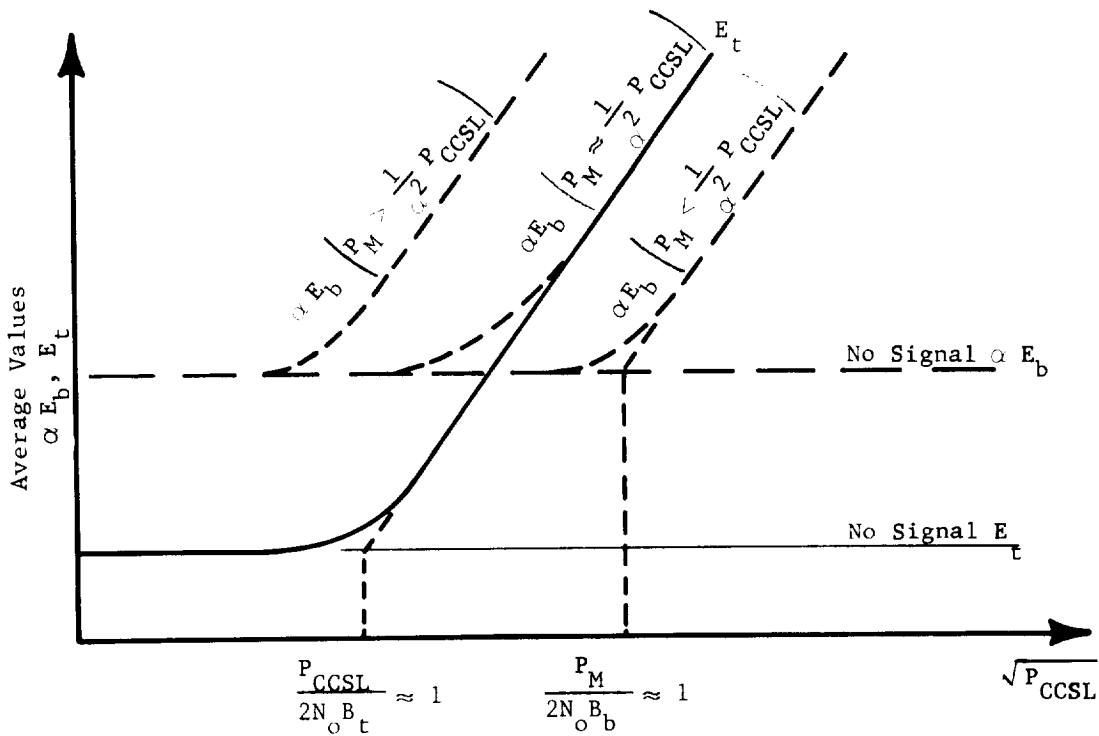


Fig. C-3. Detector outputs (Fig. C-1) versus cross-coupled sidelobe power, with P_M/P_{CCSL} as a parameter.

exceeds the noise contained in its filter, the average output rises as shown. It is seen that $\alpha E_b \text{ aver} > E_t \text{ aver}$ for $P_M > 1/\alpha^2 P_{\text{CCSL}}$ and for all low-level (SNR < 1) CCSL signals. Therefore, the average output of the differential amplifier is positive for these cases. Allowing some threshold margin, V_T , we see that the differential amplifier output cannot exceed the threshold for all cases where

$$E_t - \alpha E_b - V_T \geq 0 \quad (\text{C-5})$$

where V_T is the threshold setting, referred to the differential amplifier input. Therefore, the circuit will not lock CCSL signals for which the inequality in (C-5) is satisfied. When the mainbeam signal is in the tracker filter, the smaller CCSL signal will have only a minor effect on the acquisition operation. In this case, $E_t \gg \alpha E_b$ for all practical cases where P_M is above the tracker acquisition threshold.

B. Derivation of Capability

The circuit in Fig. C-1 will be analyzed in detail, for the case where the receiver noise is essentially thermal (i.e., assuming that there are no spikes of transmitter-receiver leakage in the doppler band). The effects of such spurious signals will be discussed later.

Of fundamental importance in analyzing the circuit performance is the bandwidth, B_b , required to contain both mainbeam and CCSL signals. This bandwidth is determined by the maximum doppler-frequency difference between the mainbeam and CCSL signals. This maximum frequency difference has been estimated to be 6.2 kHz, based on a 45° approach angle minimum burnout velocity of 220 fps, a 3σ value of lateral burnout velocity of 150 fps, and assuming that the lateral velocity component passes through the plane of beams one and three. For purpose of the following calculation, a value of $B_b = 8$ kHz will be assumed. This value was obtained from Mr. R. Dibos, Hughes Aircraft Company, has an estimate of the maximum operational spread between the center doppler frequencies of two beams.

Assume the following radar parameters:

$$\begin{aligned} B_t &= 300 \text{ Hz, narrowband mode (N.B.)} \\ &= 1500 \text{ Hz, wideband mode (W.B.)} \\ B_b &= 8000 \text{ Hz, (from discussion with R. Dibos, Hughes)} \\ B_d &= 4 \text{ Hz (for 40 msec response time as for present system)} \\ \alpha &= \frac{1}{2} \text{ (this value will be shown to give discrimination} \\ &\quad \text{capability } P_M/P_{\text{CCSL}} = 6 \text{ db)} \end{aligned}$$

It can be shown that for a linear detector, time average values and variances of E_b and E_t may be expressed as

$$\begin{aligned} \bar{E}_b &\approx k_1 \sqrt{P_M + N_o B_b} \\ \bar{E}_t &\approx k_1 \sqrt{P_{\text{CCSL}} + N_o B_t} \\ \sigma_b^2 &\approx k_1^2 N_o \sqrt{B_b B_d} \\ \sigma_t^2 &\approx k_1^2 N_o \sqrt{B_t B_d} \end{aligned} \quad (\text{C-6})$$

where k_1 = gain constant

N_o = noise density at input (assumed uniform throughout bands B_t and B_b).
Thus, (C-5) can be rewritten

$$\bar{E}_t - \alpha \bar{E}_b - V_T + \text{Random Term} \geq 0 \quad (C-7)$$

where the random term corresponds to the noise fluctuations on $E_t - \alpha E_b$.

In the absence of signals, V_T will cause the average values of the left side of (C-7) to be negative. However, false-alarm locks can occur if the random term goes sufficiently positive to overcome this average negative value. Although such false-alarms cause only a pause in the acquisition search, it is desirable that they occur only infrequently. This can be ensured by setting

$$\begin{aligned} & |\bar{E}_t (P_{CCSL} = 0) - \alpha \bar{E}_b (P_M = 0) - V_T| \\ & > > \sqrt{\sigma_t^2 + \alpha^2 \sigma_b^2} \end{aligned} \quad (C-8)$$

which is achieved by setting

$$V_T + k_1 \sqrt{N_o} \left[\alpha \sqrt{B_b} - \sqrt{B_t} \right] \gg k_1 \sqrt{N_o} B_d^{\frac{1}{2}} \left[\sqrt{B_t} + \alpha^2 \sqrt{B_b} \right]^{\frac{1}{2}} \quad (C-9)$$

For the numbers given above

$$\begin{aligned} V_T + 27.5 k_1 \sqrt{N_o} & \gg 8.9 k_1 \sqrt{N_o} \quad (\text{N.B.}) \\ V_T + 6.0 k_1 \sqrt{N_o} & \gg 11 k_1 \sqrt{N_o} \quad (\text{W.B.}) \end{aligned} \quad (C-10)$$

For a factor of 4 in this inequality, the false-alarm rate should be acceptably low (i.e., only values of the random component beyond 4σ would cause false-alarms). This value results in

$$\begin{aligned} V_T & = 8 k_1 \sqrt{N_o} \quad (\text{N.B.}) \\ & = 38 k_1 \sqrt{N_o} \quad (\text{W.B.}) \end{aligned} \quad (C-11)$$

Returning now to the general condition for CCSL lock given in (C-5), we will derive average values of P_{CCSL} and P_M which define the threshold condition between CCSL lock and no-lock. In terms of average values of E_t and E_b , this threshold is defined by the condition

$$\bar{E}_t - \alpha \bar{E}_b - V_T = 0,$$

or

$$k_1 \sqrt{P_{CCSL} + N_o B_t} - \alpha k_1 \sqrt{P_M + N_o B_b} - V_T = 0 \quad (C-12)$$

or

$$\sqrt{\frac{P_{CCSL}}{N_o B_t} + 1} - \frac{8}{\sqrt{B_t}} = \frac{1}{2} \sqrt{\frac{P_M}{N_o B_t} + \frac{B_b}{B_t}} \quad (\text{N.B.})$$

(C-13)

$$\sqrt{\frac{P_{CCSL}}{N_o B_t} + 1} - \frac{38}{\sqrt{B_t}} = \frac{1}{2} \sqrt{\frac{P_M}{N_o B_t} + \frac{B_b}{B_t}} \quad (\text{W.B.})$$

These equations have been solved for various values of $P_{CCSL}/N_o B_t$ and for the radar parameters given above, and are plotted in Fig. C-4.

Notice that for $P_M = 0$, the values of $P_{CCSL}/N_o B_t$ satisfying (C-13) correspond to the circuit's acquisition sensitivity (expressed as a SNR). This is of course the same as setting $P_{CCSL} = 0$ and assuming that the mainbeam signal is in the tracker filter rather than in the bandpass filter. Fig. C-4 shows that the acquisition sensitivity of the circuit is 5.6 db (W.B.) and 9.1 db (N.B.). This sensitivity can be improved by use of smaller α . Fig. C-4 also shows that, on the average, mainbeam signals 6 db above CCSL signals will suppress the latter. If we allow a 3 db margin to account for signal fluctuations, a signal ratio of 9 db will reliably suppress CCSL signals. The asymptotic ratio shown in Fig. C-4 is $1/\alpha^2$. Thus, a trade-off between acquisition sensitivity and CCSL suppression may be made. The above results show that $\alpha = 1/2$ is about the highest desirable; and somewhat lower values may be a better compromise.*

C. Use of a Non-Linear Attenuator

A slightly more elaborate circuit can provide more flexibility in the trade-off between acquisition sensitivity and CCSL suppression. The linear attenuator in Fig. C-1 is replaced with a non-linear attenuator of the type shown in Fig. C-5.

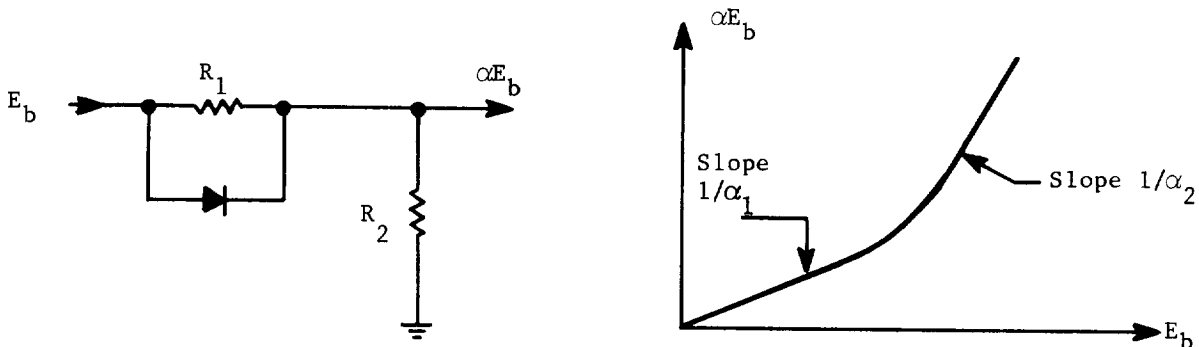


Fig. C-5. Attenuator characteristic.

This circuit permits selection of α_1 to maximize the acquisition sensitivity, while α_2 is selected to give the desired high-SNR CCSL discrimination. It is interesting to note that for $\alpha_2 > 1$ (i.e., gain), one signal may be used to suppress a

*For example, $\alpha = 1/3$ gives values of acquisition sensitivity of 5 db (W.B.) and 7.5 db (N.B.) and CCSL discrimination capability of 9.5 db.

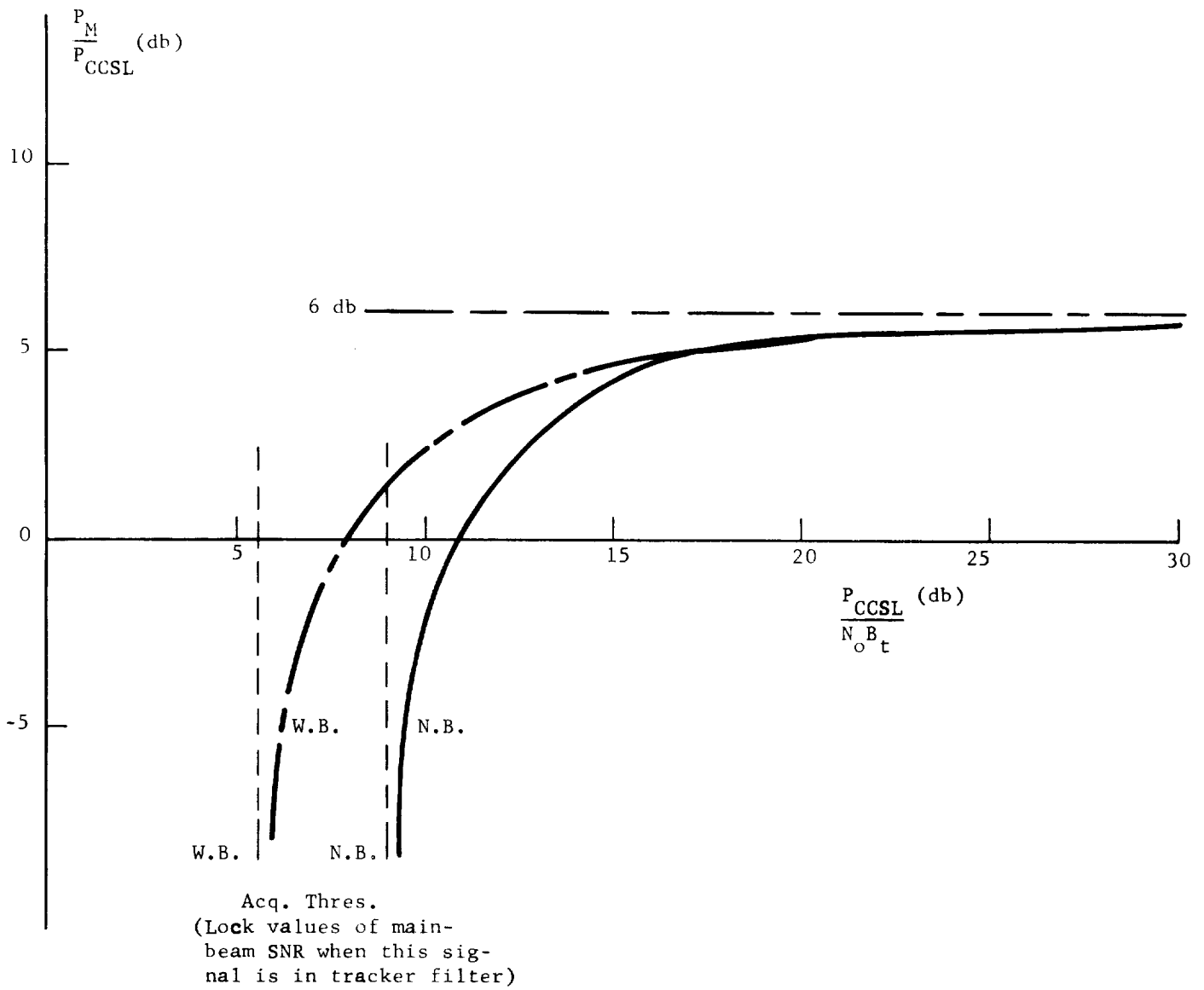


Fig. C-4. Sidelobe suppression capability of circuit in Fig. C-1 for $B_b = 8$ kHz, $B_t = 300$ Hz (N.B.), 1500 Hz (W.B.), $B_d = 4$ Hz, and $\alpha = 1/2$. Acquisition thresholds apply when P_{CCSL} and P_M are interchanged and $P_{CCSL} = 0$.

stronger signal. As an example of the use of this circuit, for $\alpha_1 = 1/3$ and $\alpha_2 = 1/\sqrt{2}$, the circuit's acquisition sensitivity will be 5 db (W.B.) and 7.2 db (N.B.) and its CCSL discrimination capability for high SNR signals will be 3 db.

D. Effects of Non-Thermal Noise Components

The previous discussion applies to the case where the pre-amplifier noise output is smoothly distributed, as for thermal noise arising in the RF crystals. Actually, of course, there will be spurious noise components in the band, arising from transmitter-receiver leakage, crystal vibration, power-supply ripple, etc. Some of these noise components may be random, but there will also be components which are essentially periodic. Difficulties arising from these components are most likely to occur in the high-gain mode, because they are expected to be below the acquisition threshold for lower-gain modes. Therefore, any system which employs noise-derived thresholds from a part of the doppler band is susceptible to desentization when a peak of spurious noise appears in the band which is used to provide the noise-derived threshold. Notice that the present RADVS and the circuit described above are such systems. The major difference between the present RADVS system and the suggested modification is that the latter uses a wider filter. It is not possible to make a broad general statement about the relative merits of the two noise-derived thresholds. Actually, the frequency spacing of spurious components is relevant to this question. If these components are spaced in such a manner that only one appears in the sampled noise band (for both the present RADVS and the suggested modification), the modified system will be better because the spurious component will represent a lesser part of the total power in the band. If a single spurious component predominates over all noise in the band the modified system is also superior; in this case the noise-derived threshold for the system in Fig. C-1 is attenuated by a greater factor (α in Fig. 1) than would be the case where the sampled band is narrower. Even if several components appear simultaneously in the sampled band, one component will most likely predominate, and the argument given above for the single component applies rather well. Another viewpoint is as follows: assume a bandpass filter is scanned throughout the doppler band and the detected output observed; in general, the fluctuations which will be observed (normalized to the average detected output) will be smaller for a given bandpass filter than for a narrower one; this just follows the standard smoothing law when a given waveform is averaged over an interval--the broader the interval, the less the variations from the mean.

E. Summary of Technique Capabilities

A study of the estimated values given in Tables C-1 and C-2 show that the capability given in Fig. C-4 should be adequate for all practical cases to be encountered, for the present RADVS system. Reference 45 data would indicate that the worst case to be encountered, without RADVS restrictions imposed on roll-angle, would be for approach angles of 25° and for a roll angle of 45° . For this case, beam 2 would point vertically downward, and CCSL signals from transmit beam 2 into receive beams 1 and 3 could cause trouble. This particular condition will probably have to be avoided (within $\pm 10^\circ$) for all missions, unless CCSL logic circuits are used between these beams. This reference also indicates that the P_M/P_{CCSL} ratio should improve as the approach angle moves on either side of 25° (i.e., toward either 0° or toward 45°).

One very important point should be made regarding the use of the circuit described above: even in the event of a false lock-up on the CCSL signal. due to the unlikely case of the required signal ratio not being exceeded, as soon as the required ratio is exceeded the circuit will cause un-lock from the CCSL signal and re-lock on the mainbeam signal. Therefore, the probability that a serious false lock-on (i.e., a continued lock-on) will occur appears to be very small.

This brief attempt to place bounds on the doppler separation and of the relative power ratio of the mainbeam and CCSL signals, and then to draw conclusive inferences regarding the degree of protection against false CCSL signal lock-on, is obviously very incomplete. A more detailed study is obviously in order, such as was done by the Monte Carlo computation described in [50].

V. EFFECTS OF SIMULTANEOUS OCCURRENCE OF MAINBEAM AND CROSS-COUPLED SIDELobe SIGNALS IN TRACKER-FILTER BANDWIDTH

When the lateral velocity components are quite small, the mainbeam signal and CCSL signals will have nearly equal doppler frequencies. The previous discussion has been concerned with those cases for which the doppler separation is sufficient to prevent both signals from simultaneously falling within the tracker-filter bandwidth. We now consider cases for which the frequencies are close enough so that both signals are within this bandwidth. The mainbeam signal power will usually exceed the CCSL power by a rather large factor; from the previous discussion and from measured pattern characteristics it appears that the ratio will in most cases be greater than 16 db; notable exceptions are those cases for which one beam is pointing almost vertically toward the lunar surface.

An exact analysis of this interference problem is very difficult and will not be attempted here. Past analysis and experience is very helpful, however. For example, when the spectra of the two signals are well separated, the illustration in FigC-6 shows that pre-discriminator limiting action causes the resultant signal to be frequency modulated at the beat rate. Even if the discriminator bandwidth responds to this beat frequency, the tracker will pass only those beats within its bandwidth (approximately 7 Hz). Because of this, doppler signals separated by 30 Hz or more should cause negligible effect on the tracker output. This effect is referred to as "capture" in FM receivers, where the AFC circuit provides extremely good discrimination against the weaker of two signals which are simultaneously present in its discriminator bandwidth.

Actually, the capture effect will still be present even for overlapping, spread spectra. In this case, however, there will be times when the amplitude of the small signal exceeds that of the large signal. During these times, it will contribute to the discriminator output, with the result that the VCO is driven slightly toward the weaker signal. Thus, for such fluctuating signal inputs, the tracker VCO will be biased slightly away from the correct frequency. Because the separation of the two spectra is proportional to lateral velocity components, resulting errors in measuring V_x and V_y will be proportional to the correct velocity. The important point is that no fixed off-set errors in measuring V_x and V_y can occur; the major effects of the interfering signal will be to increase the noise on the velocity analog outputs, and to cause small errors proportional to the lateral velocity components.

For the relative level of the mainbeam and CCSL signals to be incurred, there is essentially no danger of the latter signals causing tracker unlock, once it has acquired the mainbeam signal.

VI. CONCLUSIONS

As a result of the review and analysis described above, the following conclusions have been reached:

- (1) The cross-coupled sidelobe problem is a very serious one for the present RADVS system.
- (2) There are no inherent suppression effects caused by circuit nonlinearities which would be effective to an appreciable degree. The unintentional presence of sufficient non-linearities to do

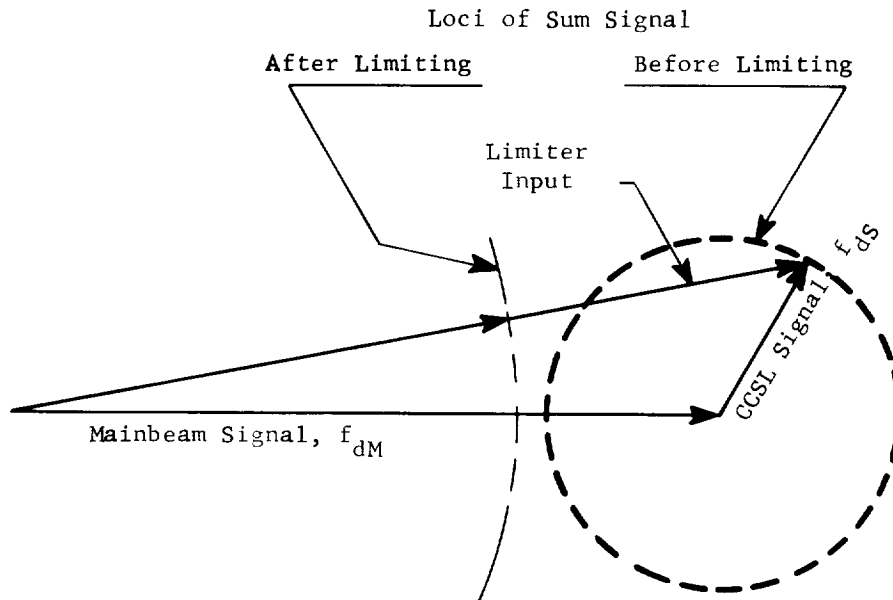


Fig. C-6. Illustration of limiting action on the resultant of a large signal plus a small signal. For well separated signals (i.e., non-overlapping), the effect is to change a non-symmetrical spectrum of the resultant (before limiting) to a symmetrical spectrum, centered at the center of the large-signal spectrum. For fluctuating signals, the effect is slightly different; small shifts of the resultant-spectrum center from that of the larger signal do occur after limiting.

- this would result in noticeable degradation in tracker sensitivity and/or in significant signal clipping. Any suppression of cross-coupled sidelobe signals obtained in this manner should be explored thoroughly to insure that no performance degradation occurs in other ways.
- (3) Gain-state switching can cause mainbeam signals to suppress cross-coupled sidelobe signals below the acquisition threshold, only for power ratios of these signals exceeding 33 db, the dynamic range between gain states. Many cases will occur for which this ratio will not be exceeded, and therefore gain-state switching does not provide effective protection against false lock-on to CCSL signals.
 - (4) The solution to the cross-coupled sidelobe problem by restriction of roll angle is not applicable to all missions. In fact, the technique appears to be most effective for lunar descents near 25° from vertical (such as Mission B), and a rather narrow margin appears for this case^[45]. The roll angle selected for Mission B does not ensure that cross-coupled sidelobe lock-up will not occur, but does give low and approximately equal probabilities for false lock-up on beams 1 and 2.
 - (5) In order to eliminate the cross-coupled sidelobe problem entirely by antenna improvement, and not impose roll-angle restrictions, each receive antenna must have sidelobes in each of the other two mainbeam directions which are at least 46 db below the mainlobe. This can be inferred from the results in reference 45 for 25° approach angle, which is believed to impose about the worst requirement. Such a specification on the antennas would probably still mean that certain roll angles for the 25° approach would have to be avoided, in order to avoid having any DVS beam pointing within about 5° of lunar vertical.
 - (6) If a partial solution is adopted of rotating the antenna (beams 2 and 3) 180° , measurements should be made to insure that all patterns relevant to the cross-coupled-lobe problem are measured or that the cross-coupled product is measured directly. Even with this solution, the data contained in reference 63 and the analysis in reference shows that difficulty could be encountered for the 25° approach over appreciable intervals of roll angle, assuming no RADVS restrictions on this angle are imposed. Thus, for this solution, each mission must be analyzed carefully to ensure that no serious CCSL problem exists.
 - (7) Reference 63 contains all the necessary data on the antenna patterns of S/N 1. Limited data on S/N 10 shows good repeatability on the -27 db sidelobe of antenna 2 in the mainbeam direction of antenna 1. However, the sidelobe of antenna 1 in the mainbeam direction of antenna 2, being at a lower level, did not repeat (values are -37 and -46 db). Because sidelobes at this lower level can influence the cross-coupled sidelobe problem, measurements should be made on each antenna in order to determine the level of the following receive-antenna sidelobes in the direction of the indicated transmit mainbeams:

<u>Receive Antenna</u>	<u>Transmit Antenna</u>
1	2
2	1
1	3
3	1
2	3
3	2

These results should then be used to evaluate cross-coupled sidelobe problems for each mission.

- (8) It appears that the use of CCSL logic circuits between all pairs of antennas can solve the problem. If this is done, care should be taken that simultaneous testing between two or more pairs is not allowed to result in false indications.
- (9) A promising method is described by which the stronger of two or more signals, in a frequency band wide enough to contain all three mainbeam signals, can suppress the weaker signals. The required margin between the stronger and weaker signals is approximately 6 db for the circuit analyzed. More complex circuits, in which a non-linear attenuator is used, can provide suppression for smaller ratios of mainbeam to sidelobe signal levels. A thorough analysis of the bandwidth requirements for this circuit and of its suppression capabilities should be made.
- (10) No serious problems of tracker unlock or false-lock occur when the mainbeam signal and cross-coupled signal are simultaneously within the tracker bandwidth. However, the noise on the analog velocity outputs may increase; this interference effect should be tested with spread-spectra signals.

APPENDIX D

AVAILABLE DETAILS OF VENDOR UNIT TESTS

I. INTRODUCTION

Information in this appendix was taken directly from the Ryan documents referenced in section V.C.1.

II. VERIFICATION TESTS

A. KPSM

1. Klystron Requirements

<u>Parameter</u>	<u>DVS Klystron</u>	<u>RA Klystron</u>
High Voltage	-2150 ± 75 vDC	-800 ± 20 vDC (reflector)
ripple	record	record
regulation	+ 0.25%	+ 0.25%
current	40 to 55 ma	0.5 microamp (max)
time delay	20.0 ± 5.0 sec	2.0 ± 0.5 sec.
Collector Voltage	-500 ± 10 vDC	-500 ± 10 vDC (cathode)
ripple	record	record
regulation	+ 1%	+ 1%
current	10 microamps	45 to 65 ma
time delay	20 ± 5 sec	20.0 ± 5. sec.
Filament Voltage	7.2 ± 0.3 vDC	6.3 ± 0.3 vDC
ripple	record	record
regulation	+ 0.15 vDC	+ 0.15 vDC
current	0.8 to 1.1 amp	0.9 to 1.3 amp
time delay	0 sec.	0 sec.

2. Modulation Characteristics Requirements

Repetition Rate	= 182 ± 5 cps
Flyback Signal Amplitude	= -2.0 to 10.0 vDC
Flyback Pulse Width	= 10 to 160 microseconds
Flyback Rise Time	= 10 microseconds
Start Sweep Pulse Amplitude	= -3.0 to -11.0 vDC
Start Sweep Pulse Width	= 3 to 30 microseconds
Start Sweep Pulse Rise Time	= 3 microseconds (max)

3. Noise on RF Output Requirements

AM sideband noise in 100 Hz BW on RA klystron in high and low dev.	125 db below carrier at 80 kHz away, rising 3db/octave to 102 db at 400 Hz away
AM sidebands in 100 Hz BW due to power supply ripple	115 db below carrier at 80 kHz away, rising 3 db/octave to 92 db at 400 Hz away

4. Modulation Rates at -20°C Requirements

Sweep time	= 5.0 ± 0.5 msec
Average rate	= 8,000 MHz/sec ± 2.4% and 800 MHz/sec ± 1.5%

5. XMTR Frequencies at -30°C Requirements

Measure at times after turn on: 30 sec., 2 min., 3 min.,
4 min., 5½ min.

RA frequency	12.9 GHz ± 25 MHz
DVS frequency	13.3 GHz ± 35 MHz

6. Thermal-Vacuum Test Requirements

Stabilize KPSM @ +75 ± 10°F, < 5 x 10⁻⁶ torr, for minimum of
4 hours. Check XMTR's freq., power, and RA high deviation rate.
Check system warm up time.

B. R/T Units

1. Power Consumption

Requirements: 225 ma from +25 vDC; 15 ma from -25 vDC

2. RF Detector Bias

Requirements: DVS beams: -3 ± 2.0 dbm
RA beams: -2.7 ± 2.0 dbm

3. Beam Angle

Requirements: E Plane	0°0' ± 4'
H Plane	12°30' ± 4'
H Plane Angle between beams	25°0' ± 8'

4. Insertion Loss with Lab Test Adapters

Requirements: XMT Flanges:	1 db
RCV Flanges:	4.5 db
Detectors	7.0 db

5. Two Way Gain

Requirements: 56 db min.

6. Two Way Beamwidth (3 db)

Requirements: E Plane: 5.3° max H Plane: 3.5° max

7. VSWR

Requirements: 1.3:1 max at XMT and RCV flanges and detectors

8. First Order Sidelobe (@ ~ 8°)

Requirements: -30 db min.

9. Noise Figure (Overall Receiver)

Requirements: DVS @ 800 Hz	25.9 db max
8 kHz	19.0 db max
80 kHz	15.8 db max
RA @ 8 kHz	23.8 db max
80 kHz	17.1 db max

10. Microwave Isolation

Requirements: between XMT feeds: 20 db (min)
between opposite XMT & RCV feeds: 55 db (min)

11. Thermal-Vacuum Test

Requirements: Stabilize at +125° ± 10°F (at preamps), < 5 x 10⁻⁶ torr,
for minimum of 4 hours. Check system warm up time.

C. SDC

Stabilize at $+105^{\circ} \pm 10^{\circ}\text{F}$ (at the LVPS), $< 5 \times 10^{-6}$ torr, for minimum of 4 hours. Check analog outputs, range marks, and sensitivity. Check system warm up time.

III. ACCEPTANCE TESTS

A. Laboratory Ambient

1. KPSM

Modulation Rate

Low Deviation Modulation Rate

Place the Klystron Power Supply/Modulator (KPSM) in the temperature chamber and allow it to stabilize at $\approx 30^{\circ}\text{C}$. Apply power to the KPSM. Measure the average deviation rate and the klystron flange temperature after $5\frac{1}{2}$ minutes.

Requirements: 800 MHz sec \pm 1.5% ; 5.0 \pm 0.5 millisecc

High Deviation Modulation Rate

Place the KPSM in the temperature chamber and allow it to stabilize at $\approx 30^{\circ}\text{C}$. Apply power to the KPSM. Measure the average deviation rate, deviation rate at the sweep extremes, and the klystron flange temperature at 1 min. time intervals thru 4 min.

Requirements: After 1st reading,

Average:	8,000 MHz/sec \pm 2.4%	Upper Limit:	8,000 MHz/sec $+ 2,000$ MHz/sec
Lower Limit:	8,000 MHz/sec $\pm 2,000$ MHz/sec	Sweep Time:	5.0 \pm 0.5 Millisecc

RA and DVS Klystron Frequency

Place the KPSM in the temperature chamber and allow it to stabilize at $\approx 30^{\circ}\text{C}$. Apply primary power to the KPSM. Measure the frequency of the RA (undeviated) and the DVS klystrons at 30 sec., 2 min., 3 min., 4 min., $5\frac{1}{2}$ min.

Requirements: (all times) RA, 12.9 GHz \pm 25 MHz; DVS, 13.3 GHz \pm 35 MHz

RA and DVS Klystron Power

Apply primary power to the KPSM. Measure RA and DVS Klystron power and record the results.

Requirements: RA, 250 mw; DVS, 8.5 \pm 1.5 w.

2. R/T Units

Two-Way Gain

Measure two-way antenna gain on all beams.

Requirements:	Beam 1 @ 13.3 GHz	56 db (min)
	Beam 2 @ 13.3 GHz	55 db (min)
	Beam 3 @ 13.3 GHz	55 db (min)
	Beam 4 @ 12.9 GHz	56 db (min)

Beam Angles

Measure E plane and H plane beam angles for all beams. Measure H plane angle between beams in each unit.

Requirement: E Plane

Beam 1 $0^{\circ}0' \pm 4'$
Beam 4 $0^{\circ}0' \pm 4'$

E Plane

Beam 2 $0^{\circ}0' \pm 4'$
Beam 3 $0^{\circ}0' \pm 4'$

H Plane

Beam 1 $12^{\circ}30' \pm 4'$
Beam 4 $12^{\circ}30' \pm 4'$

H Plane

Beam 2 $17^{\circ}23' \pm 4'$
Beam 3 $17^{\circ}23' \pm 4'$

H Plane Angle

Between Beams $25^{\circ}0' \pm 8'$

H Plane Angle

Between Beams $34^{\circ}46' \pm 8'$

Insertion Losses

Requirements:

P2 XMIT Flange 4.5 db (max)
P3 XMIT Flange 4.5 db (max)
P2 $/0^{\circ}$ Rec Flange 4.5 db (max)
P2 $/90^{\circ}$ Rec Flange 4.5 db (max)
P3 $/0^{\circ}$ Rec Flange 4.5 db (max)
P3 $/90^{\circ}$ Rec Flange 4.5 db (max)

P1 XMIT Flange 1.0 db (max)
P4 XMIT Flange 1.0 db (max)
P1 $/0^{\circ}$ Rec Flange 4.5 db (max)
P1 $/90^{\circ}$ Rec Flange 4.5 db (max)
P4 $/0^{\circ}$ Rec
Flange A 7.0 db (max)
Flange B 7.0 db (max)
P4 $/90^{\circ}$ Rec
Flange C 7.0 db (max)
Flange D 7.0 db (max)

Record insertion losses of adapters to be shipped with antennas.

VSWR

Measure the VSWR at the points given.

Requirements: 1.3:1 (max) at all RCV & XMIT flanges.

Two-Way Beam Patterns

Take beam pattern measurements on all beams and attach to report.

3. SDC

Response Time

Apply 22.4 + 0.0, -0.2 VDC primary input voltage. Apply the signals shown in the first column below until the tracker under test acquires then apply the step frequency shown in the second column. Monitor the results with the graphic recorder and retain the recorder tapes for the Report on Tests. (Response time is the time for reduction of the output error by 63 per cent.) Apply input signals at a level of 20.0 mv. Conduct each test ten times.

Requirements: 0.115 sec. max for average of 10 attempts.

V_x	Step 1	D1=1.60 kHz D2=1.33 kHz----0.930	R_z	Step 1	D1=1.33 kHz----0.930 D3=1.33 kHz----0.930 D4=1.60 kHz
	Step 2	D1=1.33 kHz----0.930 D2=1.60 kHz		Step 2	D1=1.60 kHz D3=1.60 kHz D4=5.33 kHz----5.880
V_y	Step 1	D2=1.60 kHz D3=1.33 kHz----0.930			
	Step 2	D2=1.33 kHz D3=1.60 kHz----0.930			
V_z		D1=1.33 kHz----0.930 D3=1.33 kHz----0.930			

Cross-Coupled Side Lobe Logic

Apply 22.4 +0.0, -0.1 VDC primary input voltage. Apply the signals as described in the following steps.

Step	Gain States		Freq. (kHz)		Levels	Requirements
	D ₂	D ₃	D ₂	D ₃		
1	90	90	10	10	D ₂ = 200 ±5mv; D ₃ = 200 ±5mv	Both track
2	65	90	10	10	D ₂ = 200 ±5mv; Decrease D ₃ from 280mv	D ₃ dropout at 200 ± 42mv
3	40	90	10	10	D ₃ = 250 ±5mv; Increase D ₂ from 10mv	D ₃ dropout at D ₂ = 14 ± 3mv
4	40	65	10	10	D ₂ = 30 ± 0.5 mv; Decrease D ₃ from 40mv	D ₃ dropout at 30 ± 6.2mv
5	40	65	10	vary	D ₂ = 30 ± 0.5mv; D ₃ = 20 ± 0.5mv	D ₃ acquire at 10.1 ± .02 kHz
6	90	65	10	10	D ₃ = 200 ± 5mv; Decrease D ₂ from 280mv	D ₂ dropout at 200 ± 42mv
7	90	40	10	10	D ₂ = 250 ± 5mv; Increase D ₃ from 10mv	D ₂ dropout at D ₃ = 14 ± 3mv
8	65	40	10	10	D ₃ = 30 ± 0.5mv; Decrease D ₂ from 40mv	D ₂ dropout at 30 ± 6.2mv

Thermal Sensor Data

Record serial numbers and check continuity and isolation.

B. Vibration

1. General

Vibration

Each unit shall be vibrated separately. Each unit shall be subjected to vibration in accordance with the following schedule.

Nonoperating

Sine wave 5 to 16 Hz @ 0.45 Inch Da
 16 to 125 Hz @ ± 6 G Peak
 125 to 1500 Hz @ ± 2 G Peak

The sine wave frequency shall be logarithmically swept from 5 to 1500 Hz over a two minute period. The sine wave vibration shall consist of two two minute sweeps in an axis essentially parallel to the thrust axis and in two other critical axes orthogonal to the thrust axis for a total of 12 minutes sine wave vibration time on each unit.

Operating

Upon completion of the two two minute sine wave vibration sweeps in each axis, subject the unit to white gaussian acceleration (WGA) with a power spectral density of $0.002 \text{ G}^2/\text{Hz} + 0.002 \text{ G}^2, - 0.001 \text{ G}^2$; band limited between 50 and 2000 Hz. The unit shall be subjected to two minutes of WGA on each unit. The unit shall be operating and measurements taken as described in following paragraphs.

Test Setup

Attach each unit to the vibration exciter in such a manner as to best obtain the desired acceleration without attempting to simulate the spacecraft installation. Load each unit as necessary to make it dynamically similar to the flight configuration. Observe the vibration level on the exciter as near to the supporting bracket as possible. Unless otherwise noted in the detailed unit procedure, the units shall be vibrated in an axis essentially parallel to the thrust axis and in two other critical orthogonal axes which are perpendicular to the thrust axis.

2. KPSM

Nonoperating (Sine Wave)

Subject the KPSM to sine wave vibration as described above. Upon completion of the two two minute sweeps, visually inspect the unit for any physical damage. Record any defects noted.

Operating (WGA)

Test Setup

Attach the KPSM to its vibration fixture by means of its normal mounting provisions. Mount the fixture on the exciter head for vibration along the thrust axis. Attach accelerometers. Connect the KPSM and an RA/VS antenna with the test equipment necessary to provide the voltages and to monitor the parameters noted.

Measurements

Record the voltage and current from the three power supplies. Monitor DVS frequency and power and RA frequency and power thirty seconds after turn-on and every thirty seconds through 120 seconds. On a tape recorder, record interference levels from the RA/VS antenna preamplifiers as a function of vibration frequency (using a spectrum analyzer). Play the magnetic tape into the X-Y plotter. Identify the plots and retain for the Report on Tests. Play the magnetic tape into SDC trackers and record the condition of the Tracker Lock lamps (illuminated or extinguished). Operate the SDC in the signal-plus-noise to noise mode using normal preamplifier noise.) Record the preamplifier channel and level and frequency of any interference peaks at any time the Tracker Lock lamps illuminate. This test shall be limited to 2.5 minutes maximum duration.

Requirements: XMTR Freq.,	RA = 12.9 GHz \pm 25 MHz
	DVS = 13.3 GHz \pm 35 MHz
XMTR Power,	RA = 250 mw (min)
	DVS = 7 watts (min)

(at all times)

- +25 vDC supply, $+25.0 \pm 0.25$ vDC, 60 ma (max)
- 25 vDC supply, -25.0 ± 0.25 vDC, 5 ma (max)
- 22.4 vDC supply, 22.4 ± 0.25 vDC, record current

Reference Tests

Upon completion of vibration tests, measure the parameters listed below.

PARAMETER	REQUIRED	PARAMETER	REQUIRED
RA XMT Power	350 ± 100 MW	High Dev. Rate	8.0 GHz/sec
DVS XMT Power	7 WATTS (MIN)	Low Dev. Rate	0.8 GHz/sec
RA XMT Freq.	$12.9 \text{ CC} \pm 25\text{MC}$	Deviation Repetition Rate	182 ± 5 Hz
DVS XMT Freq.	$13.3 \text{ CC} \pm 35\text{MC}$	Flyback Time	0.5 ± 0.025 Millsec
22.4 vDC Supply Voltage	Record	+25 VDC Supply Voltage	Record
22.4 vDC Supply Current	18.0 Amps (Max)	+25 VDC Supply Current	60.0 Ma (Max)
16.5 vDC Supply Voltage	Record	-25 VDC Supply Voltage	Record
16.5 vDC Supply Current	23.0 Amps (Max)	-25 VDC Supply Current	5.0 Ma (Max)
		Warm up Time Required	30 Sec (Max)

3. R/T Units

Nonoperating (Sine Wave)

Attach the antenna to its vibration fixture by means of its normal mounting provisions. Attach accelerometers. Subject the antenna to sine wave vibration as described. Upon completion of the two two minute sweeps, visually inspect the unit for any physical damage. Record any defects noted.

Operating (WGA)

Test Setup

Mount the antenna on the vibration fixture by means of its normal mounting provisions. Attach three accelerometers to each of the three mounting points for monitoring vibration in the following axes:

1. Vertical
2. Normal to the Antenna
3. Tangent to the Antenna

Attach the control accelerometer at one of the mounting points or at a point on the vibration fixture most suitable for equalization control. Show, by means of a diagram on the X-Y charts, the number and location of accelerometers. Monitor equalization at the control accelerometer with the Analyzer Equalizer and adjust the vibration input level to obtain the specified vibration levels by use of the Analyzer Equalizer and/or the peak notch filter of the vibration system. During vibration, adjust the vibration input level to maintain the specified vibration as monitored at any two of three comparable axes accelerometer outputs. Connect the Tape Recorder to monitor the preamplifier outputs. Apply the required operating voltages to the preamplifiers. Apply the required RF energy to the antenna input ports.

Measurements

- a. Prior to vibrating the antenna, monitor all preamplifier outputs on the Tape Recorder for approximately two minutes for reference.
- b. Apply the required vibration input levels and monitor each of the in-line accelerometers on the X-Y Recorder for seven minutes.
- c. During vibration, record the preamplifier outputs on the Tape Recorder for two minutes.
- d. Scan the preamplifier outputs with the Noise and Wave Spectrum Analyzer in a 100 Hz bandwidth. Record the levels of any discrete peaks.
- e. Reduce any discrete resonant peaks until the preamplifier outputs are within 10 db (nominal) of the preamplifier output level noted in the reference test (Step a). Record the vibration level and the preamplifier output level. After completion of tests, play the tape recorded preamplifier output signals through the Wave and Noise Spectrum Analyzer and record on the X-Y Recorder. Play the tapes into trackers and record the condition of the Tracker Lock lamps (illuminated or extinguished). (Operate the SDC in the signal-plus-noise to noise mode using normal preamplifier noise.)

Reference Tests

Upon completion of vibration tests, measure the parameters listed below.

Overall receiver noise figure @ 8kHz: DVS, 19.0 db max
RA, 23.8 db max

Preamp gain switch levels: DVS, before switch max
280 mv, after switch 10 +(10, -0) mv; RA, before
switch max. 317 mv, after switch 20 (+10, -0)mv.

Preamp gain state signals: 13.5 ± 1.0 vDC

Max. preamp output amplitude balance in 90 db gain state: ± 1.0 db

4. SDC

Nonoperating (Sine Wave)

Attach the SDC to its vibration fixture by means of its normal mounting provisions. Attach accelerometers. Subject the SDC to sine wave vibration as described. Upon completion of the two two minute sweeps, visually inspect the unit for any physical damage. Record any defects noted.

Operating (WGA)

Attach the SDC to its vibration fixture by means of its normal mounting provisions. Attach accelerometers. Interconnect the SDC with the test equipment. Conduct the following tests before, during and after vibration in each axis:

(a) Acquisition

Apply the simulated doppler return sine wave frequencies shown below in the signal-to-noise mode:

D1 = 24.51 kHz
D2 = 19.661 kHz

D3 = 24.51 kHz
D4 = 75.010 kHz

Set the DVS input signal levels at zero mv rms with a noise density of 2.5 mv rms in a 100 Hz bandwidth. Set the RA input signal level to 6.0 mv rms with a noise density of 0.92 mv rms in a 100 Hz bandwidth. Set the primary input voltage at $22.4 \pm 0.0, -0.2$ VDC. Turn the BURNOUT SIGNAL switch to OFF. Turn the DVS PRE-AMP GAIN STATE SIGNAL switch to 90 db. Turn the RANGE PRE-AMP GAIN STATE SIGNAL switch to 80 db. Apply RADVS power and start the recorder chart drive motor. Observe the D1, D2, D3, and R Tracker Lock lamps. Slowly increase the signal level on each channel until the Tracker Lock lamps illuminate. Record the signal level required for each channel.

Requirements: DVS, 29.0 to 51.5 mv; RA, 6.9 to 9.8 mv

Measure analog outputs $V_x, V_y, V_z,$ and R_z with the Digital Voltmeter.

Requirements: $V_x = 15.00 \pm 0.71$ vDC, $V_y = -15.00 \pm 0.71$ vDC, $V_z = 50$ vDC (saturated), $R_z = + 30.00 \pm 1.14$ vDC.

Measure voltage and current at the primary input power source.

Requirements: record voltage, current = 8.5 A (Max)

Record the SDC analog outputs for a minimum of 10 seconds on the Graphic Recorder.

(b) Analog Noise

Apply the Sine Wave signals shown below at the following levels:

D1 = D2 = D3 = 170 mv rms	D4 = 118 mv rms
D1 = 4.902 kHz	D3 = 4.902 kHz
D2 = 5.710 kHz	D4 = 10.124 kHz

Turn the BURNOUT SIGNAL switch to ON. Turn the DVS PRE-AMP GAIN STATE SIGNAL switch to 65 db. Turn the RANGE PRE-AMPS GAIN STATE SIGNAL switch to 60 db. Set the primary input power at $22.4 \pm 0.0, -0.2$ VDC. Apply primary input voltage and start the recorder chart drive motor. Measure the analog outputs with the Digital Voltmeter. Determine the peak-to-peak analog noise (at output of S/C simulation filter) over the 100-second period containing the maximum excursion. Record all results.

Requirements: Noise: $V_x = 0.100$ v p-p (max), $V_y = 0.100$ v p-p (max),
 $V_z = 0.250$ v p-p (max), $R_z = 0.400$ v p-p (max)

Accuracy: $V_x = -2.50 \pm 0.140$ vDC, $V_y = + 2.50 \pm 0.140$ vDC,
 $V_z = 10.00 \pm 0.140$ vDC, $R_z = 3.00 \pm 0.120$ vDC

Reference Test

Upon completion of the vibration tests, interconnect the SDC with the test equipment at the SDC Unit check-out station and perform the following tests.

(1) LVPS Ripple and RADVS Telemetry Signals

Measure power supply ripple in 1 kHz BW from 2 kHz to 100 kHz.

Requirements: +25 v supply ; 2.0 mv max; -25 v supply, 1.0 mv max;
+100 v supply, 20.0 mv max; -100 v supply, 20.0 mv max.

Measure telemetry signals in the "ON" and "OFF" states.

(7) Linearity, Accuracy, and Fourteen Foot Mark

(a) Linearity and Accuracy

Apply simulated signals at the frequencies and level shown below. Measure V_x , V_y , and V_z and record the results.

D1 = 0.123 kHz D3 = 0.123 kHz
D2 = 0.123 kHz D4 = 0.445 kHz

Signal level = 20 mv rms, low gain
state, BO, HI DEV.

Requirements: $V_x = 0.0 \pm 0.049$ vDC, $V_y = 0.0 \pm 0.049$ vDC,
 $V_z = 0.25 \pm 0.049$ vDC

(b) Fourteen Foot Range Mark Accuracy

With the test setup the same as above, decrease the frequency of D4 until the 14 foot mark is generated. Record the range input frequency and range analog output at which the mark is generated.

Requirements: $R_z = 0.339 \pm 0.042$ vDC, R-Freq. = 387 ± 38 Hz

(8) Acquisition Time

With the trackers in the signal-to-noise acquisition mode (preamp high gain state), apply simulated sinewave signals at the frequencies and levels shown below.

D1 = 10 kHz D3 = 10 kHz
D2 = 10 kHz D4 = 80 kHz

DVS Signal Levels = 21.7 mv rms in
a 100 Hz bandwidth.

DVS Noise Levels = 2.50 mv rms in a
100 Hz bandwidth.

RA Signal Level = 9.25 mv rms in a
100 Hz bandwidth.

RA Noise Level = 0.92 mv rms in a
100 Hz bandwidth.

Turn the Burn Out Signal ON. Momentarily remove the signals. Measure the time between reapplication of the signal and illumination of the TRACKER LOCK lamps. Record the results.

Requirements: All trackers acquire signal within 4 seconds.

(9) Response Time

Same as SDC response time test in section III.A.3 of this appendix.

APPENDIX E
DETAILS OF THE VENDOR SYSTEM ACCEPTANCE TEST

I. INTRODUCTION

Information in this appendix is taken from Ryan report 51765-2B (change 12), Part I. (Mechanical tests and inspections have been omitted.)

II. STANDARD TEST CONDITIONS

The standard test conditions for the vendor tests are listed in Table E-1, which was copied from Table 1-1 of the document referenced. Abbreviations and notes for the table are listed below:

AV	Velocity Sensor Accuracy
AR	RA Accuracy
BO	After Burnout
BBO	Before Burnout
HD	High Deviation
LD	Low Deviation
M	Analog Noise
M1	1,000 Foot Range Mark
M2	14 Foot Range Mark
NR	Operation Not Required
RV	RA Range-Velocity Capability
SR	RA Sensitivity
SV	Velocity Sensor Sensitivity
VV	Velocity Sensor Velocity Capability
①	Range for DVS Return Power
②	Vertical Trajectory
③	Based on Lambert Law Scattering
④	Return Power for 40,000 Feet Range and 45° Attitude

A description of the STC's copied from the referenced document follows:

The Standard Test Conditions provide the essential signal characteristics required to demonstrate that the RADVS will meet the requirements of the basic product specification. Each Standard Test Condition checks a number of the basic performance requirements. It will be noted that in certain instances, the equivalent range of the DVS and the RA differ. This provides a means for effectively checking system operation at two simulated points on a trajectory at the same time. The Table also indicates the mode of operation of the RA and the DVS, as well as the specific nature of the tests performed for such a condition. The detailed explanation for each condition is as follows:

- STC 1: The RA is nonoperating. The DVS is operated at maximum range and the equivalent of 3,000 FPS along each of the three doppler beams. This, therefore, checks maximum altitude and velocity capability at 45° pitch angle on all beams simultaneously.
- STC 2: Test both the RA and the DVS at pitch angles of 45° and 40,000 feet. The maximum search requirement for the RA is tested, which occurs with a V_z of 740 FPS at a range of 40,000 feet. Test the DVS at the required maximum negative linear horizontal velocity output capability.
- STC 3: Test the RA and DVS with negative simulated input signals to demonstrate that the RADVS will not acquire the main retro tankage as a target after it is jettisoned.

Table E-1. Standard test conditions (STC) for vendor tests and listing of parameters tested

STC	R _z (FT)	V _x (FPS)	V _y (FPS)	V _z (FPS)	D1 (kHz)	D2 (kHz)	D3 (kHz)	F _R (kHz)	P _{VS} (dbm)	P _{RA} (dbm)	R _{VS} (FT)	V _T (FPS)	PARA- METERS TESTED	RA/VS MODE
1	NR	0	0	3310	81.13	81.13	81.13	NR-	-106	--	50,000	3310	SV, VV	NR/BBO
2	40,000	-300	-300	740	13.31	18.15	22.99	84.45	-104	-104	40,000	853	AR, AV, SR, VV	LD/BBO BO
3	SEARCH	0	0	0	-1.60	-1.60	-1.60	-3.5	-50	-113	--	-65	NEGA- TIVE DOPPLER	LD/BO
4	36,530	+300	+300	+325	12.80	7.97	3.10	67.925	-100	-104	36,530	530	AR, VV AV, SR	LD/BBO BO
5	14,000	0	0	850	20.83	20.83	20.83	45.06	-95	-93	14,000	850	AR, AV VV	LD/BBO BO
6	2,000	0	0	67	1.64	1.64	1.64	4.995	-106	-77.4	50,000	67	SV, AR AV	LD/BO
7	VAR 1,500 to MARK	-50	+50	100	2.45	3.26	2.45	VAR 5.06- 17.26	-74	-74	6,800	122.5	ML, AV	LD-HD/ BO
8	300	0	0	38	0.93	0.93	0.93	5.88	-104 -52	-59 ²	40,000	38	SV, AV, AR	HD/BO
9	240	-50	-50	54.5	1.33	0.53	1.33	5.33	-50	-57 ²	240	89.3	AR, AV	HD/BO
10	VAR 130 to 50 to MARK	0	0	5	0.123	0.123	0.123	2.24- 1.075- MARK	-42 ²	-47 ²	100	5	M, M2, AV	HD/BO
11	29,757	VAR	VAR	67	1.64	VAR to 1.64	1.64	67.925	-102	-104	36,530	VAR	CCL, CRO	LD/BBO CRO BO

- STC 4: Test the DVS at the required maximum positive linear horizontal velocity output capability. Test V_z in the mid-range of the linear requirements and the RA for maximum sensitivity.
- STC 5: Tests the RA for a near mid-range altitude in the low deviation mode. Tests the DVS at the required maximum linear vertical velocity output capability and V_y and V_x at the null.
- STC 6: Tests the RA^x in the low deviation mode at 2,000 feet where maximum errors may be expected to occur. The DVS is tested for acquisition capability per the 50,000 foot curve of HAC Specification 232902. The DVS doppler frequencies correspond to the lowest values which can occur on the subject curve for ranges of 50,000 feet and pitch angles of 45°, with each beam in turn effectively oriented to its most unfavorable position relative to the lunar vertical and the relative velocity vector.
- STC 7: Tests the RA for the generation and accuracy of the 1,000 foot range mark and transition from the low deviation mode to the high deviation mode. The DVS is tested for accuracy and linearity at points between the mid-linear range and zero velocity.
- STC 8: Tests the RA in the high deviation mode at near mid-range of the linear requirements. The range frequency is sufficiently high so as not to require leading the RA down for lock. (Assuming the 1,000 foot mark has been generated and the unit placed in the high deviation mode.) The DVS is tested for accuracy around the null of V_x and V_y and low positive values of V_z . The problem specifically tests the DVS acquisition capability in accordance with the 40,000 foot curve of the HAC Specification No. 232902. As in STC 6 the individual doppler frequencies were selected as the minimum frequency occurring for the worst condition of 45° pitch angle and worst orientation of each beam with respect to the lunar vertical and the relative velocity vector. The two values of received DVS power correspond to the two different altitudes indicated for the DVS.
- STC 9: The STC was formerly used, in conjunction with STC 8, to measure system time constants. These tests are now conducted on a unit basis. STC 9 is used for linearity and accuracy measurements only.
- STC 10: Tests the RA for the generation and accuracy of the 14 foot range mark and the DVS at very low velocities.
- STC 11: Tests the CRO logic circuitry. The DVS is operated in its wide band mode prior to burn-out, the CRO mode after burn-out, and finally in the RO mode with narrow bandwidths after burn-out. The sequence defined in the applicable test procedures allow observation and measurement of the timing and operation of the various modes. D2 frequency is made variable to simulate the large angular dispersion which may occur at burn-out and which requires operation in the CRO mode. Cross-coupled side lobe rejection was formerly tested under this condition. With incorporation of Change 3 to these procedures, cross-coupled side lobe rejection is tested using STC 4 which is more compatible with conditions under which this parameter is tested during unit tests.

III. REQUIRED VALUES AND TOLERANCES

Table E-2 shows the total allowable RADVS system 3σ errors as listed in the Ryan document referenced. For application to system tests using the RADVS Test Equipment (RADVSTE), these errors must be adjusted in accordance with

- (1) Errors not included in RADVS/RADVSTE tests, i.e., antenna alignment and boresight errors, terrain bias errors, and the Digital Voltmeter error.
- (2) Normal RADVSTE measuring error.

Table E -2. Total allowable 3σ errors for the RADVS per Ryan report
51765-2B

STC	R _z		V _x		V _y		V _z	
	FEET	VDC	FPS	VDC	FPS	VDC	FPS	VDC
1	NR	----	0	0.0	0	0	331.	----
2	40,000	40.00 ± 2.00	-300	+15.00 ± 0.85	-300	-15.00 ± 0.85	740	37.00 ± 0.85
3	NEGATIVE DOPPLER		0	0	0	0	-65	0
4	36,530	36.53 ± 1.83	+300	+15.00 ± 0.53	+300	+15.00 ± 0.53	325	16.25 ± 0.53
5	14,000	14.00 ± 0.70	0	0 ± 0.85	0	0 ± 0.85	850	42.50 ± 0.85
6	2,000	2.00 ± 0.105	0	0 ± 0.0835	0	0 ± 0.0835	67	3.350 ± 0.0835
7	1500- 900	1.50 ± 0.081	-50	-2.50 ± 0.132	+50	+2.50 ± 0.132	100	5.00 ± 0.132
8	300	600 ± 0.310	0	0 ± 0.063	0	0 ± 0.063	38	0 ± 0.063
9	240	4.80 ± 0.245	+50	+2.50 ± 0.103	-50	+2.50 ± 0.103	54.5	2.725 ± 0.103
10	130- 9	2.60 ± 0.153	0	0 ± 0.050	0	0 ± 0.050	5	0.250 ± 0.050
11	36,530	36.53 ± 1.83	VAR		VAR		67	

Table E-3. Testing requirements and tolerances for vendor system tests using RADVSTE

STC	R _z		V _x		V _y		V _z	
	FEET	VDC	FPS	VDC	FPS	VDC	FPS	VDC
1	NR	-----	0	0 + 2.20	0	0 + 2.2	3310	
2	40,000	40.00 ± 1.52	-300	+15.00 ± 0.60	-300	+15.00 ± 0.60	740	37.00 ± 0.60
3	NEGATIVE DOPPLER		0	0	0	0	-65	0
4	36,530	36.53 + 1.38	+300	+15.00 ± 0.35	+300	15.00 ± 0.35	325	16.25 ± 0.35
5	1,400	14.00 ± 0.53	0	0 ± 0.60	0	0 ± 0.60	850	42.50 ± 0.60
6	2,000	2.00 ± 0.081	0	0 ± 0.0674	0	0 ± 0.0674	67	3.350 ± 0.0674
7	1,500- 900	1.5 ± 0.066	-50	- 2.50 ± 0.095	+50	+ 2.50 ± 0.095	100	5.00 ± 0.095
8	300	6.00 ± 0.130	0	0 ± 0.055	0	0 ± 0.055	38	1.90 ± 0.055
9	240	4.80 ± 0.115	+50	+ 2.50 ± 0.077	-50	-2.50 ± 0.077	54.5	2.725 ± 0.077
10	130- 9	2.60 ± 0.090	0	0 ± 0.049	0	0 ± 0.049	5	0.250 ± 0.050
11	36,530		VAR		VAR		67	

The adjusted values are given in Table E-3. These tolerances were selected to expedite testing and data evaluation. If RADVS performance falls outside these reduced limits, the RADVSTE accuracy must be checked to determine if the RADVSTE errors add in such a manner to justify their being eliminated from the RADVS tolerance.

IV. TESTS

A. Power Consumption

Check that power from the 22.4 v DC supply does not exceed 590 watts with the supply set at 16.5, 20.0, and 22.4 vDC.

B. Thermal Sensors

Check resistance and isolation of sensors.

C. RF Power

Conduct these test with primary input voltage at 16.5 + 0.1, -0.0 and 22.4 + 0.0, - 0.1 VDC. Measure the RF power on each beam, allowing for insertion losses. Retain all computations for this Test Report.

Requirement: DVS, 1.5 w min each beam; RA, 210 mw min.

D. XMTR Frequency

Measure the frequencies using RADVSTE. Perform these tests with primary input voltage at 16.5 +0.1, -0.0 and 22.4 +0.0, -0.1 VDC.

Requirement: RA, 12.9 GHz \pm 25 MHz; DVS, 13.3 GHz \pm 35 MHz

E. Standard Test Condition Tests

(1) Test Setup

Interconnect the RADVS with the RADVSTE. Set up the STC on the RADVSTE. Set primary input voltage at [a specified value between 16.50 and 26.0 v].

(2) Test Listing for STC's

- STC 1: (a) Thirty-seconds Warm-up at 26 VDC Primary Input power
- (b) DVS Linearity and Accuracy
- (c) DVS Maximum Slant Range Capability
- (d) DVS Maximum Total Velocity Capability
- (e) DVS Acquisition Time and Sensitivity
- STC 2: (a) RADVS Linearity and Accuracy
- (b) Maximum Horizontal Negative Linearity Output Capability
- (c) RA Maximum Slant Range Capability
- (d) RA Maximum Velocity Capability at 40,000 Feet
- (e) RA Maximum Attitude Angle
- (f) RADVS Acquisition
- STC 4: (a) RADVS Linearity and Accuracy
- (b) DVS Maximum Horizontal Positive Linear Output Capability
- (c) RADVS Acquisition
- STC 5: (a) Warm-up Time
- (b) RADVS Linearity and Accuracy
- (c) DVS Maximum Vertical Linear Output Capability
- (d) RADVS Acquisition

- STC 6: (a) RADVS Linearity and Accuracy
(b) RADVS Acquisition
(c) DVS Sensitivity
- STC 7: (a) RADVS Linearity and Accuracy
(b) 1,000 Foot Range Mark Accuracy
(c) RORA and RODVS Signal Accuracy
(d) Tracker Lock Signal Accuracy
- STC 8: (a) RADVS Linearity and Accuracy
(b) DVS Sensitivity
- STC 9: (a) Linearity and Accuracy
- STC 10: (a) RADVS Linearity and Accuracy
(b) Noise and Ripple
(c) Thirteen Foot Range Mark Accuracy
- STC 11: (a) CRO Logic Signal Accuracy in the Search
and Track Modes
(b) Cross-coupled, Side-lobe Rejection

(3) Typical Measurements

Make sure all Recorder tapes are identified by date, test, amplifier level, and signal recorded on each channel. When RADVSTE controls which effect signals being monitored on the Recorder are changed or when a normal operational function occurs, note the time of the event on the left margin of the Recorder tape. Retain all tapes for the Report On Test.

(a) Linearity and Accuracy

- 1 Start the Recorder chart drive motor. Turn the RADVS POWER switch to ON. Turn the TEST ACTIVATE switch to ON. Record the presence of the Burn Out Signal (if called for). After the RODVS and/or RORA lamps illuminate, examine the Recorder tape to verify reliable operation. Turn the VOLTMETER switch to measure V_x , V_y , V_z , and/or R_z on the Digital Voltmeter. Record the results on the data sheet. Permit the Recorder chart drive motor to run for at least 10 seconds while recording range and velocity analog outputs.
- 2 Turn the BURN OUT SIGNAL switch to OFF (if called for). Record the absence of the Burn Out Signal on the recorder. Repeat the measurements of V_x , V_y , and V_z and record the results.

(b) Acquisition Time and Sensitivity

- 1 Turn the TEST ACTIVATE switch to ON. When the RODVS and/or RORA lamps illuminate, examine the Recorder tape to verify reliable operation. Record RA and/or DVS acquisition time on the data sheet. Turn the TEST ACTIVATE switch to OFF.
- 2 Turn the TEST ACTIVATE switch to ON and repeat the measurements. Record the results on the data sheet. Turn the TEST ACTIVATE switch to OFF.

- 3 Turn the TEST ACTIVATE switch to ON and repeat the measurement. Record the results on the data sheet.
- 4 Observe (a given) TRACKER LOOP lamp. Force loss of lock of the tracker. Record the attenuator setting at which the tracker drops out on the data sheet. Decrease the attenuation until the tracker locks on. Record the attenuator setting at which the tracker acquires on the data sheet. Turn the TEST ACTIVATE switch to OFF.
- 5 Repeat step four for other trackers (as indicated).

(c) Warm-up Time

Start the Recorder chart drive motor. Turn the TEST ACTIVATE switch to ON. Turn the RADVS POWER switch to on. Record the time between application of spacecraft power and indication of the RODVS and/or RORA signals on the data sheet.

(d) Analog Transients Due to Preamplifier Gain Switching

Set the recorder channels to the following:

CHAN 1	SC FIL	CHAN 3	SC FIL
CHAN 2	SC FIL	CHAN 4	SC FIL

Zero the Recorder pens on channels 1,2,3, and 4 using the V_x , V_y , V_z , and R OFFSET-SC FILTER controls. Set the amplifier gain levels on channels 1, 2, 3, and 4 at 50 MV/LINE. Adjust the MICROWAVE INPUT SIGNAL ATTENUATION to a level to ensure that all preamplifiers are in high gain state.

- 1 When all trackers have acquired and with the Recorder chart drive motor running, decrease the MICROWAVE INPUT SIGNAL ATTENUATION on each beam until all preamplifiers switch to the mid-gain state. Observe the values recorded on channels 1, 2, 3, and 4 of the Recorder chart at gain switch. Record the results on the data sheet.
- 2 Repeat the measurements for gain switch to the low gain state on all channels.
- 3 Repeat the measurements for gain switch from the low to the mid-gain state on all channels.
- 4 Repeat the measurement for gain switch from the mid-gain state to the high gain state on all channels.

(e) Range Mark Accuracy

- 1 Measure the 1000/14 foot range mark signal in the OFF state with the Digital Voltmeter.
- 2 Turn the Function Selector switch on the Range Rate Simulator to MARK TEST. Turn the Start Test switch to START SWEEP. When the 1,000/14 foot mark lamp illuminates, record the Electronic Counter indication. Take this measurement ten times. Interrupt the primary input voltage two times during the series of tests. Allow thirty seconds minimum between each measurement. Indicate the point at which primary voltage is interrupted on the data sheet.

- 3 Measure the 1,000/Foot Range Mark signal with the Digital Voltmeter and record the results on Data.
- 4 Perform measurements at another [specified] primary voltage.
- 5 Check that the tracker remains locked at the 1000 ft. deviation rate change at the two primary voltages specified.

(f) Noise and Ripple

Set the recorder channels to the following:

CHAN 1	SC FIL	CHAN 3	SC FIL
CHAN 2	SC FIL	CHAN 4	SC FIL

Apply the simulated doppler signal frequencies and return signal levels given. Set the recorder gain levels on channel 3 and 4 at 50 MV/LINE. Zero the recorder pens on channels 1, 2, 3, and 4 with the OFFSET-SC FILTER controls. Permit the Recorder chart drive motor to run for a minimum of 60 seconds after this condition is obtained. Record the maximum excursion of the Recorder pens on the data sheet.

(g) CRO Logic Signal Accuracy in the Search and Track Modes

- 1 Turn on the Recorder chart drive motor. Turn the RADVS POWER switch to ON. When D1 and D3 TRACKER LAMPS illuminate, turn the BURN OUT SIGNAL switch to ON. When the CRO lamp illuminates, measure the time between indication of the Burn Out Signal and indication of the CRO signal. Record the results on the data sheet.
- 2 Measure the CRO DVS signal with the Digital Voltmeter and record the results on the data sheet.
- 3 Increase the frequency of D2 to 1.5 KHz. When the RODVS lamp illuminates, measure the time between indication of the D2 Tracker Lock signal and indication of loss of the CRO DVS signal. Record the results on the data sheet.
- 4 Decrease the frequency of D2 until the TRACKER LOCK D2 lamp extinguishes. Record the condition of the CRO DVS signal (ON or OFF) on the data sheet.
- 5 Measure the CRO DVS signal in the "OFF" condition with the Digital Voltmeter. Record the results on the data sheet.

(h) Cross-Coupled Side Lobe Rejection

- 1 Set up STC No. 4 on the RADVSTE with D2 at 3100 Hz. Record the actual frequency of D1, D2, D3, and D4 measured with the Electronic Counter on the data sheet.

- 2 Increase the RF signal level on Beam 2 until the D3 TRACKER LOCK lamp extinguishes. Record the D2 attenuator reading at which the D3 tracker drops out on the data sheet. Compute the difference between the attenuator reading and -100 dbm and record the results on the data sheet.
- 3 Change the frequency of D2 until the D3 TRACKER LOCK lamp illuminates. Record the frequency at which the D3 TRACKER LOCK lamp illuminates on the data sheet. Compute the difference between this frequency and 3100 Hz. Record the results on the data sheet. Adjust the frequency of D2 toward the original 3100 Hz setting until the D3 tracker drops out. Record the frequency at which the D3 tracker drops out on the data sheet.
- 4 Set D2 frequency at 3100 Hz. Decrease the RF signal level on Beam 2 until the D3 tracker acquires. Record the level at which the tracker acquires on the data sheet. Compute the difference between this level and -100 dbm and record the results on the data sheet. Set D2 signal level at -100 dbm.
- 5 Repeat the measurements in Step 2 using Beam 3.

(4) Required Test Values

- (a) Analog outputs: see Table E-3.
- (b) Sensitivities: record
- (c) Analog noise: $V_x = V_y = 0.125$ v p-p max,
 $V_z = 0.300$ v p-p max; $R_z = 1.000$ v p-p max @ simulated
 50 ft. and 200 ft., = 0.500 v p-p max @ simulated 2000 ft.
- (d) Logic signals: see Appendix D

F. Lunar Reflectivity Calibration and Preamp Gain State Signals

(1) D1 Tracker

- (a) Turn on the recorder chart drive motor. Turn the TEST ACTIVATE switch to ON. Turn the RADVS POWER switch to ON. After the RA and DVS RELIABLE OPERATE LAMPS illuminate, increase the attenuation on Beam 1 until D1 tracker drops out. Measure the D1 reflectivity signal under this condition for reference. Record the results on the data sheet.
- (b) Observe the P1 /0° signal level and decrease the attenuation of Beam 1 until the D1 tracker just locks on in the high gain state. Record the P1 /0° signal level at D1 lock-on on the data sheet. Record the attenuator setting at which the tracker locked on the data sheet.
- (c) Turn the VOLT SEL switch to P1 40 and P1 65 measure the signals with the Display Panel Voltmeter. Record the results on the data sheet. Turn the VOLT SELECT switch to REFL (DVM) D1 and adjust the attenuation on Beam 1 for a reflectivity signal level of 0.5 VDC. If the range of reflectivity signals given in this test cannot be obtained, conduct the test over the greatest reflectivity signal range obtainable. Record the attenuator setting on the data sheet.

- (d) Repeat the reflectivity measurement in Step (c) for signal levels of 1.0, 2.0 and 3.0 v DC. Record the results on the data sheet.
- (e) Decrease the attenuation on Beam 1 until the D1 preamp just switches to the mid-gain state. Record P1 preamp output just prior to and after gain switch. Record the attenuator setting at which the Pre-amp gain switched. Record the results on the data sheet. Repeat the P1 40 and P1 65 measurements for 65 db gain state and record the results on the data sheet.
- (f) Repeat the reflectivity measurement in Step (c) for the mid-gain state. Record the results on the data sheet.
- (g) Repeat the reflectivity measurements in Step (d) for the mid-gain state. Record the results on the data sheet.
- (h) Decrease the attenuation on Beam 1 until the D1 tracker just switches to the 40 db gain state. Repeat the measurements in Step (e) for 40 db gain state. Record the results on the data sheet.
- (i) Repeat the measurement in Step (c) for the 40 db gain state and record the results on the data sheet.
- (j) Repeat the measurements in Step (d) for the 40 db gain state and record the results on the data sheet.
- (k) Observe the P1 / 0^0 signal level and increase the attenuation on Beam 1 until the D1 tracker just switches to the 65 db gain state. Record the P1 / 0^0 signal level just prior to and after gain switch on the data sheet. Record the attenuator setting at gain switch on the data sheet.
- (l) Repeat the measurements in Step (k) for gain switch to the 90 db gain state. Record the results on the data sheet.

(2) Other Trackers

Repeat above steps.

(3) Required Values

The reflectivity measurements are taken for calibration purposes only. The reflectivity analog signal should not exceed 5.0 Volts for the 90 and 65 db gain states.

G. Modulation Sweep Period

Turn the RADVS POWER switch to ON. Record the sweep period indicated on the Universal Counter Timer on the data sheet.

APPENDIX F

BUYER FAT REQUIREMENTS LISTING

Information in this appendix is reproduced from HAC document No. 3023926A, Surveyor Spacecraft A-21, System Test Specification. The first table, Table F-1, is a reproduction of Table No. 3-11-g, "Test Requirements Library," (pp. 155-179) of the referenced document. In this table, requirements are arranged according to number without indication of applicability to specific test phases. Different aspects of the same requirement are denoted by dash numbers in the second column. The revision letter column allows a means of showing changes in requirements.

The second table, Table F-2 is a reproduction of Table 3-12-g, "Test Requirements Matrix," (pp. 427-429) of the referenced document. This table shows in which phases each test requirement is evaluated. Entries are in terms of the applicable dash numbers. (X's indicate places where tests cannot be conducted because of conflicting configurational requirements.)

In general, flight acceptance requires the passing of every test requirement listed. The exceptions are the System Readiness Tests (SRT) subphases, which are for operational convenience only.

Certain other details of test requirements and phases are given below with use of excerpts from the referenced document. (Section numbering is carried over from the source document.)

3.3 INITIAL SYSTEMS CHECKOUT (ISCO) TEST PHASE

3.3.1 Test Objectives

1. Perform calibration of engineering and data channels as required to support this and subsequent test phases and the flight mission.
2. Perform spacecraft performance tests which cannot be made in subsequent test phases.
3. Perform power and grounding checks.
4. Verify compatibility of each subsystem with the spacecraft TCM subsystem.
5. Provide for (1) special tests to verify new design features, and (2) interface margin tests.

3.3.2.1 Test Description: The spacecraft shall be functionally divided into test groups, each of which shall be tested in conjunction with the telecommunications equipment in such a manner that mutual interactions, if any, will be revealed. These test groups are: PO-RF/CD/SP, MS-MA/TCM, TV/TCM, FC/TCM, and FC-AM-RA-PR/TCM. (After integration, the RF/CD/SP equipments are referred to as the telecommunications (TCM) subsystem. The PO-TCM integration test requirements shall be performed first with remaining test groups tested in any order at the discretion of the test director.)

The abbreviations are explained as follows:

CD: Command Decoding
SP: Signal Processing
RF: Radio-Frequency Data Link (or Radio Communications)
FC: Flight Control
AM: Altitude Marking Radar
RA: Radar Altimeter and Doppler Velocity Sensor
PR: Propulsion
MA: Engineering Mechanisms Auxiliary
PO: Power
MS: Mechanical Subsystem
TV: Television

3.3.3.1.1 Test Access: Test tees shall provide for direct electrical access to the spacecraft. Signal injection and monitoring to satisfy the test requirements of this section shall be provided by test cables.

3.3.3.1.2 Power Requirements: The spacecraft shall be operated on an external 22 volt DC source.

3.3.3.2 Environment: All tests shall be performed at room ambient conditions. Sufficient air circulation shall be provided to maintain equipment operating temperature below the maximum

3.4 MISSION SEQUENCE/ELECTROMAGNETIC INTERFERENCE (MS/EMI) TEST PHASE

3.4.1 Test Objectives: The objectives of the Mission Sequence/Electromagnetic Interference Test shall be to:

1. Verify that the system performs in accordance with the System Functional Requirements Specification 224510, and Equipment Specification 224832, when commanded through all modes of operation in an ambient laboratory environment.
2. Verify the functional compatibility of the Surveyor spacecraft with radio frequency interference simulating the environment to be encountered at AFETR Launch Pad 36.
3. Verify that the Surveyor spacecraft is functionally compatible with the expected RFI environment created by the Atlas/Centaur launch vehicle and its AGE.

3.4.2.1 Test Descriptions: The Mission Sequence/Electromagnetic Interference Test Phase shall be divided into (1) and (2) plugs in, Time compressed (32 hour) Mission Sequence Tests and (3) plugs out, real time (66 hour) Mission Sequence/Electromagnetic Interference Test. Of the first two Mission Sequence Tests, sequence 1 shall have a constant power supply voltage and sequence 2 shall have a power supply voltage/time profile which approximates actual battery voltage. Each test sequence shall be divided into the following segments:

SRT: System Readiness Test
P/L-L: Prelaunch to launch
INJ: Injection and attitude reference acquisition
C ϕ 1: Coast phase 1
MC: Midcourse correction
C ϕ 2: Coast phase 2
TD: Terminal descent
POST TD: Post-touchdown

3.4.3.1.1 Test Access: For the first two sequences, hardline test access shall be provided as necessary to comply with the test objectives and requirements. When simulated Injection phase is reached during the third test sequence, the remainder of the sequence through Post Touchdown shall be performed with the spacecraft in a true flight configuration of no hardline access (100 percent plugs-out configuration) with the spacecraft operated by r-f link.

3.4.3.1.2 Power Requirements: During test sequence 1, a + 19V simulated battery voltage will be applied to the spacecraft. During test sequence 2, the simulated battery voltage shall be adjusted for the following levels.... During test sequence 3, the spacecraft shall utilize spacecraft battery power.

3.4.3.2 Environment: The first two test sequences shall be performed in an earth ambient environment prior to the EMI test. During the third sequence, the spacecraft shall be located in a r-f screen room where the expected EMI environment of launch pad 36 and the Atlas/Centaur Launch vehicle is simulated until Injection phase is reached. At that time, the EMI simulation shall be turned off and the remainder of the sequence shall be performed. The EMI simulation intensity levels shall be allowed to stabilize before initiating the test.

3.5 SOLAR THERMAL VACUUM (STV) FUNCTIONAL TEST PHASE

3.5.1 Test Objective: The objectives of the Solar Thermal Vacuum Test shall be:

1. Verification of correct spacecraft functional operations during a real-time transit mission sequence while exposed to a range of solar conditions in a simulated cislunar space environment.
2. Verification of correct spacecraft thermal performance during simulated STV environments.

3.5.2.1 Test Description: During the STV test phase the spacecraft shall be tested in accordance with the mission flight program as defined by HAC specifications 224550 and 224555. The test phase shall consist of 3 subphases.

1. Subphase A Low Temperature Test. This test subphase shall consist of a 66 hour real-time mission sequence under simulated transient and low level Solar Constant environments. A one hour solar eclipse shall be provided during the test. The spacecraft shall derive power from its own batteries.
2. Subphase B High Temperature Test. This test subphase shall consist of a 66 hour real-time mission sequence continued from subphase A without interrupting the Thermal-Vacuum chamber operation. A high level Solar Constant environment shall be simulated. The spacecraft derives power from the STEA.
3. Subphase C Nominal temperature plugs-out test. This test shall be conducted under a nominal STV environment. Hardline access to the spacecraft for this test shall be minimized and spacecraft operated from on-board power. The test shall be conducted as a 32-hour compressed mission sequence, involving real-time operation from launch through midcourse, followed by a temperature stabilization period, real-time terminal descent, and a postlanding assessment.

In each of the subphases, the test sequence consists of the following segments.

SRT: Systems Readiness Test
MS SEQ (DRY RUN): Mission Sequence-Dry Run (Subphases A and B only)
P/L-L: Prelaunch countdown and launch
INJ: Injection
Cφ1: Coast Phase I
MC: Midcourse correction
Cφ2: Coast Phase 2
TD: Terminal descent
POST TD: Post Touchdown
SRT: Systems Readiness Test (Subphase C only)

3.5.3.1.1 Test Access: Hardline test access to the spacecraft shall be provided through the vacuum chamber penetration plates. During the final test subphase (C) this access shall be minimized to include only spacecraft power access for emergency shutoff and thermal instrumentation with communications derived solely by RF link.

3.5.3.1.2 Power Requirements: Test subphase A and C shall be run utilizing spacecraft battery power, and subphase B run on ground power.

3.5.4.2 Environment: Three mission sequence tests shall be conducted under a Solar Thermal Vacuum environment. During these tests the spacecraft shall be subjected to a simulated environment approximating the conditions to be encountered during all phases of the transit portion of the mission. The simulated environment shall consist of a temperature -300°F or lower, a static pressure of 5×10^{-6} torr, or less, and solar radiation of 0.8, 1.1, and 1.0 solar constant for subphases A, B, and C, respectively. (A solar constant is defined as 130 w/ft^2 at the test plane.)

3.7 VIBRATION (VIB) TEST PHASE

3.7.1 Test Objectives: The objective of the Vibration Test Phase shall be to:

1. Verify functional integrity during and after simulated launch vibration environments.
2. Verify proper fabrication and assembly of the spacecraft and all system components.

3.7.2.1 Test Description: The Vibration Test Phase shall be divided into two basic parts:

1. Vibration Environments
2. Earth Ambient Environment (spacecraft functional and alignment tests before or after exposure to vibration).

————— Only the Functional/Pretest Checkout and Function Post-test Checkout concerns RADVS along with positional checks.

3.7.3.1.1 Test Access: Hardline test access shall be minimized while meeting the test objectives and requirements of this test phase. The testing shall be accomplished primarily in a plugs-out test configuration. No commands shall be sent to the vehicle during the shake periods.

3.7.3.2 Environment: All tests shall be performed at room ambient conditions. Vibration levels are specified...

3.8 VERNIER ENGINE VIBRATION (VEV) TEST PHASE

3.8.1 Test Objectives: The objective of the Vernier Engine Vibration Test Phase shall be to:

Verify the RADVS beams do not produce a false lock as a result of vernier engine vibrations.

3.8.2.1 Test Description: The Vernier Engine Vibration test phase shall be divided into two basic parts:

1. Flight control/RADVS open loop operation in a vibration environment.
2. Spacecraft functional tests before and after vibration test.

3.8.3.1 Spacecraft Configuration: The spacecraft shall be fully assembled mechanically and electrically in a flight configuration... Among required exceptions shall be the following:

1. The inert retro rocket shall not be installed.
2. The altitude marking radar shall not be mounted on the spacecraft.
3. Fuel and oxidizer tanks shall be filled with Helium gas to 10 ± 5 PSIG inside the bladder with 2 PSIG minimum differential across the bladder, positive pressure inside.
4. Thrust Chamber Assemblies shall be removed and replaced with equivalent masses.
5. RADVS feed horns shall be terminated in microwave loads to simulate a free space environment for the RF transmitters and receivers.
6. The ASPP shall be in the transit position.
7. The spacecraft legs and omni directional antennas A and B shall be extended.

3.8.3.1.1 Test Access: Hardline access to the spacecraft shall be minimized to meet the test objectives and requirements. The spacecraft shall be operated in conjunction with the STEA through the omni directional antenna RF command link.

3.8.3.1.2 Power Requirements: The spacecraft shall utilize on board battery power during vibration testing. Pre-and Post-vibration tests shall use external ground power.

3.8.3.2 Environment: The spacecraft shall be mounted on the system test stand, utilizing vibration isolation airmounts. Pressure, temperature, and humidity conditions shall be laboratory ambient. Vibration environment shall be as specified by the following subparagraphs.

3.8.3.2.1 Vibration: Vibration shall be applied simultaneously through dummy vernier engines in a direction parallel to the spacecraft roll (Z) axis. The excitation force shall be random noise having a gaussian distribution (band limited between 84 cps and 2000 cps) and an average amplitude at each dummy vernier engine of 20 lbs RMS.

3.8.3.2.2 Period of Vibration Exposure: The spacecraft shall be subjected to the vibration environment for a period of 240 seconds.

3.8.3.2.3 Tolerance: Spectral density of the summed and averaged RMS force input between 84 cps and 2000 cps shall in general be maintained within ± 3 db of their nominal level.

3.10 AIRFORCE EASTERN TEST RANGE (AFETR) TEST PHASE

3.10.1 Test Objectives:

1. Perform subsystem and system test to verify spacecraft is ready for a Joint-Flight Acceptance Composite Test (J-FACT).
2. Demonstrate during J-FACT that the spacecraft and launch vehicle are compatible for flight.
3. Perform weight, balance, and alignment, and check critical functions prior to encapsulation.
4. Verify spacecraft is ready for transport to launch pad and perform functional and operational checks on pad in preparation for launch.

3.10.2 General

3.10.2.1 Test Description: The AFETR test phase shall be comprised of nineteen separate test subphases performed in the order of the following brief test descriptions:

1. AMR-FC-SP-Subsystem Tests: This test subphase shall verify performance of subsystem level parameters which are vital to mission success and cannot be tested adequately at a system level.
2. PVT-1, PVT-2, PVT-3, and PVT-4: These test subphases shall verify that the spacecraft did not suffer any damage in shipment to AFETR and is ready for a Joint-Flight Acceptance Composite Test with the launch vehicle.
3. VPS Functional and Leakage: This test subphase shall perform Vernier Propulsion System (VPS) and Gas Jet Attitude Control (GJAC) system functional tests, low pressure system leak tests, and the high pressure decay tests.
4. SRT (Post Encapsulation): Test to demonstrate that the spacecraft is adequately prepared for transfer to the launch pad after encapsulation.
5. SRT (LP): A system Readiness Test shall be performed as a system functional check of the spacecraft via the telemetry link prior to start of J-FACT.
6. CD (LP): Countdown test shall be performed to provide system operational checks and confirmation that system can be placed in launch configuration prior to start of J-FACT.
7. J-FACT: The Joint-Flight Acceptance Composite Test subphase shall demonstrate that the spacecraft and launch vehicle are compatible in a simulated system readiness test, countdown, and flight thru Centaur retromaneuver.
8. Weigh and Align: During this test subphase, the initial spacecraft alignments and verifications shall be performed. Those requirements associated with retro-rocket installations and fueling shall be omitted.
9. PVT-5: This test subphase shall be the final spacecraft testing at the Spacecraft Checkout Facility. All critical functions shall be verified which cannot be checked after spacecraft encapsulation.

10. WB&A, Fuel Load, Pressure: Final Weight, balance, and alignment after retro rocket installation and fueling operations shall be performed during this test subphase.
11. PVT-6: This test phase shall consist of connector pin retention tests to demonstrate connector mating integrity, squib circuit, verification, and SS and AD checks.
12. SRT (Post-Encapsulation): A System Readiness Test shall be performed during this test subphase to demonstrate that the spacecraft is adequately prepared for transfer to the launch pad after final encapsulation.
13. SRT (LP): A System Readiness Test - (Launch Pad) test shall be performed to verify that the spacecraft is adequately prepared to be launched.
14. Countdown (LP): A countdown (Launch Pad) test shall be performed to allow final spacecraft operational checks and to place the spacecraft system in a launch configuration.
15. SRT LP-Final and CD LP-Final: Same tests as SRT (LP) and CD (LP) which are performed at the appropriate time in the launch vehicle countdown procedure.

3.10.3.1.1 Test Access: Hardline test access and RF link control shall be provided as determined from test requirements set forth in the AFETR zone of the test requirements matrix, Table F-2.

3.10.3.1.2 Power Requirements: Ground power and spacecraft battery power shall be provided as determined from test requirements set forth in the AFETR zone of the Test Requirements Matrix, Table F-2. and spacecraft configuration requirements.

3.10.3.2 Environment: During the various test subphases the spacecraft shall be either encapsulated or on a test stand in room ambient conditions. In either case sufficient air conditioning shall be provided to maintain equipment operating temperature below the maximum specified ...

TABLE F - 1

TEST REQ'T NO.	DASH NO.	REV LTR	REQUIREMENT TITLE	REQUIREMENT DESCRIPTION	S/C APPLICABILITY						
					3	4	5	6	7		
RA101	1	A	Power Consumption	The total power consumption of the RADVS system when tested between the input voltage range of 16.5 to 22.5 VDC shall not exceed 590 watts.	X	X	X	X	X	X	X
RA102	1	A	Reliable Operate RA Signal (RORA)	The Reliable Operate Radar Altimeter signal (RORA) shall be indicated by TM signal FC-33 and shall indicate the ON state only when trackers for beams 1, 3, and 4 are tracking simultaneously.	X	X	X	X	X	X	X
RA102	2	A	Reliable Operate RA Signal (RORA)	RORA shall indicate OFF by TM signal FC-33 at all times when no return signals to the microwave receivers are being simulated.	X	X	X	X	X	X	X
RA103	1	A	Reliable Operate DVS (RODVS)	The Reliable Operate Doppler Velocity Sensor (RODVS) TM signal FC-34 shall be in the ON state only when any one of the following conditions are satisfied <u>Conditions:</u> 1. Before retro burnout with beams 1,2,3, locked and tracking simultaneously. 2. After retro burnout plus 4 seconds - when any combination of beams 1,2,3 are tracking. This condition is defined as the CRODVS mode. 3. Subsequent to retro burnout plus 4 sec - After beams 1,2,3 have locked and tracked simultaneously for 1.1 sec minimum, then RODVS shall indicate the ON state only when beams 1,2,3 are tracking simultaneously.	X	X	X	X	X	X	X
RA103	2	A	Reliable Operate DVS (RODVS)	RODVS shall indicate OFF by TM signal FC-34 at all times when no return signals to the microwave receivers are being simulated.	X	X	X	X	X	X	X

TABLE F-1 Continued

TEST REQ'T NO.	DASH NO.	REV LTR	REQUIREMENT TITLE	REQUIREMENT DESCRIPTION	S/C APPLICABILITY						
					3	4	5	6	7		
RA103	3	A	Reliable Operate DVS (RODVS)	<p>The Reliable Operate DVS(RODVS) TM signal FC-34 shall be in the ON state only when each of the following conditions are satisfied separately.</p> <p><u>Conditions:</u></p> <ol style="list-style-type: none"> 1. Before retro burnout with beams 1, 2, 3 locked and tracking simultaneously. 2. From retro burnout to burnout plus 4 seconds when any combination of beams 1, 2, 3 are tracking. This condition is defined as the CRODVS mode. 3. Subsequent to retro burnout plus 4 sec - After beams 1, 2, 3 have locked and tracked simultaneously for 1.1 sec minimum, then RODVS shall indicate the ON state only when beams 1, 2, 3 are tracking simultaneously. 	X	X	X	X	X	X	
RA104	1	A	Tracker Lock Signals	Each RADVS tracker lock signal as indicated by TM channels R-15, R-16, R-17 and R-18 shall indicate the ON state when simulated microwave input signals are applied to that individual antenna feedhorn and shall indicate OFF at all other times.	X	X	X	X	X	X	
RA104	2	A	Tracker Lock Signals	Each RADVS tracker lock signal as indicated by TM channels R-15 through R-18 shall indicate OFF at all times in the absence of simulated microwave return signals.	X	X	X	X	X	X	
RA105	1	A	RA XMTR Frequency	The altimeter transmitter frequency (undeviated) shall be 12,900 + 25 MHz following time-in of the transmitter. The frequency shall be measured at 1.0 + 0.5 minutes and 4.0 + 0.5 minutes after application of power to the RADVS	X	X	X	X	X	X	

TABLE F-1 Continued

TEST REQ'T NO.	DASH NO.	REV LTR	REQUIREMENT TITLE	REQUIREMENT DESCRIPTION	S/C APPLICABILITY						
					3	4	5	6	7		
RA106	1	A	DVS XMTR Frequency	The DVS transmitter frequency shall be 13,000 ± 35 MHz following time-in of the transmitter. The frequency shall be measured at 1.0 ± 0.5 minutes and 4.0 ± 0.5 minutes after application of power to the RADVS.	X	X	X	X	X	X	X
RA107	1	A	RA XMTR Power	The altimeter microwave power output at the altimeter antenna feedhorn shall be 210 MW/±23.22 dbm minimum following time-in of the transmitter. The power shall be measured at 1.0 ± 0.5 minutes after application of power to the RADVS.	X	X	X	X	X	X	X
RA108	1	A	DVS XMTR Power	The DVS transmitter microwave power output at each DVS antenna feedhorn shall be 1.5 W/±31.76 dbm minimum following time-in of the transmitter. The microwave power shall be measured at 1.0 ± 0.5 minutes after application of the power to the RADVS.	X	X	X	X	X	X	X
RA109	1	A	Receiver Sensitivity	<p>1. Purpose:</p> <p>The purpose of this test is to measure the receiver acquisition and dropout sensitivities as a function of frequency.</p> <p>2. S/C Configuration:</p> <p>Waveguide shall be connected to RADVS - STEA.</p> <p>3. Test Input Requirements:</p> <p>Simulated microwave signals shall be inserted in the antenna Feedhorns for beams D₁, D₂, D₃, and D₄ at the frequencies specified below. The signal level shall be below locking threshold and gradually increased until the respective tracker locks as indicated by tracker lock signals R-15, R-16, R-17 and R-18. The signal level shall then be decreased</p>							

TABLE F-1 Continued

TEST REQ'T NO.	DASH NO.	REV LTR	REQUIREMENT TITLE	S/C APPLICABILITY						
				3	4	5	6	7		
RA109 (cont)	1	A								
			<p>until the trackers unlock. The KPSM shall be undeviated and the Burnout signal applied as indicated. Power levels shall be measured within ± 1 db accuracy of the actual values inserted and frequencies shall be maintained within ± 5 Hz. Relative beam accuracy values shall be known to within 1 db.</p> <p>D₁ D₂ D₃ D₄ P PRA Burnout STC (Hz) (Hz) (Hz) (Hz) (dbm) (dbm) Signal</p> <p>1. 81,130 81,130 81,130 -111.4 - -111.4 - OFF</p> <p>2. - - 84,450 - -113.3 -</p> <p>5. 20,830 20,830 20,830 - -109.5 - OFF</p> <p>5. 20,830 20,830 20,830 - -116.5 - ON</p> <p>6. 1,640 1,640 1,640 4,995 -111.5 -102 ON</p> <p>7. - - 10,000 - -109 -</p> <p>7. 2,450 3,260 2,450 28,000 -113.5 -112 ON</p> <p>8. 930 930 930 - -103 - ON</p> <p>8. 930 930 930 - -90.0 - OFF</p> <p>4. S/C Performance Requirements:</p> <p>The receiver acquisition and dropout sensitivities shall be recorded and the acquisition sensitivity shall be more sensitive than the values specified in the previous table. There is no requirement for drop out sensitivity other than recording the values observed.</p> <p>5. Data Analysis:</p> <p>A calibration curve of acquisition sensitivity vs. frequency shall be developed for each channel.</p>							

TABLE F-1 Continued

TEST REQ'T NO.	DASH NO.	REV LTR	REQUIREMENT TITLE	REQUIREMENT DESCRIPTION	S/C APPLICABILITY																																							
					3	4	5	6	7																																			
RA109	2	A	Receiver Sensitivity	<p>1. Purpose: The purpose of this test is to verify that the acquisition sensitivity at the beginning of a simulated dynamic terminal descent is equal to or greater than the minimum required sensitivity for a given set of initial conditions.</p> <p>2. S/C Configuration The waveguide shall be connected to the RADVS-STE and the closed loop simulator shall be adjusted and calibrated for initial conditions A, B, C, or D.</p> <p>3. Test Input Requirements: With the KPSM undeviated the simulated microwave signals input power levels to the Antenna feedhorns for beams D₁, D₂, D₃, and D₄ shall be set to the following levels dependent on the set of initial conditions chosen for that particular descent. These power levels shall be applied after burn-out has occurred.</p> <table border="1"> <thead> <tr> <th>Initial Condition</th> <th>R (feet)</th> <th>V_x (FPS)</th> <th>V_y (FPS)</th> <th>V_z (FPS)</th> <th>P_{RA} (dbm)</th> <th>P_{DVS} (dbm)</th> </tr> </thead> <tbody> <tr> <td>A</td> <td>20,000</td> <td>+20</td> <td>+20</td> <td>200</td> <td>-112</td> <td>-114</td> </tr> <tr> <td>B</td> <td>20,000</td> <td>-20</td> <td>-20</td> <td>200</td> <td>-112</td> <td>-114</td> </tr> <tr> <td>C</td> <td>25,000</td> <td>+50</td> <td>+50</td> <td>500</td> <td>-112.5</td> <td>-115</td> </tr> <tr> <td>D</td> <td>25,000</td> <td>-50</td> <td>-50</td> <td>500</td> <td>-112.5</td> <td>-115</td> </tr> </tbody> </table>	Initial Condition	R (feet)	V _x (FPS)	V _y (FPS)	V _z (FPS)	P _{RA} (dbm)	P _{DVS} (dbm)	A	20,000	+20	+20	200	-112	-114	B	20,000	-20	-20	200	-112	-114	C	25,000	+50	+50	500	-112.5	-115	D	25,000	-50	-50	500	-112.5	-115	X	X	X	X	X
Initial Condition	R (feet)	V _x (FPS)	V _y (FPS)	V _z (FPS)	P _{RA} (dbm)	P _{DVS} (dbm)																																						
A	20,000	+20	+20	200	-112	-114																																						
B	20,000	-20	-20	200	-112	-114																																						
C	25,000	+50	+50	500	-112.5	-115																																						
D	25,000	-50	-50	500	-112.5	-115																																						

TABLE F-1 Continued

TEST REQ'T NO.	DASH NO.	REV LTR	REQUIREMENT TITLE	REQUIREMENT DESCRIPTION	S/C APPLICABILITY																									
					3	4	5	6	7																					
RA109 (cont)	2	A		<p>4. S/C Performance Requirements:</p> <p>Upon application of the input signals the tracker lock signals R-15, R-16, R-17, and R-18, shall go from an "OFF" state to an "ON" state and remain on.</p> <p>5. Data Analysis</p> <p>Record that satisfactory performance has occurred.</p>																										
RA111	1	A	Preamp Gain State Signals	<p>The Preamp Gain State Signals ON and OFF shall be indicated and verified as follows:</p> <p>Indicated by:</p> <table border="1" style="margin-left: 20px;"> <thead> <tr> <th>D₁</th> <th>D₂</th> <th>D₃</th> <th>D₄</th> </tr> </thead> <tbody> <tr> <td>R-19, R-20</td> <td>R-21, R-22</td> <td>R-23, R-24</td> <td></td> </tr> <tr> <td>1</td> <td>1</td> <td>1</td> <td>GS 40 1 1 GS 40</td> </tr> <tr> <td>0</td> <td>0</td> <td>0</td> <td>GS 65 0 1 GS 60</td> </tr> <tr> <td>0</td> <td>0</td> <td>0</td> <td>GS 90 0 0 GS 80</td> </tr> </tbody> </table> <p>The Gain Switching shall occur at simulated power levels within +3 db of the indicated switch points according to the Lunar Reflectivity Calibration Curves in RAL22-1.</p>	D ₁	D ₂	D ₃	D ₄	R-19, R-20	R-21, R-22	R-23, R-24		1	1	1	GS 40 1 1 GS 40	0	0	0	GS 65 0 1 GS 60	0	0	0	GS 90 0 0 GS 80	X	X	X	X	X	X
D ₁	D ₂	D ₃	D ₄																											
R-19, R-20	R-21, R-22	R-23, R-24																												
1	1	1	GS 40 1 1 GS 40																											
0	0	0	GS 65 0 1 GS 60																											
0	0	0	GS 90 0 0 GS 80																											
RA111	2	A	Preamplifier Gain State Signals	<p>Preamp Gain State signals as indicated by TM channels R-19 through R-26 (Inclusive) shall indicate OFF at all times in the absence of simulated microwave return signals.</p>	X	X	X	X	X	X																				

TABLE F-1 Continued

TEST REQ'T NO.	DASH NO.	REV LTR	REQUIREMENT TITLE	REQUIREMENT DESCRIPTION	S/C APPLICABILITY
R112	1	A	Analog Output Accuracy	<p>1. Purpose: The purpose of this test is to verify the transfer function of the RADVS analog signals and develop a calibration curve of the RADVS - Flight Control-TM combination.</p> <p>2. S/C Configuration: Waveguide shall be connected to RADVS-STEA and a test tee between the SDC and Flight Control for access to the analog signals from the SDC. The TM shall be in mode 2 at 1100 BPS.</p> <p>3. Test Input Requirements: With the KPSM undeviated and RORA and RODVS signals present, simulated microwave signals single side-band modulated with the following frequencies and power levels shall be inserted in the antenna feed-horns for beams D₁, D₂, D₃, and D₄ as indicated below: Power levels shall be maintained within ± 2 db and frequencies within ± 5 Hz.</p>	3 4 5 6 7

TABLE F-1 Continued

TEST REQ'T NO.	DASH' NO.	REV LTR	REQUIREMENT TITLE		REQUIREMENT DESCRIPTION										S/C APPLICABILITY					
			R _z (Ft.)	V _x (FPS)	V _y (FPS)	V _z (FPS)	D ₁ (Hz)	D ₂ (Hz)	D ₃ (Hz)	D ₄ (Hz)	P _{DVS} (dbm)	P _{RA} (dbm)	3	4	5	6	7			
2			40,000	-300	-300	740	13,310	18,150	22,990	84,450	-100	-104								
4			36,530	+300	+300	325	12,800	7,970	3,100	67,925	-100	-104								
5			14,000	0	0	850	20,830	20,830	20,830	45,060	-95	-94								
7			1,100	-50	+50	100	2,450	3,260	2,450	4,412	-72	-72								
7			900	-50	+50	100	2,450	3,260	2,450	17,257	-72	-72								
9			240	+50	-50	54.5	1,330	530	1,330	5,330	-50	-57								
10			20	0	0	5	123	123	123	456	-42	-49								
-			Search Search Search Search																	
			$D_1 = \frac{16.23 V_x + 16.23 V_y + 49.021 V_z}{2}$																	
			$D_2 = \frac{-16.23 V_x + 16.23 V_y + 49.021 V_z}{2}$																	
			$D_3 = \frac{-16.23 V_x - 16.23 V_y + 49.021 V_z}{2}$																	
			$D_4 = AR_z + 26.23 V_z$																	
			where $A = 1.626$ for $R_z > 1000$ ft. $A = 16.26$ for $R_z < 1000$ ft.																	

TABLE F-1 Continued

TEST REQ'T NO.	DASH NO.	REV LTR	REQUIREMENT TITLE	REQUIREMENT DESCRIPTION	S/C APPLICABILITY																																																																												
RA112 (cont)	1	A		<p>4. S/C Performance Requirements:</p> <p>The voltages of the analog outputs from the SDC shall indicate the following values.</p> <p>V_x & V_y inputs (FPS)</p> <table border="0"> <tr><td>0</td><td>0 ± 0.070</td></tr> <tr><td>-50</td><td>-2.500 ± 0.095</td></tr> <tr><td>+50</td><td>$+2.500 \pm 0.079$</td></tr> <tr><td>-300</td><td>-15.000 ± 0.460</td></tr> <tr><td>+300</td><td>$+15.000 \pm 0.350$</td></tr> <tr><td>Search</td><td>0 ± 0.100</td></tr> </table> <p>Voltage outputs (DCV)</p> <table border="0"> <tr><td></td><td>0.250 ± 0.055</td></tr> <tr><td></td><td>2.725 ± 0.077</td></tr> <tr><td></td><td>5.000 ± 0.095</td></tr> <tr><td></td><td>16.250 ± 0.350</td></tr> <tr><td></td><td>37.500 ± 0.460</td></tr> <tr><td></td><td>42.500 ± 0.700</td></tr> <tr><td></td><td>0.080 ± 0.100</td></tr> </table> <p>V_z inputs (FPS)</p> <table border="0"> <tr><td>5</td><td></td></tr> <tr><td>54.4</td><td></td></tr> <tr><td>100</td><td></td></tr> <tr><td>325</td><td></td></tr> <tr><td>740</td><td></td></tr> <tr><td>850</td><td></td></tr> <tr><td>Search</td><td></td></tr> </table> <p>Voltage output (DCV)</p> <table border="0"> <tr><td></td><td>0.400 ± 0.085</td></tr> <tr><td></td><td>4.800 ± 0.115</td></tr> <tr><td></td><td>18.000 ± 0.380</td></tr> <tr><td></td><td>1.100 ± 0.051</td></tr> <tr><td></td><td>14.000 ± 0.530</td></tr> <tr><td></td><td>40.000 ± 1.500</td></tr> </table> <p>R_z inputs (FT.)</p> <table border="0"> <tr><td>20</td><td></td></tr> <tr><td>240</td><td></td></tr> <tr><td>900</td><td></td></tr> <tr><td>1,100</td><td></td></tr> <tr><td>14,000</td><td></td></tr> <tr><td>40,000</td><td></td></tr> </table> <p>Voltage output (DCV)</p> <table border="0"> <tr><td></td><td>0.400 ± 0.085</td></tr> <tr><td></td><td>4.800 ± 0.115</td></tr> <tr><td></td><td>18.000 ± 0.380</td></tr> <tr><td></td><td>1.100 ± 0.051</td></tr> <tr><td></td><td>14.000 ± 0.530</td></tr> <tr><td></td><td>40.000 ± 1.500</td></tr> </table> <p>For V_x, V_y, and V_z Output Voltage = $0.050 V_{(x,y,z)}$ (FPS)</p>	0	0 ± 0.070	-50	-2.500 ± 0.095	+50	$+2.500 \pm 0.079$	-300	-15.000 ± 0.460	+300	$+15.000 \pm 0.350$	Search	0 ± 0.100		0.250 ± 0.055		2.725 ± 0.077		5.000 ± 0.095		16.250 ± 0.350		37.500 ± 0.460		42.500 ± 0.700		0.080 ± 0.100	5		54.4		100		325		740		850		Search			0.400 ± 0.085		4.800 ± 0.115		18.000 ± 0.380		1.100 ± 0.051		14.000 ± 0.530		40.000 ± 1.500	20		240		900		1,100		14,000		40,000			0.400 ± 0.085		4.800 ± 0.115		18.000 ± 0.380		1.100 ± 0.051		14.000 ± 0.530		40.000 ± 1.500	3 4 5 6 7
0	0 ± 0.070																																																																																
-50	-2.500 ± 0.095																																																																																
+50	$+2.500 \pm 0.079$																																																																																
-300	-15.000 ± 0.460																																																																																
+300	$+15.000 \pm 0.350$																																																																																
Search	0 ± 0.100																																																																																
	0.250 ± 0.055																																																																																
	2.725 ± 0.077																																																																																
	5.000 ± 0.095																																																																																
	16.250 ± 0.350																																																																																
	37.500 ± 0.460																																																																																
	42.500 ± 0.700																																																																																
	0.080 ± 0.100																																																																																
5																																																																																	
54.4																																																																																	
100																																																																																	
325																																																																																	
740																																																																																	
850																																																																																	
Search																																																																																	
	0.400 ± 0.085																																																																																
	4.800 ± 0.115																																																																																
	18.000 ± 0.380																																																																																
	1.100 ± 0.051																																																																																
	14.000 ± 0.530																																																																																
	40.000 ± 1.500																																																																																
20																																																																																	
240																																																																																	
900																																																																																	
1,100																																																																																	
14,000																																																																																	
40,000																																																																																	
	0.400 ± 0.085																																																																																
	4.800 ± 0.115																																																																																
	18.000 ± 0.380																																																																																
	1.100 ± 0.051																																																																																
	14.000 ± 0.530																																																																																
	40.000 ± 1.500																																																																																

TABLE F-1 Continued

TEST REQ'T NO.	DASH NO.	REV LTR	REQUIREMENT TITLE	REQUIREMENT DESCRIPTION	S/C APPLICABILITY
RA112 (cont)	1	A		<p>For Range.</p> <p>Output Voltage = $0.001 R_z$ (FT) ($R_z > 1000$ ft)</p> <p>Output Voltage = $0.020 R_z$ (FT) ($R_z < 1000$ ft)</p> <p>5. Data Analysis:</p> <p>Record values of the TM in BCD for channels FC-35, FC-39, FC-40, FC-41, and FC-77 simultaneously with the hardline readings. A TM calibration curve for each of the V_x, V_y, V_z, and Range signals shall be developed (input vs TM in BCD) by subtracting FC-77 from each of the other TM channel readings.</p>	3 4 5 6 7
RA112	2	A	Analog Output Accuracy	<p>1. Purpose:</p> <p>The purpose of this test is to verify the analog output accuracy thru TM during a dynamic terminal descent.</p> <p>2. S/C Configuration:</p> <p>Waveguide shall be connected to RADVS-STEPA and the computed V_x, V_y, V_z, and R_z inputs from the Flight Control Simulator to the RADVS STEPA shall be recorded with the same time base as the TM signals.</p> <p>3. Test Input Requirements:</p> <p>With the KPSM undeviated and RORA & RODVS signals present, simulated microwave signals for a terminal descent shall be inserted in the antenna feedhorns for beams D₁, D₂, D₃, & D₄ and the recorded computed values of V_x, V_y, V_z, & R_z</p>	X X X X X

TABLE F-1 Continued

TEST REQ'T NO.	DASH NO.	REV LTR	REQUIREMENT TITLE	REQUIREMENT DESCRIPTION	S/C APPLICABILITY						
					3	4	5	6	7		
RA112 (Cont)	2	A		<p>shall agree with the actual inserted frequencies within ± 0.8 ft for ranges < 1000 ft., ± 5.0 ft. for ranges of 1000 ft $\leq R \leq 12,500$ ft., ± 0.3 FPS for V_x, V_y, & $V_z < 200$ FPS, and \pm FPS for $V > 200$ FPS. The microwave signal power levels shall be as defined in test requirement RA122-2.</p> <p>4. S/C Performance Requirements:</p> <p>Verify that the range analog output signal on FC-35 shall not deviate from the true simulated range by more than the RSS of 44 ft. and $\pm 5\%$ of the true simulated range (high deviation mode) or the RSS of ± 30 ft. & $\pm 5\%$ of true simulated range (low deviation mode). Verification shall be performed within $\pm 10\%$ of points at 10,000 ft., 5,000 ft., 1000 ft mark, 50 ft., & 14 ft. mark.</p> <p>Verify that the velocity analog outputs on FC-39, FC-40, and FC-41 do not deviate from the true velocity signals by more than the RSS of \pm FPS and $\pm 2.0\%$ of the true total velocity vector. Verification shall be performed within $\pm 10\%$ of points at 150, 100, 50 & 10 FPS for V_x and at 0 FPS for V_x & V_y.</p> <p>5. Data Analysis:</p> <p>Verification of TM data vs input signals from the Flight Control Simulator shall be made from tabulation runs of taped TM & input data. The Calibration curve developed in RA-112-1 shall be used after the raw TM data has been corrected for line drop (FC-77), time delay and offsets in the Flight Control Conditioning circuits, and relative word position of discrete data points.</p>							

TABLE F-1 Continued

TEST REQ'T NO.	DASH NO.	REV LTR	REQUIREMENT TITLE	REQUIREMENT DESCRIPTION	S/C APPLICABILITY						
					3	4	5	6	7		
RA112	3	A	Analog Output Accuracy	<p>1. Purpose: The purpose of this test is to verify that no tracker locks occur and that V_x, V_y, & V_z are providing a nominal zero FPS indications and Range is providing the proper sweep pattern when all 4 trackers are searching.</p> <p>2. S/C Configuration: All 8 antenna feedhorns shall be terminated in microwave dummy loads with no significant leakage about their flanges.</p> <p>3. Input Test Requirements: None</p> <p>4. S/C Performance Requirements: Verify that TM signal FC-35 indicates a varying search pattern between 0 & 5 volts at a repetition rate of 0.650 ± 0.10 Hz when averaged over a one minute period. Verify that the TM signals on FC-39 & FC-40 are zero ± 2 FPS and FC-41 is 1.63 ± 2 FPS.</p> <p>5. Data Analysis: Verification shall be obtained by using the calibration curve developed in RA-112-1 after the raw TM data has been corrected for line drop FC-77 and offsets in the Flight Control conditioning circuits.</p>	X	X	X	X	X	X	

TABLE F-1 Continued

TEST REQ'T NO.	DASH NO.	REV LTR	REQUIREMENT TITLE	REQUIREMENT DESCRIPTION	S/C APPLICABILITY						
					3	4	5	6	7		
R114	1	A	1000 Ft. Mark	<p>During the period subsequent to burnout plus 4 sec. when RORA signal is present and when simulated $V_z = 105 \pm 25$ fps, and when simulated range rate $= 105 \pm 21$ fps, the 1,000 ft. range mark shall occur when the input range freq F_r is: $FR = (1626 + 26.23 V_z)$ cps plus or minus 115 cps for every one of 10 separate trials. The average of the 10 trials and the 3σ dispersions shall meet the following criteria:</p> <p>$\bar{x} + 3\sigma \leq 1707 + 26.23 V_z$ cps</p> <p>$\bar{x} - 3\sigma \geq 1545 + 26.23 V_z$ cps</p> <p>\bar{x} is defined as $= \frac{\sum x_i}{10}$ where x_i is each individual measurement.</p> <p>3σ is defined as $= \sqrt{\sum (x - x_i)^2}$ for 10 samples</p>	X	X	X	X	X	X	
R114	2	A	1000 Ft. Mark	<p>The 1000 ft mark as indicated by TM channel FC-37 shall indicate ON when the decreasing simulated input range signal to the RADVS is 1000 ± 71 ft. The 1000 ft mark shall indicate OFF prior to this time.</p>	X	X	X	X	X	X	
R114	3	A	1000 Ft. Mark	<p>The 1000 ft mark as indicated by TM channel FC-37 shall indicate OFF in the absence of simulated RF input signals.</p>							
R115	1	A	14 Ft. Mark	<p>When both RORA and 100 ft. mark signals are present and when simulated $V_z = 5 \pm 3$ fps, and when simulated range rate $= 5 \pm 1$ fps, then the 14 ft. range mark shall occur when $F_r = 255 + 26.23 V_z + 65$ cps for everyone of 10 separate trials. The average of the 10 trials and the 3σ dispersion shall meet the following criteria:</p>							

TABLE F-1 Continued

TEST REQ'T NO.	DASH NO.	REV LTR	REQUIREMENT TITLE	REQUIREMENT DESCRIPTION	S/C APPLICABILITY						
					3	4	5	6	7		
RA115 (Cont)	1	A		$\bar{x} + 3\sigma \leq 304 + 26.23 V_z$ cps $\bar{x} - 3\sigma \geq 206 + 26.23 V_z$ cps \bar{x} is defined as $= \frac{\sum x_i}{10}$ where x_i is each individual measurement 3σ is defined as $= \sqrt{\frac{\sum (x_i - \bar{x})^2}{10}}$ for 10 samples							
RA115	2	A	14 Ft Mark	The 14 ft. mark as indicated by TM channel FC-38, shall indicate ON when the decreasing input range signal is 14 + 4 ft. The 14' mark shall indicate OFF prior to this time.	X	X	X	X			X
RA115	3	A	14 Ft. Mark	The 14 ft. mark as indicated by TM channel FC-38 shall indicate OFF in the absence of simulated RF input signals.	X	X	X	X			X
RA116	1	A	RA XMTR Deviation	As measured on the RADVS STEA Polarad Analyzer, the RA Tx deviation shall be 40 + 1 mc in high deviation and 4.0 ± 0.4 mc in low deviation. The deviation rate shall change from low to high upon generation of the 1000 ft mark.	X	X	X	X			X
RA117	1	A	SDC Temperature	The SDC Temperature as indicated by TM channel R-9 shall be between +60°F and +150°F when tested in an ambient environment with a TM bit rate of 1100 BPS or less.	X	X	X	X			X
RA117	2	A	SCD Temperature	The SDC Temperature as indicated by TM channel R-9 shall have a start temperature between +45 ± 30°F for φA, + 83 ± 83 + 30°F for φB, and + 68 ± 30°F for φC when tested in a thermal vacuum environment. The SDC temperature shall not exceed + 150°F during its ON time. The TM bit rate shall be 1100 BPS or less.	X	X	X	X			X

TABLE F-1 Continued

TEST REQ'T NO.	DASH NO.	REV LTR	REQUIREMENT TITLE	REQUIREMENT DESCRIPTION	S/C APPLICABILITY						
					3	4	5	6	7		
RA118	1	A	KPSM Temperature	The KPSM temperature as indicated by TM channel R-8 shall be between +60°F and +145°F when tested in an ambient environment with a TM bit rate of 1100 BPS or less.	X	X	X	X	X	X	X
RA118	2	A	KPSM Temperature	The KPSM temperature as indicated by TM channel R-8 shall have a start temperature between +7 + 25°F for φA, + 40 + 25°F for φB, and +28 + 25°F for φC when tested in a thermal vacuum environment. The KPSM temperature shall not exceed 145°F during its ON time. The TM bit rate shall be 1100 BPS or less.	X	X	X	X	X	X	X
RA119		A	DVS Antenna Temperature	The DVS Antenna Temperature as indicated by TM channel R-10 shall be between +60°F and +112°F when tested in an ambient environment with a TM bit rate of 1100 BPS or less.	X	X	X	X	X	X	X
RA119	2	A	DVS Antenna Temperature	The DVS Antenna Temperature as indicated by TM channel R-10 shall have a start temperature between -1 +35°F for φA, + 35 +35°F for phase B, and +36 +35°F for phase C when tested in a thermal vacuum environment. The DVS Antenna shall not exceed 112°F during its ON time. The bit rate shall be 1100 BPS or less.	X	X	X	X	X	X	X
RA120	1	A	A/VS Antenna Temperature	The A/VS Antenna temperature as indicated by TM channel R-13 shall be between + 60°F and +110°F when tested in an ambient environment with a TM bit rate of 1100 BPS or less.	X	X	X	X	X	X	X
RA120	2	A	A/VS Antenna Temperature	The A/VS Antenna temperature as indicated by TM channel R-13 shall have a start temperature between + 8 + 35°F for phase A, + 42 + 35°F for phase B, and + 49 + 35°F for phase C when tested in a thermal vacuum environment. The A/VS Antenna shall not exceed +110°F during its ON time. The TM bit rate shall be 1100 BPS or less.	X	X	X	X	X	X	X

TABLE F-1 Continued

TEST REQ'T NO.	DASH NO.	REV LTR	REQUIREMENT TITLE	REQUIREMENT DESCRIPTION	S/C APPLICABILITY						
					3	4	5	6	7		
RA121	1	A	Warm up Time	<p>The total warm up time from application of primary power to transmission of microwave power shall not exceed 30 sec.</p> <p>1. Purpose:</p> <p>The purpose of this test is to provide a calibration curve of the Lunar Reflectivity hardline and TM signals for channels R-2, R-3, R-4, and R-5.</p> <p>2. S/C Configuration:</p> <p>Waveguide shall be connected to RADVS-STEA and a test tee connected at the SDC output for access to the Lunar Reflectivity signals. The TM shall be in mode 2 at 1100 BPS.</p> <p>3. Test Input Requirements:</p> <p>With the KPSM undeviated, simulated microwave signals shall be inserted in the antenna feedhorns for beams D₁, D₂, D₃ and D₄. The input doppler frequency shall be greater than 80 KHz for D₄ and greater than 12 KHz for D₁, D₂, and D₃. The input signal levels, beginning at -130 dbm (no lock condition) shall be increased in 5 db input increments or 0.5 volt output increments, which ever occurs first, up to -40 dbm. End point values at preamplifier gain switching shall be accurately determined for both increasing and decreasing signal power levels. Recorded values of input power shall be within \pm 1db of the actual inserted power.</p>	X	X	X	X	X	X	
RA122	1	A	Lunar Reflectivity Signals		X	X	X	X	X	X	

APPENDIX G

DISCUSSION OF THE STEA SIGNAL SIMULATION TECHNIQUE

I. INTRODUCTION

The simulated return signal provided by STEA is obtained by single-sideband modulation of the spacecraft's transmitted signal, as shown in Fig. 5-1. (Some unit test equipment uses a similar method.) In open loop tests, the modulating signal is developed from a crystal oscillator or from a manually operated variable frequency oscillator. For tests with the spacecraft in closed loop simulation, the oscillator is controlled in accordance with computed simulated motion. In both cases, therefore, the simulated return signal spectrum is essentially a single line which tracks the transmitted signal frequency variations. (The tracking is delayed, of course, by the signal transit time between STEA and S/C.)

An actual return signal also tracks the transmitted frequency variations, but with a much greater delay. For instance, the transit delay using STEA is less than about 10^{-7} seconds while the actual propagation delay from high altitudes is in the range of 10^{-5} - 10^{-4} seconds. This difference has an appreciable effect on the seriousness of problems caused by transmitter short term frequency incoherence. The same situation pertains to the effects of nonlinear modulation of the altimeter klystron.

Important differences between actual signals and simulated ones also exist in both spectral and time characteristics. The long-term power density spectrum of a true lunar echo will rather closely match the two-way antenna gain pattern, while the simulated signal spectrum is nearly a single line. The expected lunar echo will also fluctuate in time in a random, noise-like manner due to the scattering properties of the rough surface; the simulated signal is essentially deterministic.

The main purpose of this Appendix is to discuss how differences due to frequency coherence and nonlinear modulation affect testing results. Problems due to doppler spread have already been discussed in Sections VI.A.3 and VII.A.1d.

II. TRANSMITTER INCOHERENCE

Undesirable transmitter frequency fluctuations result in a spreading of the mixing-product spectrum. This spreading can cause signal power loss in subsequent filters, called "coherence loss," and possible false locks and tracking errors. To determine the seriousness of the effect, consider the result of mixing two signals from a sinusoidally frequency-modulated source, one delayed in time and shifted in frequency (by doppler). Assuming that the doppler shift is negligibly perturbed by the sinusoidal modulation, these signals can be expressed as

$$e_t(t, \omega_c) = E_1 \cos [\omega_c t + \phi \sin \omega_r t] \quad (G-1)$$

and

$$\begin{aligned} e_r(t, \omega_c) &= K e_t(t - T_d, \omega_c + \omega_d) \\ &= K E_1 \cos [(\omega_c + \omega_d)(t - T_d) + \phi \sin \omega_r(t - T_d)] \quad (G-2) \end{aligned}$$

where $K =$ a constant,

$\omega_c =$ transmitter carrier frequency,

$\omega_d =$ doppler frequency shift,

$\omega_r =$ frequency of the modulating sinusoid,

$\phi =$ modulation index of the transmitted signal,

$T_d =$ time delay between transmission and reception.

The low frequency component of the mixing of these two signals is

$$e_3 = E_3 \cos [\omega_d t + 2\phi \left| \sin \frac{\omega_r T_d}{2} \right| \sin \omega_r (t - T_d + \alpha)] \quad (G-3)$$

where E_3 is a constant, and α is a constant dependent on $\omega_r T_d$ [75, p.89].

The one-sided Fourier spectrum of the waveform in eq. (G-3) is composed of lines at frequencies $|\omega_d \pm n \omega_r|$, $n=0, \pm 1, \pm 2, \dots$, with amplitudes proportional to the Bessel functions

$$J_n(2\phi \left| \sin \frac{\omega_r T_d}{2} \right|).$$

The power level of each component relative to the total signal power is, therefore,

$$S_n = 20 \log [| J_n (2\phi \left| \sin \frac{\omega_r T_d}{2} \right|) |] \text{ decibels} \quad (G-4)$$

Representative numerical values for (G-4) will be obtained for typical causes of frequency incoherence. These numbers directly indicate the magnitude of the incoherence problem, which would go unnoticed in STEA type simulation testing.

A. Power Supply Ripple

The maximum allowable sensitivity to anode voltage supply variations specified for the DVS klystron is 100 kHz/volt [56]. (The RA klystron, being a reflex klystron, is likely to be 10 times more sensitive.) The major component of power supply ripple will normally occur either at the converter frequency, 2.4 kHz, or twice that frequency.* Choosing the latter value, the modulation index of the major ripple component applied to a maximally sensitive DVS klystron is

$$\phi = \frac{100 \times 10^3 \text{ V} \times \sqrt{2}}{4.8 \times 10^3} \approx 30 \text{ V} \quad (G-5)$$

where V is the rms value of the ripple component at 4.8 kHz. (The effects of other ripple components are assumed to be negligible.)

The minimum value of V for which false lock could occur is easily computed by assuming that the total return signal is 28 db above the acquisition level; any

* Later model KPSM's might operate at 3.8 to 4.0 kHz.

higher signal would cause a preamp gain switch to effectively suppress the sideband signal by about 25 db. The solution to

$$20 \log [J_1 (60V)] = -28 \text{ db}$$

is $V_{\min} = 1.33 \text{ mv}$. (Such a situation could occur at a beam slant range of 50 kft and an angle of incidence of about 20° off the lunar vertical. The corresponding spacecraft slant range could be anywhere between 46 kft and 90 kft.)

A more serious problem occurs when the ripple is high enough for lock of a sideband to persist an appreciable time. For example, a 10 mv ripple is sufficient to keep the upper beam of a spacecraft at 25° attitude locked over slant ranges of 50 kft to 10 kft, where gain state switching would occur. (The after-burnout sensitivity was used for this computation.) As another example, one of the worst situations involves the upper beam of a spacecraft at 5° attitude. A ripple of about 8 mv before burnout or 2 mv after burnout would be sufficient to maintain lock on the first sideband down to about 20 kft. Some other levels are shown in Fig. G-1.*

It can be shown that the first sideband levels (in db) relative to the acquisition threshold vary approximately as $20 \log V$ and independently of range for situations of interest. A consequence of the independence toward range is that false locks will not normally be broken unless gain states are switched or appreciable attitude change occurs.

The amount of power lost due to sideband generation should also be considered. In the case of the DVS klystron, the fundamental component is reduced less than one db for a ripple of less than about 16 mv. This amount, of course, is not serious.

As a final consideration of ripple, it should be noted that there is no pertinent test requirement specified. The vendor test simply requires that ripple be recorded. It is not measured anywhere else nor are its frequency modulation effects observed.

B. Vibration

The vibration sensitivity specification for the DVS klystron is that the frequency modulation must not exceed 200 kHz peak-to-peak for 25 g vibration between 10 Hz and 2 kHz [56]. A reasonable value for frequency deviation at the expected g levels, therefore, would be 1 kHz. The frequency of modulation would probably be less than 1.5 kHz because mechanical resonances are most likely within that region [61]. For cases of interest in this range, a good approximation to eq. G-4 is

$$S_n \approx 20 \log [J_n (2\Delta f \frac{2\pi r}{c})] \quad (G-6)$$

* Computations are based on an expected return power of -94 dbm at 50 kft and the following acquisition thresholds:

Typical Sensitivities

<u>R</u>	<u>BBO</u>	<u>ABO</u>
50 kft	-111 dbm	-118 dbm
40	-110	-117
30	-109	-116
20	-107	-114
10	-105	-112

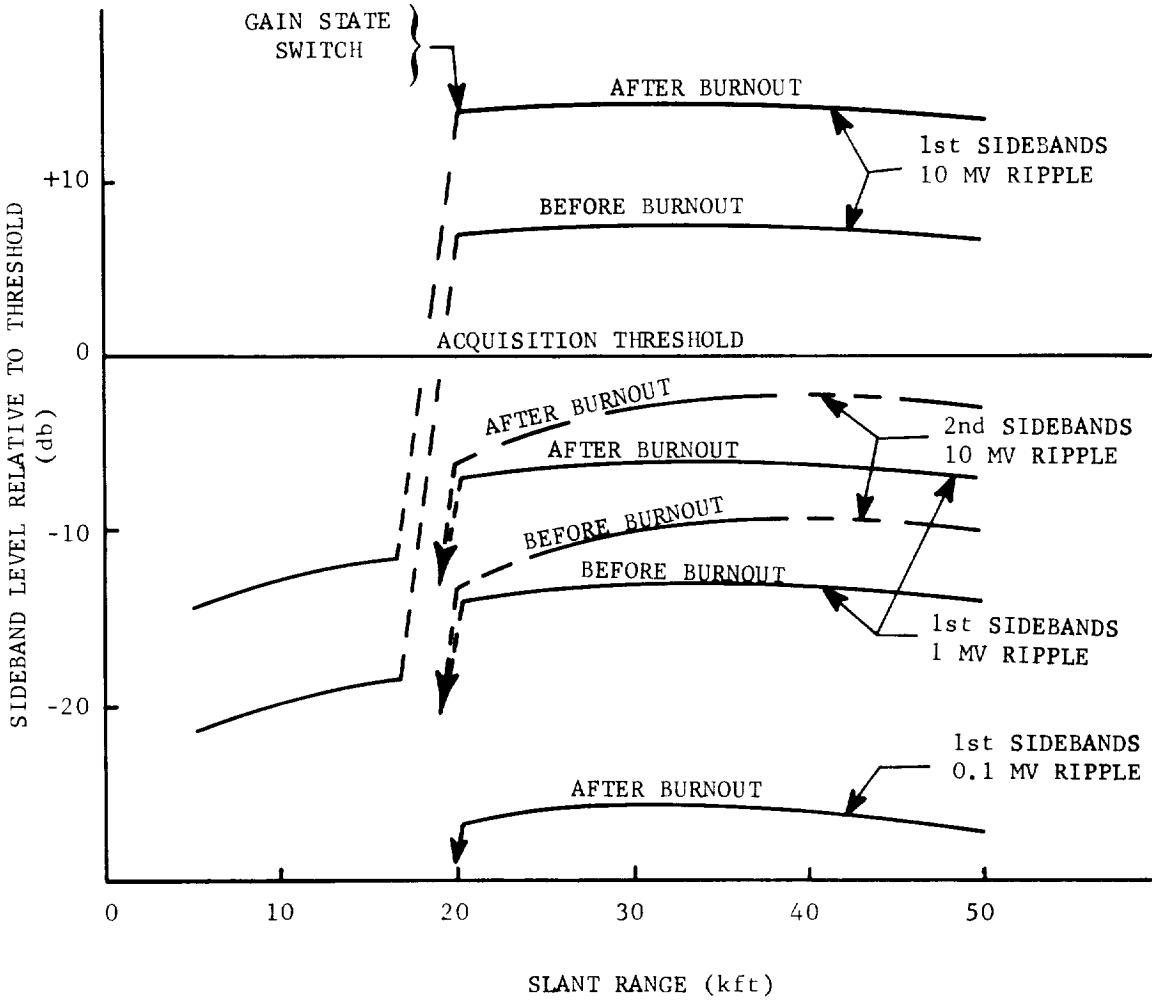


Fig. G-1. Sideband levels relative to the signal acquisition threshold vs roll axis slant range for the upper DVS beam of a spacecraft at 5° angle to the lunar vertical.

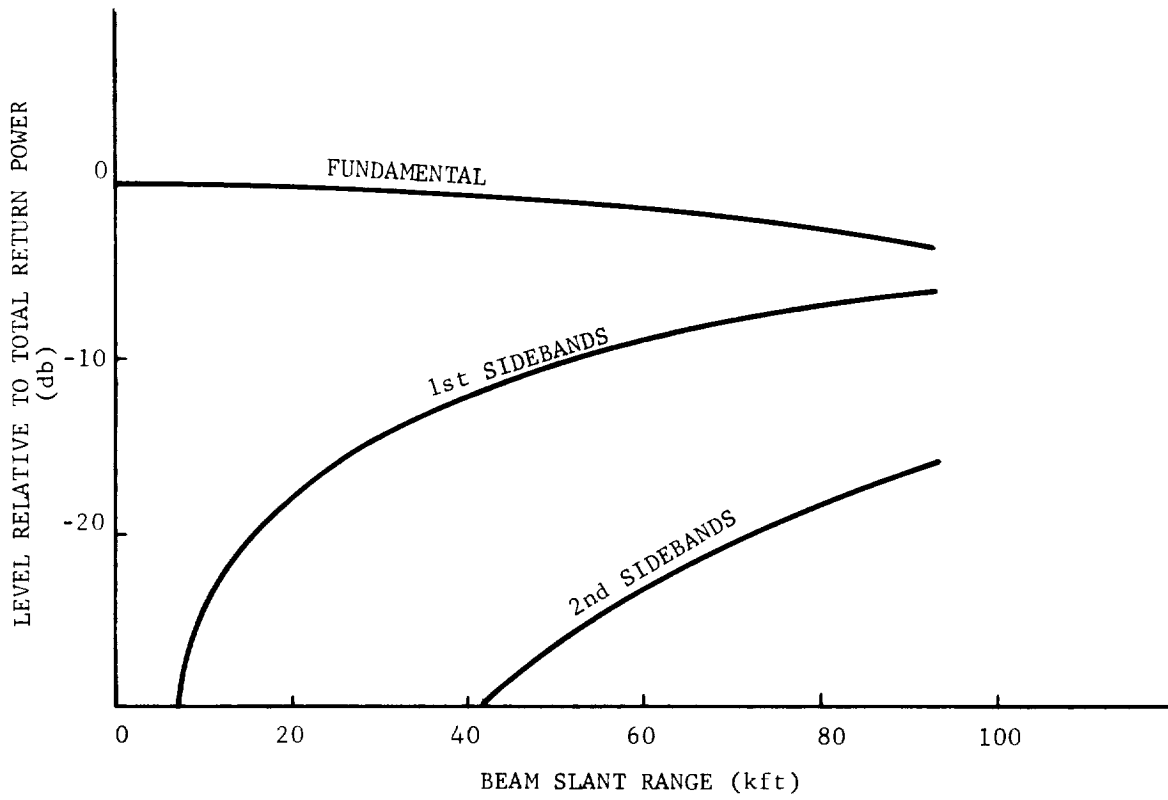


Fig. G-2. Signal component levels vs. range for sinusoidal frequency modulation of 1 kHz deviation at modulating frequencies up to about 1.5 kHz.

where Δf is the frequency deviation, c is the velocity of propagation, and r is the beam slant range. (Notice that eq. G-6 is independent of modulating frequency.)

Equation G-6 is plotted in Fig. G-2 (for $n = 0, 1, \text{ and } 2$) for the case of 1 kHz maximum deviation. The high altitude effects are similar to those caused by about 50 mv ripple. As mentioned in the discussion of ripple effects, situations can be found for which false lock can occur on any sideband within about 28 db of the total power. Loss of power in the fundamental component is also seen to be a problem for the vibration case. In fact, if the frequency deviation were greater than about 2 kHz, the fundamental would disappear completely at some beam range below 90 kft.

C. EMI

High frequency EMI is not likely to cause problems because associated modulation indices would probably be low. The contrary is true for low frequency EMI, however. (Such frequencies commonly arise from converters and commutators.) Also, shielding against these lower frequencies is generally found to be more difficult.

No special cases are considered here because EMI effects can cover a wide range. For inputs which essentially have a single frequency, the results would be similar to those described in the preceding sections.

III. EFFECTS OF NONLINEAR MODULATION OF THE RA KLYSTRON

Common sweep nonlinearities can often be adequately modeled by addition of a quadratic term to the frequency function. For example, suppose the transmitted function is

$$e_t(t) = E_1 R(t) * \left\{ W(t) \cos [(\omega_0 - mt + \alpha t^2)t] \right\} \quad (G-7)$$

- where E_1 = a constant,
 ω_0 = undeviated center frequency,
 m = linear sweep rate,
 α = coefficient of the quadratic nonlinearity,
 $W(t)$ = the "window" function defined as
 $= 1$ for $\frac{-T + \epsilon}{2} \leq t \leq \frac{-T + \epsilon}{2}$
 $= 0$ elsewhere
 $R(t)$ = the "repeat" function defined as
 $= \sum_{m=-\infty}^{\infty} \delta(t - mT)$
 T = sweep repetition period,
 ϵ = "flyback" period,
 $*$ indicates convolution

(The shape of the waveform during "flyback" is not important to this example.)
The ideal return function would then be

$$e_r(t) = Ke_t(\omega_o + \omega_d, t - T_d) \quad (G-8)$$

where ω_d and T_d have the same meanings as in previous sections and K is a constant. Consequently, the low frequency mixing component (after blanking) would be

$$e_3(t) = E_3 R(t) * \left\{ B(t) \cos [\omega_d t + 2m T_d t + 3\alpha T_d^2 t - 3\alpha T_d t^2 + \varphi] \right\} \quad (G-9)$$

where E_3 and φ are constants and $B(t)$ is a "window" function which provides the blanking effect.

The third frequency term in eq. G-9 represents the steady range error due to the assumed nonlinearity. The percent error is

$$\epsilon = \frac{150 \alpha T_d}{m} \% \quad (G-10)$$

This equation shows one of the effects of the small delay factor (T_d) in STEA simulations; the indicated error would be about 100 times less than that which would actually exist over most of the descent.

The spectrum of $e_3(t)$ is composed of lines spaced 180 Hz apart by the $R(t)$ term with an envelope determined by the other factor. It can be shown that the spectral width for this case is approximately [76, pt. IV, Ch. 2]

$$W = \frac{6\alpha T_d T_s}{2\pi} \quad (G-11)$$

where T_s = sweep period after blanking.

To obtain a number for the spectral width, suppose αT_d is such a value as to produce a 0.01% range error. Then, from (G-10)

$$\alpha T_d = \frac{0.01m}{150}$$

and
$$W = \frac{0.06m T_s}{2\pi(150)}$$

If T_s is roughly 5×10^{-3} seconds and

$$m = 2\pi (8 \times 10^8) \quad (\text{at low deviation}),$$

then
$$W = 1.6 \text{ kHz.}$$

This shows how the true spectrum can easily become quite wide. At the same time, the simulated width would still be very narrow.